The Early Secretory Pathway in Immunity

by

Stephanie H. Kim

A dissertation submitted in partial fulfillment
of the requirements for the degree of
Doctor of Philosophy
(Immunology)
in the University of Michigan
2020

Doctoral Committee:

Professor Pavan Reddy, Chair
Professor Cheong-Hee Chang
Professor David Ginsburg
Assistant Professor Rami Khoriaty
Professor Malini Raghavan

Stephanie H. Kim

stephkim@umich.edu

ORCID iD: 0000-0002-8397-1616

DEDICATION

For 엄마, 아빠, James, and Raymond

ACKNOWLEDGEMENTS

Like the activation of a naïve T cell, the development of this thesis was made possible by the integration of three critical signals. The enigma of the early secretory pathway in immunity began as a foreign antigen to me, but one that was presented in partnership with a perfectly matched mentor. The work summarized was strengthened by a wonderful thesis committee and collaborators, and performed in a propelling milieu of support. Surely, I will develop long-lasting memory of this experience.

First, I'd like to express my utmost gratitude to my thesis mentor, Pavan Reddy, for guiding me in this work and in my development as a physician-scientist. Pavan was always open to discussing and challenging new ideas, regardless of the time of day. In the process, he both instilled in me an enduring wonder for science and trained me to think both rigorously and methodically about it. I will always look up to his own indefatigable curiosity and humanism as a touchstone for leading my academic career. I am also grateful to the members of my thesis committee, Cheong-Hee Chang, Malini Raghavan, Rami Khoriaty, and David Ginsburg, whose combined expertise guided the direction of this thesis. Drs. Chang and Raghavan were educators from early in my PhD training, and their mentorship since has left an indelible mark on my resolve to pursue a career in immunology research. I'd also like to thank Drs. Khoriaty and Ginsburg who developed a strong and fascinating scientific foundation for this thesis and generously provided critical mice and reagents that made this work possible. I was also fortunate to have collaborated with Rafi Ahmed and Raj Valanparambil from Emory University, whose independent appraisal of our mice

not only enabled the addition of LCMV data to this work, but also uncovered novel elements that will surely lead to interesting stories and fun collaborations.

This thesis was supported by past and present members of the Reddy Lab. I'm grateful to have spent these years in such a collaborative and intellectually stimulating environment. A special thanks to Julia Wu, who trained me as a new student and helped launch this project. Dan Peltier, Hideaki Fujiwara, Israel Henig, Tomomi Toubai, Austin Taylor, and Yaping Sun were like older brothers to me. The countless conversations we had in lab inspired and informed the human work and BMT experiments in this thesis. Cynthia Zajac, David Sokol, Molly Radosevich, and Lu Li provided critical technical support and I'm grateful for their boundless generosity and willingness to lend a helping hand. Finally, I am thankful to Kay Oravecz-Wilson for both administrative and personal support, and for her hard work in cultivating a lab atmosphere of support and optimism.

Thank you to the support from the University of Michigan MSTP including Ron Koenig, Justine Hein, Gretchen Aland, Liz Bowman, and past members of the administration, as well as the Immunology Graduate Program including Beth Moore, Zarinah Aquil, and the new leadership. In addition, I am lucky to have entered into these programs with fellow students who inspire me, provided critical Signal 3 factors, and whom I am grateful to call some of my best friends.

A special thanks to my partner, Ray, the kindest person I know. Thank you for both keeping me grounded through this process and being a constant source of love and encouragement. Finally, I am grateful for the support from my mom, dad, and brother James. While I am the first in my family to pursue a career in research or medicine, they embody and taught me so much of what I learned is important in science: a passion for serving others, fearless creativity, a healthful mindset in nurturing slow but steady progress, and a sense of humor if all else fails. This thesis is dedicated to them more than I can express.

TABLE OF CONTENTS

LIST OF FIGURES

LIST OF TABLES

LIST OF ABBREVIATIONS

Allo-HCT – Allogeneic hematopoietic cell transplant

APC – Antigen Presenting Cell

ATP – Adenosine Triose Phosphate

BFA – Brefeldin A

BMDC – Bone Marrow-Derived Dendritic Cell

BMT – Bone Marrow Transplantation

Cas9 – CRISPR Associated Protein 9

CD – Cluster of Differentiation

CDAII – Congenital Dyserythropoietic Anemia Type II

CFSE – Carboxyfluorescein succinimidyl ester

CLSD – Cranio-lenticulo-sutural Dysplasia

COPII – Coat Protein Complex II

CRISPR – Clustered Regularly Interspaced Short Palindromic Repeats

CTL – Cytotoxic Lymphocyte

ELISA – Enzyme Linked Immunosorbent Assay

ER – Endoplasmic Reticulum

ERAD – Endoplasmic Reticulum Associated Degradation

ERES – Endoplasmic Reticulum Exit Site

GAP - GTPase activating protein

GM-CSF – Granulocyte-Macrophage Colony Stimulating Factor

GTP – Guanosine Triose Phosphate

GVHD – Graft-versus-Host Disease

GVT – Graft-versus-Tumor

HLA – Human Leukocyte Antigen

IL – Interleukin

KO – Knockout

LCMV - Lymphocytic Choriomeningitis Virus

MHC – Major Histocompatibility Complex

MLR – Mixed Lymphocyte Reaction

PBMC – Peripheral Blood Mononuclear Cell

PMA – Phorbol 12-myristate 13-acetate

qRT-PCR – Quantitative Real Time Polymerase Chain Reaction

RBC – Red Blood Cell

SCAP – SREBP Cleavage Activating Protein

SREBP – Sterol Regulatory Element Binding Protein

T_H – T helper cell

T_{reg} – T regulatory cell

TCR – T cell receptor

TEM – transmission electron microscopy

WT – Wild-type

ABSTRACT

A central problem faced by T cells is the need to meet the demands of changing landscapes in health and disease while adapting to rapid intracellular changes in gene expression and protein flux. However, significant gaps remain in our understanding of the fundamental molecular and cellular pathways that are critical in T cell immunity. An estimated one-third of the eukaryotic proteome is transported by the classical secretory pathway, which underlies not only the transport of proteins destined for secretion, but also important homeostatic and metabolic functions. In this pathway, proteins are co-translationally inserted into the endoplasmic reticulum (ER), and transported to the Golgi compartment where they undergo further processing, and delivered to other intracellular compartments, or the extracellular space. Coat Protein Complex II (COPII) drives the critical step in this pathway that transports proteins from the ER to the Golgi apparatus. The critical ER-to-Golgi pathway in T cells has heretofore not been characterized. This thesis aims to explore the role of COPII secretory pathways in T cell immunity.

Structurally, COPII consists of an outer layer that facilitates the budding of vesicles from the ER membrane, and an inner layer that comprises the protein SEC23. To study the role of COPII in T cells, we generated novel conditional T cell-specific *Sec23* knock-out mice. The mammalian genome consists of two SEC23 paralogs, SEC23A and SEC23B. We found that in murine T cells, SEC23B critically regulated the T cell secretome and metabolic reprogramming *in vitro*, as well as protective and pathogenic functions in experimental models of viral infection and allogeneic hematopoietic cell transplantation *in vivo*.

Biallelic loss-of-function mutations in *Sec23b* lead to Congenital Dyserythropoietic Anemia Type II (CDAII) in humans. We tested T cells derived from a patient with CDAII and discovered that they did not exhibit the same phenotype as those derived from our SEC23B knock-out mice. Mechanistic studies demonstrated that unlike murine knock-out T cells, T cells derived from patients with CDAII harbored increased levels of the closely related paralog, SEC23A. We thus examined T cells from mice that lack functional SEC23B, but express the *Sec23a* coding sequence from the *Sec23b* genomic locus. T cells from these mice exhibited normal functions, suggesting that SEC23A can functionally compensate for SEC23B in T cells. Together, our data demonstrate a critical role for the COPII pathway in T cell immunity, with evidence for functional overlap in vivo between the two SEC23 paralogs in regulation of T cell immunity in both mice and humans.

CHAPTER 1

A Rationale for Studying the ER-to-Golgi Transport Pathway in T cells

1.1 Statement of research problem

Approaching the immune system can occur at multiple levels including the molecular, cellular, physiological, and population. At each, our understanding of immune cell biology has both benefited from and advanced other fields of science. Early genetic approaches in yeast, combined with biochemical and imaging approaches, elucidated genes critical for secretion (designated "Sec" genes) and other aspects of vesicular transport. These studies established the molecular basis of the early secretory pathway and the broader phenomenon of vesicle transport systems, and was honored with the Nobel Prize for Physiology or Medicine in 2013[1].

Since the characterization of these genes, understanding their specific roles in different cell types continues to be an area of great interest[2]. As a result, the exploration of the COPII system in different cell types is shedding new light on the roles of COPII in development, organ physiology, and disease pathophysiology. This thesis specifically explores the role of Sec23 in T cell immunity. The goal of Chapter 1 is to introduce relevant background information that provides the framework for the experiments conducted, and to provide context for the significance of our findings.

1.2 Introduction to the immune system and T cell biology

Introduction to innate and adaptive immunity

The human immune system integrates two systems, the innate and adaptive, to defend the host from infectious organisms and disease. The cells that participate in the innate immune system represent the first line of defense after the host's physical and chemical barriers to infection. Innate immune cells recognize conserved structures and biochemically invariant molecules of microbes with hard-coded sensors such as Toll-like receptors, C-type lectin receptors, and cytosolic NOD-like receptors to mount a rapid unified response against a pathogen. Broadly, this recognition is followed by generation of inflammatory cytokines, uptake and degradation of the pathogen, and presentation of foreign antigen to the adaptive immune system. Antigen presenting cells thus serve as a bridge between the innate and adaptive immune systems. In contrast to innate immune cells, adaptive immune cells undergo genetic recombination during development to generate a diverse pool of receptors and thus allows the host to adapt to microbial variation. Among these, T cell immunity is developed via the clonal expansion of antigen specific cells that encounter cognate peptide antigen presented by the Major Histocompatibility Complex (MHC), in combination with co-stimulation and cytokine stimuli. The development of specific immunity and long-lasting memory are hallmark features of an adaptive immune response.

T cell development

T cells are derived from hematopoietic stem cells that undergo a series of developmental checkpoints in the thymus[3]. The significance of these checkpoints lies in the notion that a given T cell is capable of selecting from a vast diversity of antigen receptors through V(D)J recombination. However, a rigorous selection of the repertoire T cells that exit into the periphery is required to

ensure both self-MHC restriction and self-tolerance. T cell development is initiated upon the interaction of lymphoid progenitor cells with thymic epithelial cells, which stimulate their proliferation and activate a program of gene expression further committing the cell to the T cell lineage[4]. The sequence of T cell developmental stages can be broadly categorized by the expression of CD4 and CD8 on the T cell surface. T cell precursors referred to as double negative cells express neither CD4 nor CD8. As the T cells progress to commit to their expression of either the α:β or γ:δ T cell receptor (TCR), T cells enter the double positive stage at which they express both CD4 and CD8. The presence of both molecules in addition to the TCR enables the T cell to interact with peptide-bound MHC on thymic cortical epithelial cells, and commit to either the CD4 or CD8 single positive lineage[5,6]. $CD8^+$ cytotoxic T cells interact via their TCR to peptides presented on MHC class I, and $CD4^+$ helper T cells with those on MHC class II[7].

T cells undergo another phase of development that is comprised of apoptotic and anti-apoptotic events and ensures the egress of T cells that are restricted to self-MHC, but tolerant to self antigen.T cells that recognize self-MHC molecules are positively selected in the thymic cortex, whereas T cells that do not recognize self-MHC do not progress past the double positive stage. Positively selected T cells that have an excessively strong affinity for self antigens are removed by the process of negative selection, as they could potentially be reactive to host tissue and increase the risk of autoimmune disease. Taken together, these selection events in principle promote the survival only of T cells that have a diverse repertoire of antigen receptors which can survey for a wide array of foreign antigens including bacterial and viral proteins, but which are not reactive to self[8].

T cell activation

The engagement of three signals coordinates the activation of naïve T cells after they leave the thymus[9,10]. The interaction between the TCR on $CD8^+$ and $CD4^+$ T cells with a cognate antigen presented on MHC class I and MHC class II respectively provides the first critical signal. The TCR complex includes CD3 which is required to carry out signal transduction following peptide:MHC engagement. Signal 2 follows the engagement of T cell co-stimulatory receptors by ligands on an antigen presenting cells[9]. The predominant co-stimulatory pathway involves the binding of CD28 on the T cell with B7 (CD80 or CD86) on the antigen presenting cell. Interaction with both antigen and co-stimulatory ligands is critical for initiating the intracellular signaling cascade that promotes T cell proliferation, survival, and effector functions. In addition to these two signals, Signal 3 which is provided by surrounding cytokines, further drives the fate of the activated T cell. Signal 3 controls the differentiation of T helper (T_H) subsets, influences the polarization of specific T effector responses, and shapes the balance between immune activation and tolerance[10-14]. In addition to receiving cytokine signals, T cell activation is followed by a program of increased protein synthesis and cytokine secretion by T cells themselves[9]. T cell-derived secreted factors can influence both activating and inhibitory immune cell functions. Among T cell-derived cytokines, IL-2 regulates important aspects of T cell survival, differentiation, and proliferation. While it is critical for the development of T effector cell responses, it also is involved in the development and maintenance of T regulatory cells (T_{regs})[15]. The cytokines that signal to – and are secreted by – T cells signal through distinct pathways, and thus dysregulation of cytokine secretion can impair protective immune responses against pathogens, or exacerbate pathologic autoimmune events.

Cytokines and Acute Graft-versus-Host Disease

The biological significance of T cell secretory functions is underscored by human diseases that arise when the regulation of cytokine networks is aberrant. Indeed, understanding the specificity of the immune system and its molecular regulators has been a driving force in basic science research, and the fine-tuning of its response in humans continues to be a primary objective in the clinic. One disease that illustrates this, and is of particular interest to the Reddy lab, is acute Graft-versus-Host Disease (GVHD). Acute GVHD is a major cause of non-relapse morbidity and mortality in patients receiving allogeneic hematopoietic stem cell transplantation (allo-HCT)[16,17]. Allo-HCT holds curative potential for many hematological disorders. However, the pathophysiology of the desired graft-versus-tumor effect is linked to life-threatening complications of acute GVHD. While the development of GVHD is dependent on numerous factors, HLA polymorphisms that trigger antigen-induced activation of donor-derived T cells and their activity against recipient tissue is a key determinant in the induction and severity of GVHD[16].

The cytokine milieu in patients following bone marrow transplantation is complex, and includes both immune cell and target tissue sources. Prior to transplantation, patients first receive conditioning treatments that are damaging to host tissue and lead to the release of inflammatory cytokines including IL-1, IL-6, and TNFα[18-20]. These cytokines activate antigen presenting cells that subsequently activate donor alloreactive T cells, leading to the increased production of additional effector molecules. These include cytokines and cytotoxic factors that are directly damaging to tissue, or indirectly form the milieu that support T cell proliferation and differentiation. Thus, in GVHD, cytokines are released following conditioning treatments and amplified by tissue destruction from T cell-mediated lysis[21].

In both experimental models of allo-HCT and in patients affected by GVHD, cytokines significantly impact the alloreactive T cell response[22]. Many current existing therapies for GVHD are aimed at targeting donor T cells, and a number of therapeutic approaches aim to target Signal 1 and Signal 2 in alloreactive T cell activation in the prevention and treatment of GVHD[23-25]. However, donor T cells are also critical for the Graft-versus-tumor (GVT) effect, and as such, balancing therapies has been a challenge to preserve sufficient GVT activity while minimizing GVHD-related tissue damage.

One strategy has been to target the inflammatory byproducts of immune cells including cytokines that promote alloreactive T cell toxicity, and also cause direct inflammation-related organ damage, thus contributing to symptoms and pathology. While the success of these approaches has been modest thus far, a growing basic science understanding of relevant cytokines, the regulation of cytokine secretion, and the specific impact each has on immune and target cells will inform future strategies for the prevention and treatment of GVHD. Selectively targeting the cytokines that promote alloreactive T cells remains an attractive therapeutic strategy, and further exploring the intracellular transport pathways that are utilized by T cells and are shared by these effector molecules may shed light on new translational opportunities.

1.3 Overview of the early secretory pathway

Introduction to intracellular membrane transport

A characteristic feature of eukaryotic cells is the spatial organization of cellular processes in discrete organelles. The presence of distinct organelles separated by membrane bilayers enables the maintenance of distinct biochemical environments and unique resident proteins. Inherent in this is the existence of regulated transport systems via which molecules reach their correct

intracellular locations. One way this is achieved is via protein coats that transport membrane bound vesicles between specific compartments. The entry point for proteins into the classical secretory pathway is the ER, and proteomic studies suggest that about one-third of the proteins encoded by mammalian cells traffic from this multifunctional organelle[26,27]. Signal sequences play an important role in targeting many secreted and membrane proteins for insertion into the ER[28]. Following entry into the ER lumen, proteins undergo a series of modifications that enable protein folding and oligomerization, after which they are able to exit the ER toward their final destinations including various intracellular organelles, the plasma membrane, and the extracellular space. ER quality control mechanisms not only facilitate the proper folding of these newly synthesized proteins, but also they direct misfolded proteins toward degradative processes, including proteasomal degradation through the ER associated protein degradation (ERAD) pathway, or autophagosomal pathways[29,30]. Properly folded proteins exit the ER and proceed distally toward the Golgi apparatus where they may be further modified.

Introduction to the COPII pathway

A complex of proteins collectively known as COPII represents the required machinery for generating transport vesicles from the ER membrane[31]. COPII drives the formation of ER-derived vesicles that transport newly synthesized proteins to the ER-Golgi intermediate compartment and Golgi compartment[31-34]. Many early discoveries about COPII are derived from studies that performed genetic analysis in *Saccharomyces cerevisiae*[32,35]. The identification of proteins that play a role in secretion was first achieved by genetic screens that focused on isolating secretory (sec) mutants that exhibited ER distension and defective secretory capabilities under restrictive growth temperatures[35,36]. Structurally, COPII is comprised of an inner and outer coat whose core

subunits are conserved in all eukaryotes and represent the components required to form COPII coats. These subunits are Sar1, Sec23, Sec24, Sec13, and Sec31[31,37,38] (**Figure 1.1**).

COPII formation begins with the activation of the small GTPase Sar1 by the ER resident membrane protein Sec12 on the cytoplasmic side of the ER membrane[39,40]. The activation of Sar1 induces a conformational change that exposes an alpha helix that lodges in the ER membrane and initiates membrane curvature[41,42]. Membrane-bound SAR1-GTP binds the SEC24-SEC23 heterodimer by direct association with SEC23, which together form the COPII inner layer also referred to as the pre-budding complex that represents a crucial intermediate for full COPII assembly[43-45]. SEC23 is a GTPase activating protein (GAP) that activates the SAR1-GTPase, and the transition from SAR1-GTP to SAR1-GDP ultimately leads to the dissociation of the COPII coat[14]. SEC24 is the primary subunit that engages in cargo recognition and serves to select the repertoire of cargo molecules incorporated into COPII vesicles by association with ER export motifs located on cargo proteins[43,45-51]. Together, the SEC23-SEC24 heterodimer recruits the SEC13-SEC31 complex which forms the outer layer. SEC13-SEC31 by its structural nature drives further membrane curvature, vesicle budding, and scission from the ER membrane at ER exit sites[50,52-54]. It also serves to facilitate the uncoating of COPII coats by optimally positioning SEC23 with SAR1 to stimulate GTPase activation[55]. Mammals exhibit greater complexity of the COPII system, in part by the presence of multiple COPII subunit paralogs. Mammals have two paralogs of SAR1, two paralogs of SEC23, four paralogs of SEC24, and two paralogs of SEC31[56].

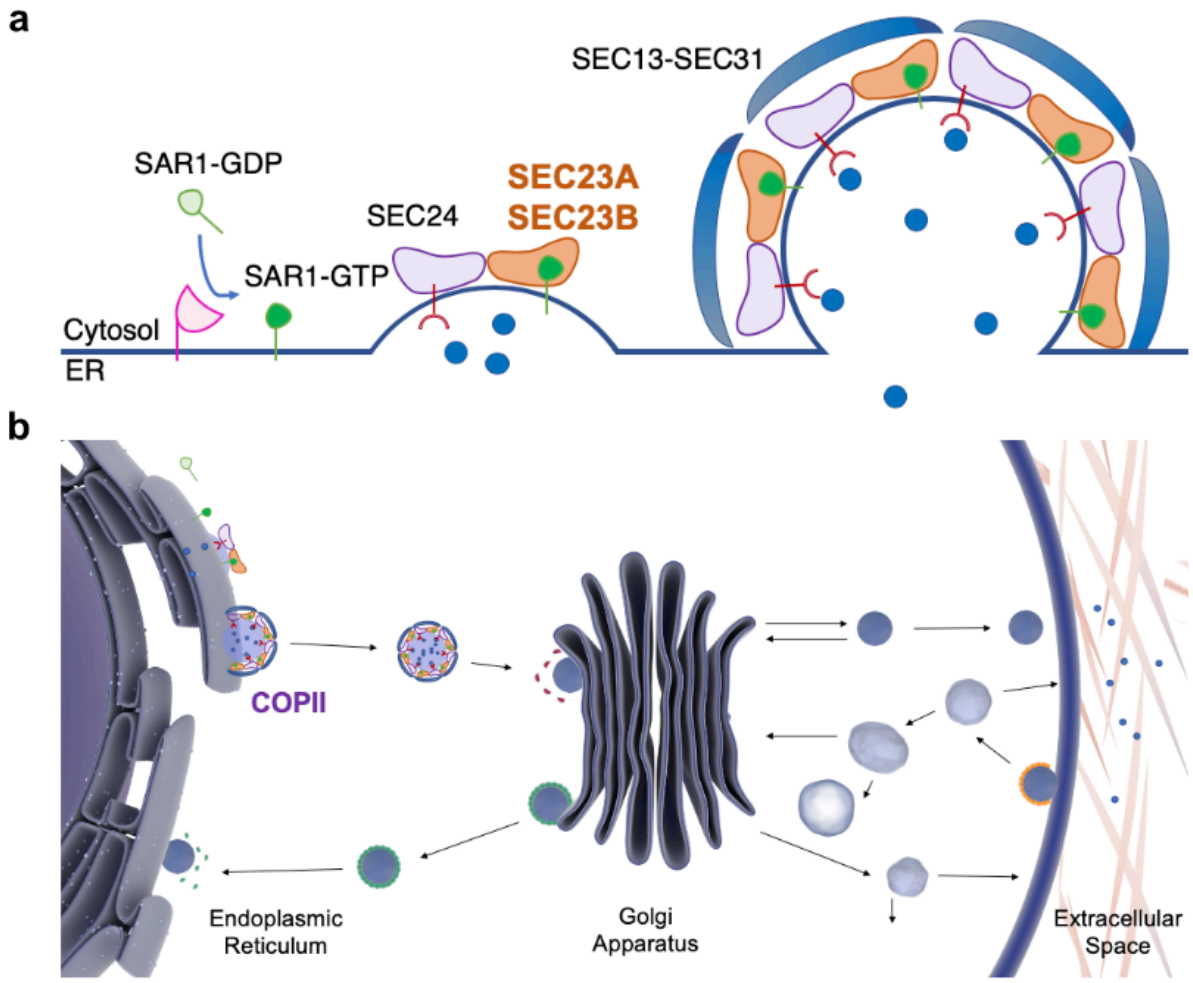

Figure 1.1 Overview of COPII vesicle formation and function in the secretory pathway

The COPII coat drives the population and formation of vesicles from the ER membrane. (**a**) Coat formation is initiated by the activation of SAR1. SAR1-GTP recruits the SEC23-SEC24 heterodimer, which binds SAR1 by SEC23, and form the COPII inner coat. Cargo receptors (red) mediate the interaction of COPII with cargo proteins, and can facilitate the incorporation of select transport molecules. SEC13-SEC31 which forms the outer layer of the COPII coat, facilitates vesicle budding and scission. (**b**) Fully formed COPII vesicles are targeted to the ERGIC and cis-Golgi compartment from where they are further sorted to other intracellular compartments or to the extracellular space.

The COPII pathway is primarily associated with the transport of secretory cargoes, but its impact is multifaceted. In the following section, we focus on the SEC23 subunit and highlight the diverse biological functions that depend on its activity.

1.4 Introduction to SEC23

SEC23 is a critical component of the COPII inner layer, and it is highly conserved across eukaryotes[38]. It is a GTPase activating protein (GAP) that directly binds SAR1, and contributes to SAR1-GTP hydrolysis. Humans and mice carry two SEC23 paralogs, SEC23A and SEC23B. These paralogs share 85% identity in amino acid sequence[43]. Structural homology combined with functional studies suggest that the functions of SEC23A and SEC23B are highly conserved and overlapping. It has been demonstrated that SEC23A and SEC23B can functionally compensate for each other, but and are expressed differentially in particular tissues in mice and humans due to evolutionary shifts in gene expression[57].

SEC23 has five domains: a zinc finger domain, β-barrel domain, α-helical domain, gelsolin domain, and a trunk domain[58]. Several binding partners of SEC23 have been described in addition to other COPII subunits. Among them, SEC23 interacts with dynactin which facilitates ER exit and vesicle transport between the ER and ER-Golgi Intermediate Compartment (ERGIC)[59]. SEC23 also binds TRAPPI, which facilitates tethering of COPII vesicles to the ERGIC and Golgi membrane[60,61]. The soluble NSF-attachment protein receptor (SNARE) protein SEC22 is another known SEC23 binding partner that is critical for trafficking of COPII vesicles to the ERGIC and cis-Golgi compartment[62,63].

SEC23 in human disease

The significance of the COPII pathway is demonstrated by a spectrum of diseases that arise in humans who carry mutations in core COPII proteins. Mutations in *SEC23A* result in Cranio-lenticulo-sutural Dysplasia (CLSD)[64,65]. CLSD is an autosomal recessive disorder that results in abnormal craniofacial development and skeletal dysplasia. Clinical features include late-closing

fontanelles, sutural cataracts, and other facial dyspmorphisms[64,65]. It is thought that a defect in the secretion of collagen contributes to the disease, with fibroblasts being characterized by dilated ER due to intracellular accumulation of procollagen[66].

By contrast, homozygous or compound heterozygous mutations in *SEC23B* give rise to Congenital Dyserythropoietic Anemia Type II (CDAII), also known as hereditary erythroblastic multinuclearity with positive acidified serum lysis test (HEMPAS)[56,67]. CDAII is characterized primarily by red blood cell abnormalities[67-69]. Patients with CDAII exhibit a mild to moderate anemia, ineffective erythropoiesis, and other erythroid abnormalities including bi- and multi-nucleated erythroblasts in the bone marrow, abnormal lipid glycosylation of some red blood cell membrane proteins such as Band3, and double membrane appearance by electron microscopy, with the inner membrane representing remnant ER[56,70]. No abnormalities to date have been reported in other hematopoietic cells. A diverse mutational landscape has been characterized for CDAII, and variants have been described along the entire *Sec23b* coding sequence[69]. However, no patients to date have been reported to harbor two nonsense mutations, suggesting that complete absence of SEC23B is not compatible with life. *SEC23B* variants have also been described in association with Cowden syndrome, thyroid cancer, and colorectal cancer metastasis, and mutations in *SEC23B* have been hypothesized to increase risk of tumorigenesis by dysregulated ER stress responses that favor cell survival, or by inhibiting the surface transport of cell adhesion molecules and thus promoting metastasis[71-73].

Mouse models used to study SEC23B

Genetically modified animal models have demonstrated roles for SEC23 in development, while illuminating other aspects of its biology. Humans with biallelic loss-of-function mutations

in *SEC23B* develop CDAII. However, the generation of a mouse model that contains a gene-trap cassette insertion in the *Sec23b* genomic locus demonstrated that mice lacking SEC23B do not develop the same anemia phenotype[74]. Rather, they exhibit abnormalities in the pancreas and other exocrine tissues that upregulate the unfolded protein response and pro-apoptotic pathways, and die shortly after birth. Gene-trap insertion in the murine *Sec23a* locus is lethal at the mid-embryonic stage, and is associated with failure of neural tube closure in the midbrain, and defects in collagen secretion[75]. Mice generated to have a SEC23B deficiency restricted to the pancreas demonstrated that pancreatic SEC23B deficiency was sufficient to cause the perinatal lethality observed in mice with germline *Sec23b* deletion[76]. Further restricting the *Sec23b* deletion to pancreatic acinar cells highlighted the importance of SEC23B specifically in the highly exocrine compartment of the pancreas[77]. The generation of another mouse model in which SEC23B deficiency was restricted to the hematopoietic cell compartment enabled the analysis of the adult hematopoietic lineage, as these mice survive into adulthood[78]. Unlike humans, however, mice with SEC23B deficiency in the hematopoietic compartment did not display an anemia phenotype, or other abnormalities in RBCs associated with CDAII such as a double membrane, or defect in band 3 glycosylation[78]. The discrepancy in phenotype between mice and humans harboring mutations in homologous genes has raised questions about the underpinnings of these observations. A recent study reports the generation of a novel *Sec23*$^{b\text{-}a/b\text{-}a}$ mouse model that harbors the *Sec23a* coding sequence in the endogenous genomic *Sec23b* locus[57]. Analysis of mice with this modification demonstrated that when expressed at adequate levels , SEC23A can rescue the pancreatic degeneration and perinatal lethality phenotype that results from the loss of SEC23B. Taken together, these findings support a unifying theory that SEC23 paralogs are functionally overlapping, but are expressed with a tissue- and species-specific pattern. The generation of these mice presented an opportunity to study the

role of the COPII pathway in T cells. In this work, we utilized *Sec23a*$^{fl/-}$ *Vav1*^{Cre}, *Sec23b*$^{fl/-}$ *Vav1*^{Cre}, and *Sec23*$^{b\text{-}a/b\text{-}a}$ mice generated in previous studies[57,76,78]. We also generated *Sec23a*$^{fl/-}$ *Cd4*^{Cre} and *Sec23a*$^{fl/-}$ *Cd4*^{Cre} mice to focus on the role of this protein in T cells.

1.5 The post-Golgi apparatus transport of secreted factors in T cells

In mammalian cells, the secretory cargoes from the ER travel to the ERGIC and the cis-Golgi compartment[79-81]. The Golgi apparatus, which consists of stacked cisternae with cis to trans orientation, represents a major site for post-translational modification and sorting of cargoes. From the Golgi apparatus, cargoes are further targeted towards the extracellular space, plasma membrane, endosomal and lysosomal compartments, or back to the ER[79]. Activated T cells undergo morphologic changes that affect intracellular cytokine transport by first establishing polarity and forming immune synapses with antigen presenting cells. A dynamic cytoskeleton enables T cells to both adhere to the APC, and transport secretory vesicles containing cytokine cargoes[82].

$CD8^+$ cytotoxic T lymphocytes (CTLs) directly kill virally infected cells and tumor cells, and deficiencies in their cytotoxic function are associated with a range of disorders as well as an increased risk of prolonged viral infection and cancer in humans. In the 1980s, it was discovered that this killing is mediated by the secretion of two main proteins, perforin[83,84], and granzymes[85]. Perforins induce pore-like membrane lesions in the cell, and granzymes which are cytotoxic granules capable of inducing apoptosis, enter through the pores destroying the target cell. Subsequent studies described the post-Golgi transport of these important factors, showing that $CD8^+$ T cells engaged with cognate APCs reorient their microtubule organizing center toward the immunological synapse, and transport secretory granules along microtubules towards the point of

cell-cell contact for targeted lysis of the APC[86]. Defects in cytotoxic function are associated with a number of human diseases. While some disorders are due to mutations in perforin itself, others are secondary to defects in exocytosis of cytotoxic granules and secretory granule transport to the immunological synapse. One example is Familial Hemophagocytic Lymphohistiocytosis, which arises both from mutations in perforin and mutations in proteins involved in membrane fusion preceding exocytosis[87]. The molecules that regulate secretion are thus critical to immune homeostasis, and studies of the pre-Golgi transport of these proteins would complement current understanding of post-Golgi processes that have thus far been illuminated.

$CD4^+$ T cells remain less well characterized in their regulated secretory pathways than $CD8^+$ T cells. There is growing evidence that like $CD8^+$ T cells, $CD4^+$ T cells contain secretory lysosomes for secretion of some proteins. It is likely that the secretory lysosomes of $CD4^+$ T cells use an analogous system and depend on the same or similar molecules that carry out key functions in $CD8^+$ T cells. CTLA-4 and FasL produced in $CD4^+$ T cells co-localize with secretory lysosome associated proteins, suggesting these are among the cargo proteins that are exported via this pathway[88,89]. $CD8^+$ T cells directionally secrete perforin and granzymes toward the immunological synapse, and this phenomenon was also observed in $CD4^+$ T cells in which cytokines can be found concentrated at the site of contact with an interacting cell[90]. This was corroborated in studies that showed $CD4^+$ T cells release their cytokines near the area of receptor cross-linking under activated conditions[91]. However, some important questions remain about how these processes are regulated.

One study by Huse et al offers a cell biological mechanism by which specificity of cytokine secretion is controlled[92]. Using video microscopy and intracellular staining techniques, they demonstrated that while cytokines such as IL-2, IFNγ, IL-3, and IL-10 were directed toward the interface between T cells and cognate antigen presenting cells, others such as TNFα, CCL3, and

CCL5 showed a different staining pattern. Over the course of the T cell activation response, TNFα migrated to all edges of the cell and not just at the site of cell-cell contact[92]. Mechanistically, whether cytokines moved toward the synapse or in every direction was shown to be coordinated by their co-localization with different trafficking proteins such as SNARE protein Syntaxin 3, or Rab GTPases Rab3D and Rab19 respectively[92]. Thus, two pathways are proposed: a unidirectional pathway that directs cytokines toward the immunological synapse and minimizes non-specific cytokine release, and a multi-directional pathway to promote more generalized inflammation[92]. Since this study, several others have followed up on the consequences of directional and multi-directional secretion[93,94]. However, more in-depth studies to elucidate the molecular mediators of $CD4^+$ T cell regulated secretion are still needed and would help illuminate our understanding of T cells under homeostasis and in disease.

Studies to elucidate the molecular mediators of regulated T cell secretion may enable novel approaches toward controlling targeted cytokine release in disease states. These studies and others underscore that in addition to cytokine expression, regulation of the membrane-bound organelles that transport them significantly impact the consequences of T cell activation. However, to date, studies have been limited to understanding the secretory pathway of cytokines through events that occur after their egress from the Golgi apparatus.

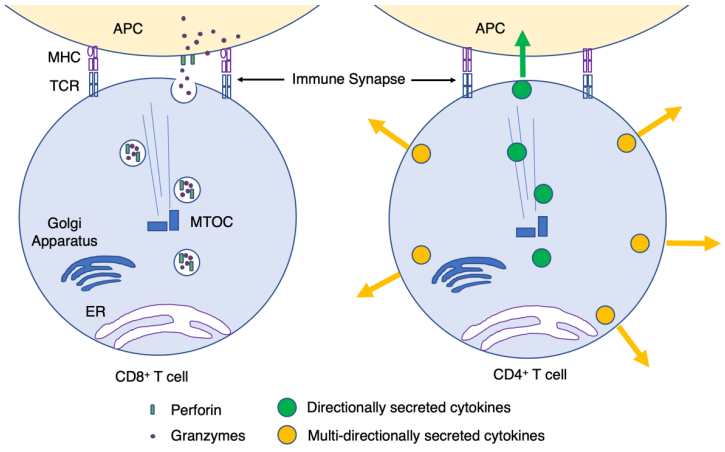

Figure 1.2 Post-Golgi pathways that transport effector molecules in $CD8^+$ and $CD4^+$ T cells

In $CD8^+$ T cells, perforin and granzymes travel directionally toward the immune synapse to efficiently lyse infected cells. $CD4^+$ T cells have at least two main pathways of cytokine secretion. Factors including IL-2 and IFNγ are transported directionally toward the immune synapse. Other cytokines like TNFα which serve to promote inflammation are secreted in a multi-directional manner[92,93]. Whether T cells utilize COPII-mediated ER to Golgi transport is unknown.

1.6 Organization of thesis

While COPII vesicles play a fundamental role in the secretory pathway, gaps remain in our knowledge about their role in immunity. This thesis seeks to build on published peer-reviewed literature to characterize the COPII pathway in immune cells with a primary focus on T cells. Chapter 1 provides background information and highlights studies that provide a foundation for our experiments. Chapter 2 investigate the consequences of *Sec23b* knock-out (KO) in murine T cells, from which we gain novel basic biological insights into the role of the COPII pathway in T cell secretion *in vitro*, and in experimental models of antiviral and alloimmunity *in vivo*. Chapter 3 utilizes *Sec23a* KO mice and *Sec23*$^{b\text{-}a/b\text{-}a}$ mice to gain insight into the role of Sec23 paralogs in mammalian T cells. Chapter 4 expands on findings from Chapter 2 to propose complementary effects of T cell metabolism on our observed phenotypes. Chapter 5 describes our findings in T cells from both healthy humans, and humans with CDAII, a disorder caused by *Sec23b* mutation. Finally, in Chapter 6, we provide a discussion on the conclusions of this thesis, future directions, and a framework for how our findings can be interpreted for clinical translation.

CHAPTER 2

The COPII Pathway Regulates T Cell Functions *in vitro* and *in vivo*

2.1 Abstract

T cell-mediated responses are dependent on their secretion of key effector molecules including cytokines and cytotoxic factors as a fundamental mechanism of cell-cell communication. However, the critical molecular determinants of the secretory pathway in immune cells are largely undefined. Herein, we characterize ER-to-Golgi transport mechanisms that are critical for T cell functions *in vitro* and *in vivo*. To study the functional role of this pathway, we generated mouse models with a conditional hematopoietic- or T cell-specific deficiency in SEC23B, a core COPII subunit. We demonstrate that unlike other hematopoietic cells, murine naive T cells express both SEC23 paralogs, and harbor greater baseline expression of SEC23B than SEC23A. Our mice demonstrated that SEC23B was not critical for T cell development, but played a key role in T cell functions. The loss of SEC23B led to reduced secretion of select effector cytokines, an altered functional phenotype *in vitro*, reduced pathogenicity in murine *in vivo* models of allogeneic hematopoietic stem cell transplantation, and reduced protective functions in an *in vivo* model of viral infection. Together, our findings offer the first demonstration that the COPII pathway is critical for T cell immunity.

2.2 Introduction

Naive T cells undergo a program of increased protein synthesis following their activation, which includes secreted proteins that facilitate their growth and effector functions. In Chapter 1, we highlight literature that describes the post-Golgi transport of effector molecules by $CD8^+$ and $CD4^+$ T cells. These findings are significant not only because they shed light on molecular mechanisms of T cell functions, but also because they suggest the existence of a sophisticated system for secreting soluble factors.

T cells contribute to protective immune responses such as those targeting viral infections and tumors, but also disease processes including autoimmunity and alloimmunity[95]. For a productive immune response, T cells must tightly control the release of numerous cytokines and cytotoxic factors that direct their functions, but the intracellular pathways that lead up to their release are not well known. Despite the significant consequences of T cell secretion in health and disease, the intracellular pathways and molecular determinants that regulate this process remain poorly characterized[93,94]. Specifically, the pathways of protein transport prior to their access to the Golgi compartment and whether they regulate T cell functions are not known.

COPII drives the formation of ER-derived vesicles that transport newly synthesized proteins to the Golgi compartment. Among their critical roles, COPII-coated vesicles enable the extracellular transport of proteins and their localization to other intracellular compartments[31-34]. While the fundamental COPII pathway is conserved in all eukaryotes, the presence of multiple COPII subunit paralogs in mammals enables increased complexity and regulation of protein secretion in mammalian cells[38,96]. Mammals express both SEC23A and SEC23B, which share 85% identity in amino acid sequence.

In this chapter, we demonstrate our initial observation that wild-type (WT) T cells engage the ER following activation, suggesting that the COPII pathway is engaged in this cell type. We endeavored to build on this observation by characterizing the consequence of targeting *Sec23b* in murine T lymphocytes. Specifically, we examined *Sec23b*$^{fl/-}$ *Vav1*^{Cre} and *Sec23b*$^{fl/-}$ *Cd4*^{Cre} mice, which lack SEC23B in hematopoietic cells and T cells respectively. Using both models, we report that the absence of SEC23B does not impair T cell development. However, it leads to an altered secretome that impacts select cytokine secretion, and results in reduced T cell proliferative capacity *in vitro*.

We further hypothesized that the disruption of SEC23B-dependent COPII vesicles would impact T cell-mediated immune responses. To test this, we determined the *in vivo* ramifications of disrupting COPII following clinically relevant T cell-dependent models. We found that in the absence of SEC23B, T cells demonstrated reduced Graft-versus-Host Disease (GVHD) in experimental models with both major and minor histocompatibility mismatch. Additionally, in a separate Lymphocytic choriomeningitis (LCMV) based model of acute viral infection, T cell protective functions were impaired. Taken together, these data identify SEC23 as a critical regulator of T cell immunity, and demonstrate that T cells utilize the COPII pathway to mediate effector functions.

2.3 Materials and Methods

Mice

All animal work in this thesis was performed in accordance with the recommendations of the Institutional Animal Care and Use Committee of the University of Michigan. The generation of *Sec23b*$^{fl/-}$ has been previously reported[57,76,78]. *Sec23b*$^{fl/-}$ mice were bred with *Cd4*^{Cre} (017336) or *Vav1*^{Cre} (008610) mice obtained from The Jackson Laboratory. Genotyping was performed using primers previously described and listed in Table 1 below[57,76,78]. C57BL/6C (027) and BALB/c (028) mice used as recipients in BMT experiments were obtained from Charles River Laboratories, and C3H.SW (000438) recipient mice were obtained from The Jackson Laboratory.

Primer	Sequence (5' to 3')
Sec23b F1	ATAGACCAGGCTGGCCTCAGTC
Sec23b F2	AACAGCCCAGGTGACTAGGA
Sec23b R	CAAGTGAGTGCCTCCTCACA
Sec23a A	GGAGCTGTTCCAAGCACATTCTCT
Sec23a E2	TCCCTGGGTCAAAGTGCTGTCCA
Sec23a D	CCACGCAGTCCTGGCTCTCCTGA
RMCE F1	CCCAGCCATGATCTCTGTTTA
RMCE R1	CCAATGATGAGGACCCAGAG
Vav1 intPC F	CTAGGCCACAGAATTGAAAGATCT
Vav1 intPC R	GTAGGTGGAAATTCTAGCATCATCC
Vav1 TG F	AGATGCCAGGACATCAGGAACCTG
Vav1 TG R	ATCAGCCACACCAGACACAGAGATC
Cre F	TTACCGGTCGATGCAACGAGT
Cre R	TTCCATGAGTGAACGAACCTGG

Table 2.1 List of all primers used to genotype mice in this dissertation

T cell isolation and in vitro cell culture

Primary murine T cells were purified by magnetic separation (Miltenyi Biotec) from single cell homogenates of spleens and lymph nodes, and cultured in cell media (1640 RPMI supplemented with 10% heat inactivated FBS, 2 mM L-glutamine, Penicillin-Streptomycin 100U/mL, 100mM HEPES, Non-essential amino acids, 1 mM sodium pyruvate, and 50 μM β-mercaptoethanol). T cells were cultured alone, or with 5 μg/mL αCD3 (145-2C11; Biolegend) and 2.5 μg/mL αCD28

(37.51; Biolegend) soluble antibodies for the specified timepoints. For proliferation studies, T cells were first labeled on day 0 with 5 μM CFSE (ThermoFisher) for 10 min at 37°C. Prior to analysis of cytokine production by intracellular flow cytometry, T cells were additionally stimulated on day 3 with a phorbol 12-myristate 13-acetate (PMA) and ionomycin (Invitrogen) in the presence or absence of BFA (Biolegend) for 5 h at 37°C.

Preparation of T cells for TEM Analysis

Cells were fixed in 2.5% glutaraldehyde in 0.1 M Sorensen's buffer, pH 7.4 (overnight, 4°C), and rinsed 0.1 M Sorensen's buffer. Cells were then fixed in 1% osmium tetroxide in 0.1 M Sorensen's buffer for 1 h, and rinsed in double distilled water to remove phosphates. Samples underwent en bloc staining with 3% uranyl acetate in double distilled water for 1 hour, and were dehydrated for 5 min each in 50%, 70%, 90%, and two changes of 100% ethanol. Samples were soaked in Epon per the following: 3:1 100% ethanol:resin for 1 hour, 1:1 100% ethanol:resin for 3 hours, 1:3 100% ethanol:resin overnight, full strength resin for several hours, new full-strength resin for several hours. Samples were arranged in molds with new full-strength resin and allowed to sit for several hours. Samples were polymerized at 60°C for 24 hours and analyzed on a JEOL JEM-1400 transmission electron microscope.

Flow cytometric analysis

Flow cytometric analysis was performed using fluorophore-conjugated antibodies to mouse CD3 (145-2C11), CD4 (GK1.5), CD8 (53-6.7), CD69 (H1.2F3), CD25 (3C7), IL-2 (JES6-5H4), TCRβ (H57-597), pZAP70 (n3kobu5), pERK1/2 (6B8B69), Annexin V, and 7-AAD (Biolegend). For surface immunophenotyping, single cell suspensions were incubated with the relevant antibodies

for 30 min at 4°C, washed, and fixed with 1% paraformaldehyde prior to analysis. Intracellular staining was performed following surface staining and fixation, in permeabilization buffer (eBioscience) for 30 min at room temperature. Staining of phosphorylated proteins was performed on methanol-fixed cells permeabilized with True-Phos Perm Buffer (Biolegend) according to manufacturer's instructions. All samples were run on an Attune NxT flow cytometer and analysis was performed using FlowJo v10.3.

T cell immunofluorescence confocal microscopy

Purified T cells were fixed on coverslips with 3% paraformaldehyde in PBS, and quenched with 50 mM NH_4Cl in PBS. Cells were then permeabilized in 0.3% Triton X-100 in PBS and blocked with 10% normal goat serum. Cells were then sequentially stained with IL-2 (JES6-5H4, Biolegend), and Calnexin (ab2595, abcam) or SEC23B (PA5-52533, Invitrogen) followed by staining with secondary antibodies against Rat IgG2bκ and Rabbit IgG respectively. DAPI (Life Technologies) was used to detect nuclei. Acquisition of images was performed using an inverted point-scanning confocal microscope with standard PMT detectors (Nikon A1).

Quantitative RT-PCR

RNA was isolated from T cells with the Qiagen RNeasy kit. cDNA was synthesized using the High Capacity cDNA Reverse Transcription Kit (Applied Biosystems), and quantified on a NanoDrop Lite Spectrophotometer (ThermoFisher). Quantitative RT-PCR was performed using PowerUP SYBR Green Master Mix (Applied Biosystems) and the primers listed in **Table 2.12** on a Mastercycler RealPlex^2 (Eppendorf).

Primer	Sequence (5' to 3')
Eif2a F	CACCGCTGTTGACAGTCAGAG
Eif2a R	GCAAACAATGTCCCATCCTTACT
Atf6a F	CTTCCTCCAGTTGCTCCATC
Atf6a R	CAACTCCTCAGGAACGTGCT
Grp94 F	TCGTCAGAGCTGATGATGAAGT
Grp94 R	GCGTTTAACCCATCCAACTGAAT
BiP F	CATGGTTCTCACTAAAATGAAAGG
BiP R	GCTGGTACAGTAACAACTG
IL-2 F	GCAGCTCGCATCCTGTGT
IL-2 R	GGGAGTTTCAGGTTCCTGTAATTCTC
IL-10 F	CAGTACAGCCGGGAAGACAA
IL-10 R	AGCTGGTCCTTTGTTTGAAAGAA
TNFa F	TGACAAAGAAGGCTGGATTCTCA
TNFa R	CACCAGCCCTTGAATGAGGT
GAPDH F	ATGGTGAAGGTCGGTGTGA
GAPDH R	TCGTTGATGGCAACAATCTC

Table 2.2 List of primers used for qRT-PCR in Chapter 2

Western Blotting

Whole cell lysates obtained from purified T cells were fractionated by gel electrophoresis through a 10% Bis-Tris gel and transferred onto polyvinylidene difluoride membrane (Millipore) in a semi-dry transfer cell (Bio-Rad). Blots were blocked and stained in 5% nonfat milk in TBST, with primary antibodies against SEC23B and SEC23A[78], and anti-β-Actin (8226; Abcam). Binding affinity of these antibodies were determined following normalization of anti-GFP antibody against GFP-conjugated SEC23A and SEC23B. Normalization is reflected in densitometric analysis. according to Incubation with secondary antibody conjugated to HRP (Santa Cruz) was performed for 2 h at room temperature. Blots were detected using the SuperSignal ECL substrate system (ThermoFisher), on a Konica SRX-101A film processor. Densitometric analysis was performed with ImageJ software.

Bone Marrow Transplantation (BMT)

BMTs were performed as previously described[97,98]. Briefly, syngeneic [C57BL/6J→C57BL/6C] and allogeneic [C57BL/6J→BALB/c or C57BL/6J→C3H.SW] recipients received lethal total

body irradiation on day -1. BALB/c recipients received a total of 8 Gy (^{137}Cs, split dose separated by 3 h), and C57BL/6C and C3H.SW recipients received a single dose of 10 Gy (^{137}Cs, single dose). All mice received 1×10^6 T cells from the specified donors, and 5×10^6 WT T cell-depleted bone marrow cells. Survival was monitored daily, and recipient GVHD clinical scores were measured weekly according to the severity of disease on recipient weight loss, posture, mobility, skin, and fur integrity as described previously[97].

Collection of T cell secretome samples

Purified T cells were stimulated by plate-bound αCD3 (10 μg/mL) and soluble αCD28 (5 μg/mL) in CTS OpTmizer serum free medium (37ºC, 5% CO_2). After 24 h, cultures were centrifuged (400xg, 10 min). Cells underwent flow cytometric analysis to confirm activation (CD69) and degree of cell death (Annexin V, 7-AAD). Supernatants were passed through a 40μm filter and underwent ultracentrifugation (120,000 x g, 90 min) to remove exosomes. Samples were then concentrated using a 3kD cutoff ultrafilter (5,000xg, 40 min). Protein concentration was determined by BCA protein assay, and samples were stored at -70ºC until use. **ProteomeXchange Accession Number**: PXD015766

Protein Identification and relative quantitation by TMT labeling and LC-Tandem MS

TMT labeling and offline fractionation: The Tandem Mass Tag (TMT) labeling was performed using TMT-10plex isobaric labeling kit (ThermoFisher, 90110). The labeling of the sample was performed according to the manufacturer's protocol with minor modifications. Briefly, 50 ug of protein from each sample was reduced with DTT (5 mM) at 45 °C for 1 h followed by alkylation with 2-chloroacetamide (15 mM) at room temperature for 30 min. Proteins were precipitated by

adding 6 volumes of ice cold acetone and incubating overnight at -20 °C. Precipitated proteins were pelleted by centrifuging at 8,000xg for 10 min at 4 °C and supernatant was discarded. The pellet was resuspended in 100 ml of 100 mM TEAB and digested overnight at 37 °C by adding 1.5 mg of sequencing grade, modified porcine trypsin (Promega, V5113). TMT reagents were reconstituted in 41 mL of anhydrous acetonitrile and digested peptides were transferred to the TMT reagent vial and incubated at room temperature for 1 h. The reaction was quenched by adding 8 mL of 5% hydroxylamine and incubating it for further 15 min. The samples were combined and dried. Prior to MS analysis, two dimensional separation of the samples was performed. For the 1st dimension, an offline fractionation of an aliquot each sample mix (200 mg) using high pH reverse phase fractionation kit into 10 fractions was performed following the manufacturer's protocol (Pierce, Cat #84868). Fractions were dried and reconstituted in 12 μL of loading buffer (0.1% formic acid and 2% acetonitrile).

Liquid Chromatography-mass spectrometry analysis (LC-Multinotch MS3): In order to obtain superior quantitation accuracy, recently developed multinotch-MS3 method was employed (McAlister GC et al). Orbitrap Fusion (ThermoFisher) and RSLC Ultimate 3000 nano-UPLC (Dionex) were used to acquire the data. Two ml of each fraction was resolved in the 2nd dimension on a nano-capillary reverse phase column (Acclaim PepMap C18, 2 micron, 75 mm i.d. x 50 cm, ThermoFisher) using a 0.1% formic/acetonitrile gradient at 300 nl/min (2-22% acetonitrile in 150 min;22-32% acetonitrile in 40 min; 20 min wash at 90% followed by 50 min re-equilibration) and directly sprayed on to Orbitrap Fusion using EasySpray source (ThermoFisher). Mass spectrometer was set to collect one MS1 scan (Orbitrap; 120K resolution; AGC target 2x105; max IT 100 ms) followed by data-dependent, "Top Speed" (3 seconds) MS2 scans (collision induced

dissociation; ion trap; NCD 35; AGC 5x103; max IT 100 ms). For multinotch-MS3, top 10 precursors from each MS2 were fragmented by HCD followed by Orbitrap analysis (NCE 55; 60K resolution; AGC 5x104; max IT 120 ms, 100-500 m/z scan range).

Data analysis: Proteome Discoverer (v2.3; ThermoFisher) was used for data analysis. MS2 spectra were searched against UniProt homo sapien database (release 2019-06-20; 20353 sequences) using the following search parameters: MS1 and MS2 tolerance were set to 10 ppm and 0.6 Da, respectively; carbamidomethylation of cysteines (57.02146 Da) and TMT labeling of lysine and N-termini of peptides (229.16293 Da) were considered static modifications; oxidation of methionine (15.9949 Da) and deamidation of asparagine and glutamine (0.98401 Da) were considered variable. Identified proteins and peptides were filtered to retain only those that passed ≤1% FDR threshold. Quantitation was performed using high-quality MS3 spectra (Average signal-to-noise ratio of 6 and <40% isolation interference).

Statistics

Experiments were conducted with technical and biological replicates at an appropriate sample size, as estimated by our prior experience. An unpaired Student t-test (two-tailed) was used for statistical evaluation of data between two groups, using a statistical software package (GraphPad Prism). Bars and error bars represent the mean and SEM respectively. Survival curves were plotted using Kaplan-Meier estimates. The Mann-Whitney U-test was used for statistical analysis of GVHD clinical scores, and the Mantel-Cox log-rank test was used to analyze survival data. P values <0.05 were considered significant: *p<0.05, **p<0.01, ***p<0.001, and ****p<0.0001. Sample sizes and statistical tests used are detailed in each figure legend.

2.4 Results

2.4.1 T cells demonstrate ER dilation following activation

We first sought to examine ER morphology following T cell activation. To do this, we examined naive WT T cells by transmission electron microscopy (TEM) before and after activation with αCD3 and αCD28 antibodies, and analyzed rough ER size in a blinded manner. Unstimulated T cells exhibited narrow cisternae of the rough ER typical of resting cells. Upon activation, the rough ER demonstrated a significant dilation of the cisternae (**Figure 2.1a**). This change was associated with increased induction of the ER stress-associated genes *Eif2a*, *Atf6a*, *Grp94,* and *Bip* (**Figure 2.1b**).

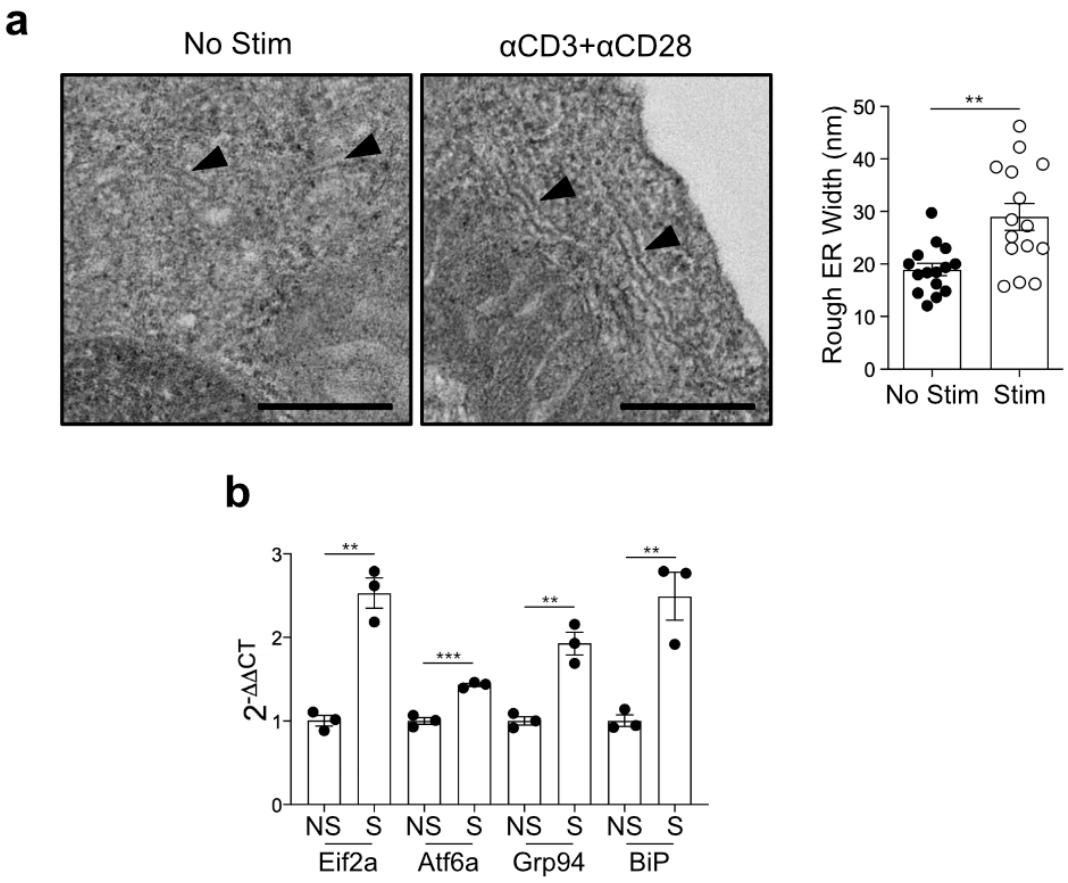

Figure 2.1 Murine T cells exhibit expansion of the rough ER cisternae and upregulation of the unfolded protein response following activation

(**a**) Transmission electron micrographs of WT murine T cells that received no stimulation, or stimulation with αCD3 and αCD28 for 3 days. Measurements of rough ER widths were taken from three different ERs from five cells in each group (n=15). Scale bar = 100 nm. (**b**) qRT-PCR analysis of ER stress-associated genes in WT murine T cells that received no stimulation, or 24 h stimulation with αCD3 and αCD28 (n=3). Data are mean ± SEM, : **p < 0.01, ***p < 0.001, (two-tailed unpaired Student's t-test).

2.4.2 A mouse model for studying SEC23B deficiency in murine T cells

We next hypothesized that the increase in ER size following T cell activation may reflect an upregulation of proteins that traffic from the ER and depend on COPII vesicles for export to the ERGIC and Golgi compartment. To test this, we examined the consequence of abrogating COPII-dependent protein transport following naive T cell activation. To this end, we generated *Sec23b*$^{fl/-}$ *Vav1*^{Cre} mice which carry a hematopoietic cell-specific SEC23B deficiency (**Figure 2.2a**). We also generated *Sec23b*$^{fl/-}$ *Cd4*^{Cre} mice which harbor a T cell-specific deficiency in SEC23B (**Figure 2.2a**). The addition of another mouse model added rigor to our findings, and helped rule out potential confounding factors from the absence of SEC23B in other hematopoietic cells. Of note, WT murine T cells expressed both paralogs, but harbored a greater baseline level of SEC23B than SEC23A. The relative expression of paralogs was corrected for affinity of our western blot antibodies via analysis of their binding to GFP-tagged SEC23B and SEC23A. Using these antibodies, we confirmed the selective downregulation of SEC23B in both models by western blot and observed no significant differences in SEC23A expression (**Figure 2.2b**).

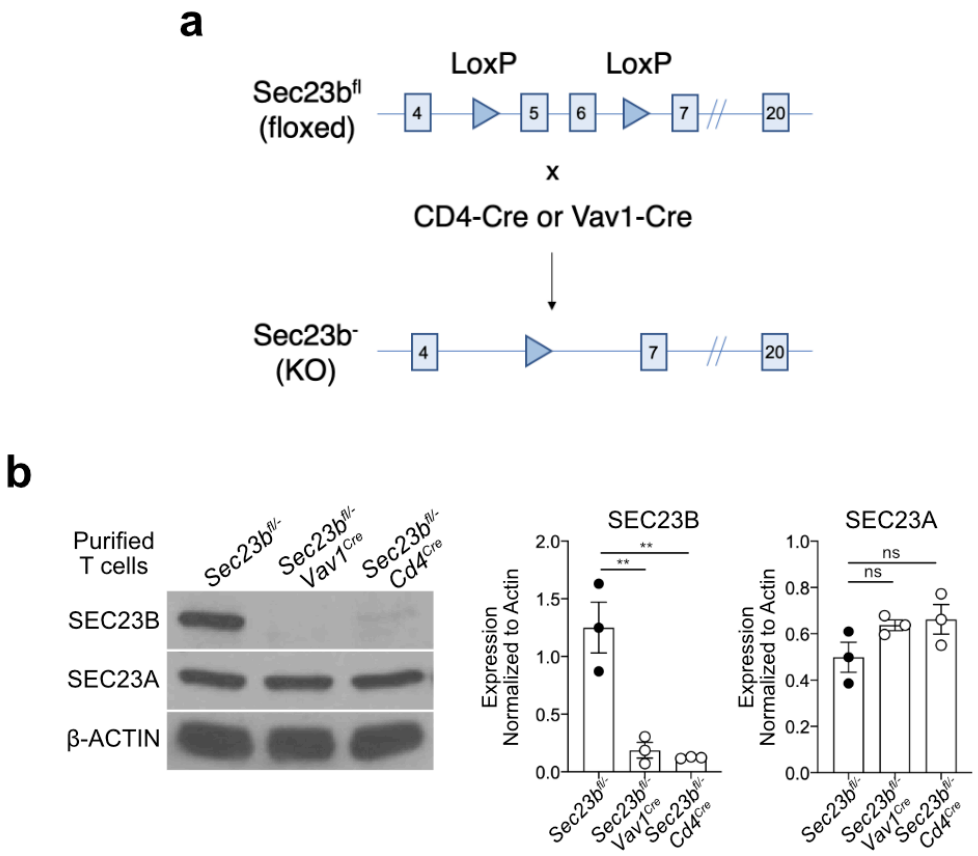

Figure 2.2 Characterization of the T cells derived from conditional *Sec23b* KO mouse models

(a) Breeding of mice carrying *Sec23b-floxed* alleles with mice that express Cre-recombinase driven by the Cd4 or Vav1 promoter results in a conditional excision in *Sec23b* exons 5 and 6 in T cells and hematopoietic cells respectively that results in a frameshift mutation and the presence of a stop codon in exon 7[78] (**b**) Western blots showing protein levels of SEC23B, SEC23A, and β-actin in *Sec23b*$^{fl/-}$ *Cd4*^{Cre} T cells relative to *Sec23b*$^{fl/-}$ controls. Densitometric analysis on the right plot indicates normalized levels of SEC23A and SEC23B relative to β-actin expression (n=4). Data are mean ± SEM: **p < 0.01, (two-tailed unpaired Student's t-test).

We reasoned that in the absence of SEC23B, T cells would demonstrate a greater increase in dilation of the rough ER cisternae secondary to accumulation of COPII cargo proteins. Compared with *Sec23b*$^{fl/-}$ controls, *Sec23b*$^{fl/-}$ *Cd4*^{Cre} T cells displayed significantly distended rough ER as shown by TEM, both when unstimulated, and following stimulation with αCD3 and αCD28 antibodies (**Figure 2.3**). Similar results were observed in *Sec23b*$^{fl/-}$ *Vav1*^{Cre} T cells (data not

shown). These data suggest that T cells depend on adequate levels of SEC23B for secretory proteins to exit the ER.

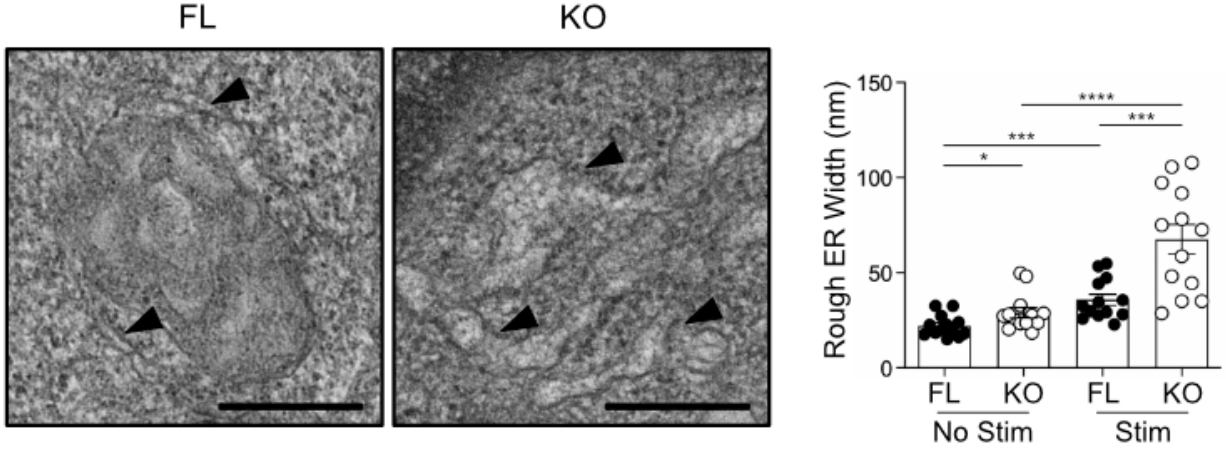

Figure 2.3 TEM reveals increased ER dilation in activated T cells in the absence of Sec23b

TEM highlighting an increase in rough ER dilation in *Sec23b*$^{fl/-}$ *Cd4*^{Cre} T cells when compared with *Sec23b*$^{fl/-}$ controls following activation with αCD3 and αCD28 for 3 days (n=15). Scale bar = 100 nm in representative micrographs. Data are mean ± SEM, :*p < 0.05, ***p<0.001, and ****p < 0.0001 (two-tailed unpaired Student's t-test).

2.4.3 SEC23B KO does not affect mature T cell development but regulates its secretome

Because SEC23B-dependent COPII formation appeared to be essential for the efficient egress of proteins from the ER in activated T cells, we next determined whether SEC23B was critical for T cell development *in vivo*. We examined both *Sec23b*$^{fl/-}$ *Cd4*^{Cre} and *Sec23b*$^{fl/-}$ *Vav1*^{Cre} models and found that absolute numbers and ratios of thymic subsets (double negative, double positive, single positive) and the various mature T cell subsets from spleen and lymph nodes from both models were similar when compared to age matched WT animals, suggesting that the deficiency of *Sec23b* did not affect T cell development (**Figures 2.4 and 2.5**).

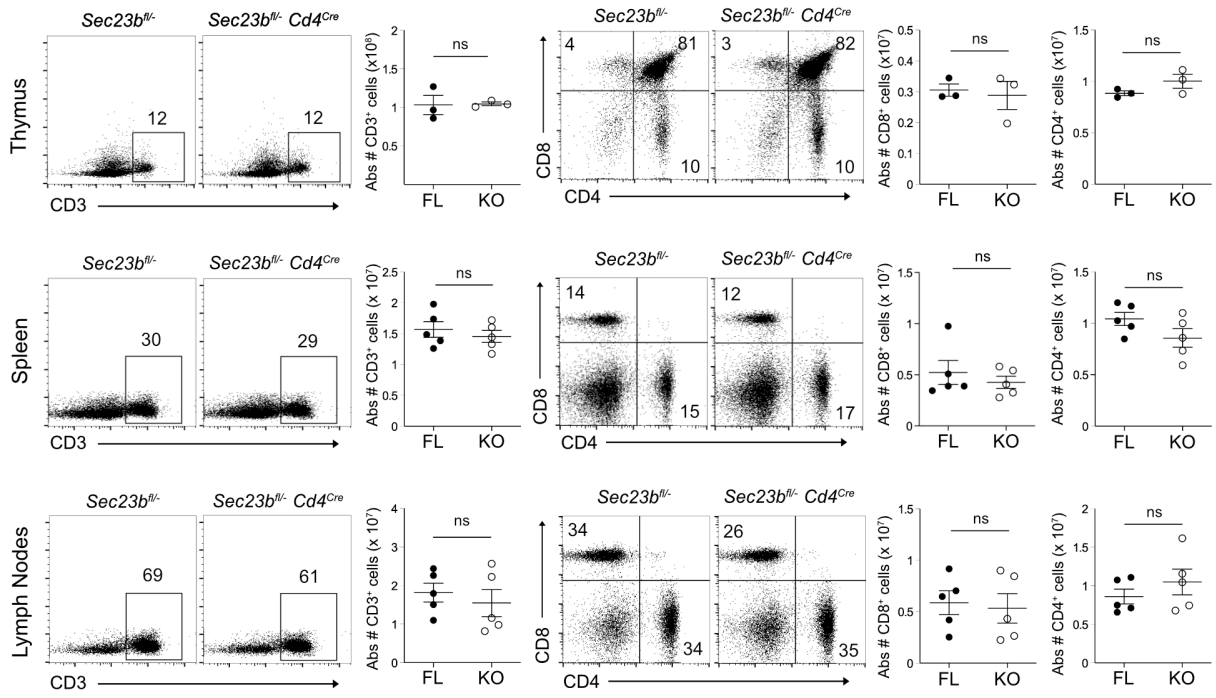

Figure 2.4 Mature T cell development in *Sec23b$^{fl/-}$ Cd4^{Cre}* mice

Percentages and absolute numbers of *Sec23b$^{fl/-}$* (FL) and *Sec23b$^{fl/-}$ Cd4^{Cre}* (KO) CD3$^+$ T cells in whole thymus (n=3), spleen (n=5), and lymph node (n=5) homogenate samples (left), and those of CD4$^+$ and CD8$^+$ T cell subsets gated on CD3$^+$ cells (right). Significance was determined by two-tailed unpaired Student's t-test, and ns is $p > 0.05$.

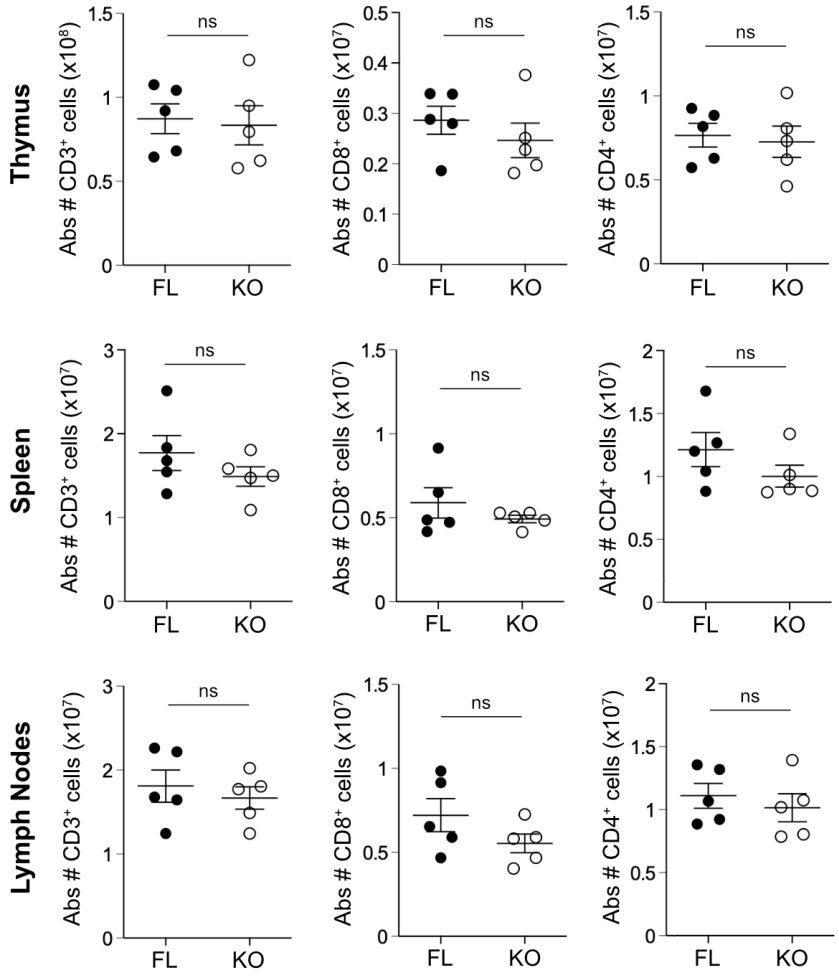

Figure 2.5 Mature T cell development in *Sec23b*$^{fl/-}$ *Vav1*^{Cre} mice

Absolute numbers of CD3$^+$ T cells and CD4$^+$ and CD8$^+$ T cell subsets gated on CD3$^+$ cells derived from whole thymus, spleen, and lymph node homogenate samples from *Sec23b*$^{fl/-}$ *Vav1*^{Cre} (KO) compared to *Sec23b*$^{fl/-}$ (FL) littermates (n=5 for all). Significance was determined by two-tailed unpaired Student's t-test, and ns is $p > 0.05$.

We next tested whether disrupting SEC23B-mediated COPII formation would impact the profile of T cell secreted proteins following their activation. To enable high-throughput identification of secreted proteins, we analyzed the T cell secretome with LC-MS/MS. We stimulated WT and *Sec23b*$^{fl/-}$ *Cd4*^{Cre} naive T cells with αCD3 and αCD28, and enriched the protein fraction in the supernatant for mass spectrometric analysis. Activated *Sec23b*$^{fl/-}$ *Cd4*^{Cre} T cell

supernatants exhibited a gross reduction in the amount of secreted proteins when compared with WT T cells. Among the reduced secreted proteins were those involved in the inflammatory response such as IFNγ (**Figure 2.6a**). Next, we validated the protein secretion pattern by focusing on cytokines utilizing a multiplex assay, and confirmed decreased levels of IFNγ and other cytokines such as IL-2 and TNFα in SEC23B-deficient T cell supernatants. Of note, the secretion of a few other cytokines by SEC23B-deficient T cells were similar to that by WT T cells, indicating that reduced secretion of cytokines by COPII deficient T cells was not a global phenomenon (**Figure 2.6b**).

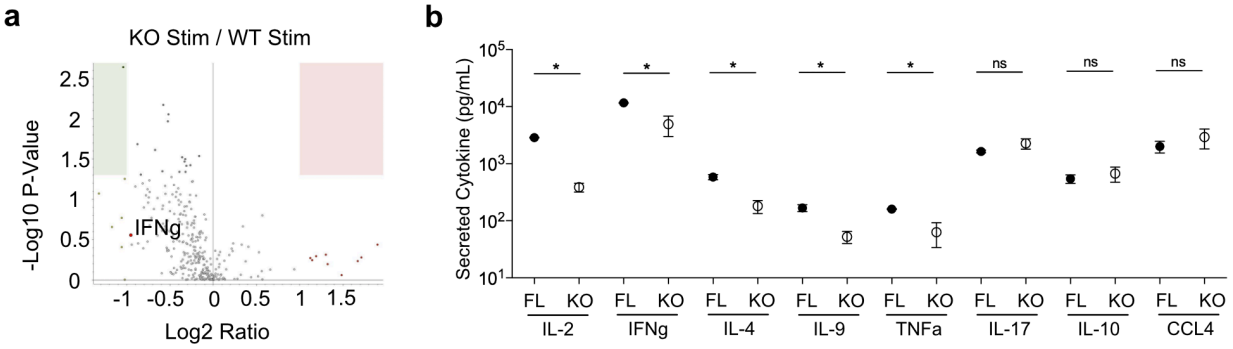

Figure 2.6 Targeting SEC23B regulates the T cell secretome

(**a**) Volcano plot representing 3 biological replicates of SEC23B-deficient T cell secretomes after 24 h of stimulation compared with WT. Log2 ratios were calculated based on p-values. (**b**) Luminex panel showing mean cytokine levels derived from *Sec23b*$^{fl/-}$ (FL) and *Sec23b*$^{fl/-}$ *Cd4*^{Cre} (KO) T cell supernatants following 3 days of stimulation with αCD3 and αCD28. Plots represent mean ± SEM, with *$p < 0.05$ (two-tailed unpaired Student's t-test).

2.4.4 Deficiency of SEC23B-dependent COPII leads to accumulation of secreted proteins

The reduction in secreted proteins we observed could be secondary to differences in activation of T cells in the absence of SEC23B. Therefore, we next analyzed whether the reduction in the secretome was secondary to defects in T cell activation. When compared to WT T cells,

Sec23b$^{fl/-}$ *Cd4*^{Cre} T cells expressed similar levels of surface TCRβ (**Figure 2.7a**) and phosphorylated TCR signaling components such as ZAP-70 and ERK1/2 (**Figure 2.7b**) following activation. Furthermore, *Sec23b*$^{fl/-}$ *Cd4*^{Cre} T cells expressed similar levels of the activation marker CD69 after stimulation (**Figure 2.7c**). These data suggest that abrogating SEC23B-dependent COPII formation does not affect TCR activation.

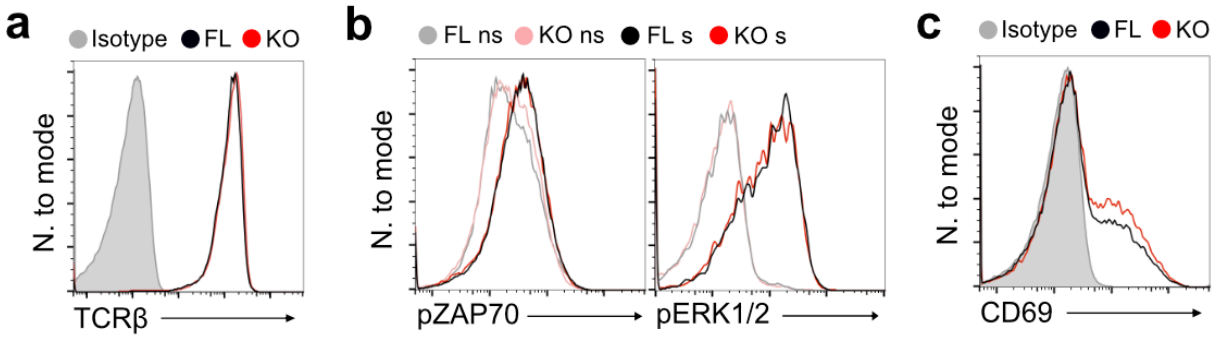

Figure 2.7 The absence of SEC23B does not impair T cell activation

(**a**) Histograms based on flow cytometry of surface TCRβ on *Sec23b*$^{fl/-}$ and *Sec23b*$^{fl/-}$ *Cd4*^{Cre} T cells relative to isotype levels present on naive unstimulated WT T cells. (**b**) Flow cytometry of phosphorylated ZAP70 and ERK1/2 molecules in *Sec23b*$^{fl/-}$ and *Sec23b*$^{fl/-}$ *Cd4*^{Cre} T cells that received no stimulation, or stimulation with αCD3 and αCD28 for 30 min. (**c**) Flow cytometry of surface CD69 present on *Sec23b*$^{fl/-}$ and *Sec23b*$^{fl/-}$ *Cd4*^{Cre} T cells stimulated with αCD3 and αCD28 for 6 h compared to isotype levels present on naive unstimulated WT T cells.

We next determined whether the reduction of secreted proteins in the supernatants is secondary to defects in protein synthesis, with a focus on IL-2. SEC23B-deficient T cells expressed normal levels of IL-2, as well as IL-10 and TNFα , at the mRNA level post-stimulation with αCD3 and αCD28 (**Figure 2.8**), suggesting that T cell activation was intact, and that the SEC23B-deficient T cells were able to produce, but unable to secrete, IL-2.

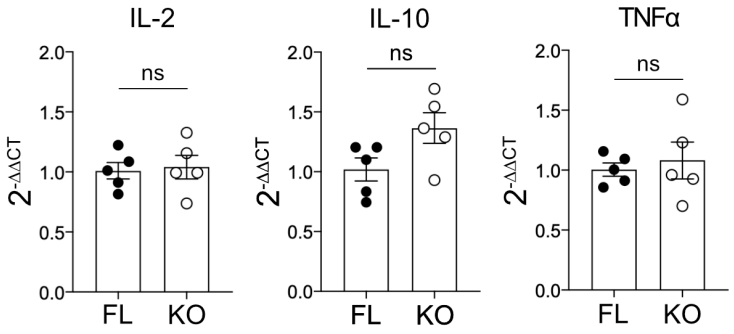

Figure 2.8 Transcription of cytokines is normal in the absence of SEC23B

qRT-PCR of IL-2, IL-10, and TNFα in SEC23B-deficient T cells compared to WT following stimulation with αCD3 and αCD28 for 4 days (n=5/group). Plots represent mean ± SEM, with ns $p > 0.5$ (two-tailed unpaired Student's t-test).

To confirm this, we stimulated cytokine production in T cells with phorbol 12-myristate 13-acetate (PMA) and ionomycin in the presence or absence of Brefeldin A (BFA), an inhibitor of anterograde transport between the ER and Golgi apparatus[99]. In the presence of BFA, both WT and SEC23B-deficient T cells demonstrated similar levels of intracellular IL-2 following activation (**Figure 2.9a**), suggesting that the absence of SEC23B does not impact IL-2 protein synthesis. By contrast, in the absence of BFA, WT T cells contained less intracellular IL-2 than in the presence of BFA, suggesting that some intracellular IL-2 was secreted by WT T cells in a COPII-dependent manner. However, in SEC23B-deficient T cells, the intracellular levels of IL-2 remained high despite the absence of BFA in culture (**Figure 2.9a**).

To further confirm SEC23B expression levels and to localize IL-2 intracellularly, we examined T cells by immunofluorescence confocal microscopy. T cells lacking SEC23B displayed greater accumulation of intracellular IL-2 when compared with WT cells, and importantly, in WT cells, IL-2 co-localized with SEC23B (**Figure 2.9b**). We also stained IL-2 with Calnexin, an ER-localized chaperone protein, and observed overlapping fluorescence (**Figure 2.10**). Together, these

data demonstrate that SEC23B-dependent COPII-mediated ER-to-Golgi transport is critical for the release of T cell secreted proteins such as IL-2.

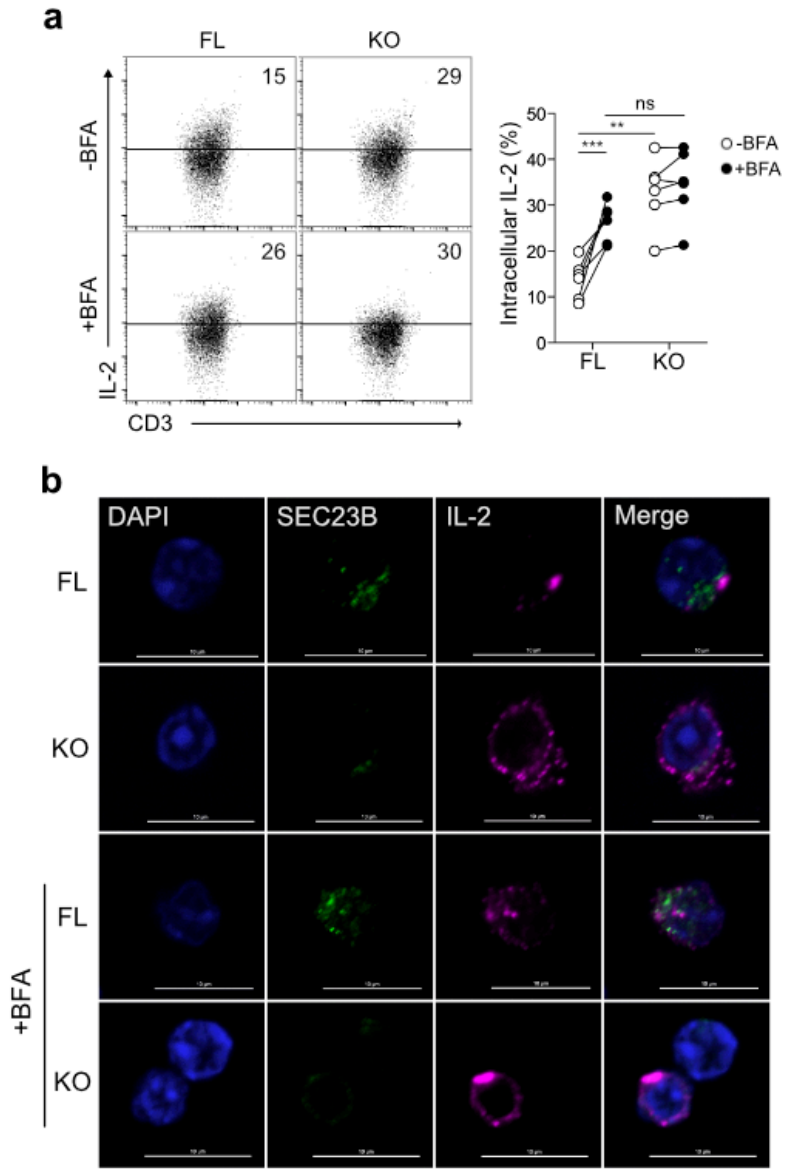

Figure 2.9 Deficiency of SEC23B leads to accumulation of IL-2 intracellularly

(**a**) Flow cytometry measuring intracellular IL-2 levels. T cells were stimulated with αCD3 and αCD28 for 3 days followed by a 5 h stimulation with PMA and ionomycin in the presence or absence of BFA (n=6/group). (**b**) Immunofluorescence confocal micrographs of SEC23 (green) and IL-2 (pink) in WT or SEC23B-deficient T cells after 3 day αCD3 and αCD28 stimulation, and 5 h PMA and ionomycin stimulation with or without BFA. Data are mean ± SEM, $^{**}p < 0.01$, $^{***}p < 0.001$ (two-tailed unpaired Student's t-test).

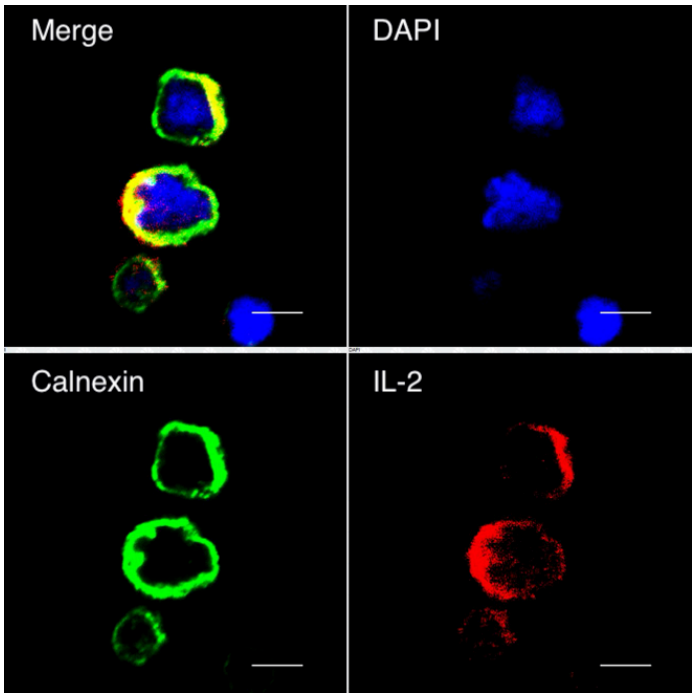

Figure 2.10 IL-2 co-localizes with Calnexin in WT T cells

(**a**) Immunofluorescence confocal micrographs of Calnexin (green) and IL-2 (red) in WT T cells after 3 day αCD3 and αCD28 stimulation, and 5 hour stimulation with PMA and ionomycin in the presence of Brefeldin A.

2.4.5 SEC23B-dependent COPII regulates naive T cell functions in vitro

Given the importance of cytokine secretion for T cell-mediated functions, we next investigated the functional consequences of abrogating the COPII pathway in T cells. Because of the differential effects observed on cytokine release, we first determined the impact of SEC23B deficiency on the ability of naive $CD4^+$ T cells to differentiate into helper T subsets. Helper T cell differentiation is plastic and subject to the surrounding cytokine milieu. Differentiating cytokines serve as signals to induce different programs of transcription that lead to the development of Th subsets[100]. When cultured in polarizing media, naive *Sec23b*$^{fl/-}$ *Cd4*^{Cre} $CD4^+$ T cells exhibited a normal capacity to differentiate into T_H1, T_H2, and T_H17 cells as measured by lineage-specifying transcription factors T-bet, GATA3, and RORγt respectively (**Figure 2.11**).

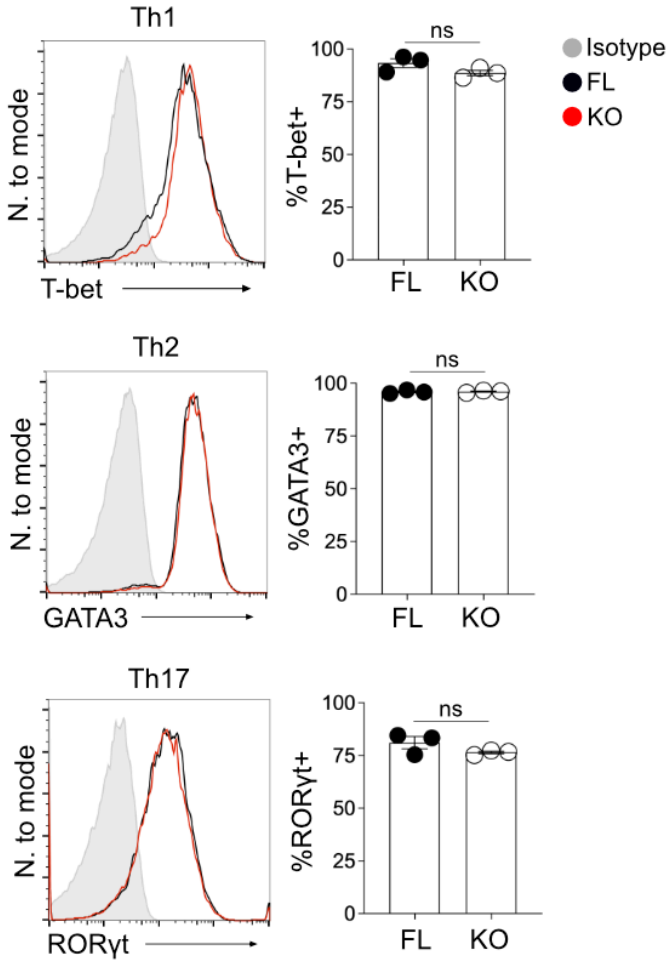

Figure 2.11 Absence of SEC23B does not impair capacity for T_H cell differentiation

Overlay of histograms based on flow cytometry plots indicating expression of intracellular T-bet, GATA3, and RORγt compared to isotype controls in WT and SEC23B-deficient naive $CD4^+$ T cells that were cultured in media containing T_H1, T_H2, and T_H17-polarizing cytokines respectively (n=3). Plots represent mean ± SEM, with ns $p > 0.5$ (two-tailed unpaired Student's t-test).

We next analyzed the impact of SEC23B deficiency on T cell proliferation *in vitro*. T cells were stimulated with αCD3 and αCD28 for 3 days following staining with carboxyfluorescein diacetate succinimidyl ester (CFSE). CFSE is a fluorescent dye that non-specifically and covalently binds to cellular proteins. Proliferation of CFSE-stained T cells can thus be measured by a dilutional decrease in fluorescence intensity by flow cytometry with each cell division[101]. As

measured by CFSE dilutions, SEC23B-deficient T cells exhibited reduced proliferative capacity when compared with WT T cells (**Figure 2.12a**). Proportions of Annexin V and 7-AAD were similar in SEC23B-deficient and WT T cells (**Figure 2.12b**), suggesting that this observation was primarily due to defects in proliferation and not secondary to increased cell death. We next examined whether the proliferation defect was secondary to decreased COPII-dependent secretion of proteins such as IL-2, a critical T cell growth factor. The addition of exogenous recombinant murine IL-2 partially corrected the proliferation defect *in vitro*, suggesting that the altered secretome, and specifically the release of IL-2, contributed only in part to the reduction in proliferation (**Figure 2.12a**). Taken together, these data demonstrate that SEC23B regulates *in vitro* T cell proliferation, but not differentiation.

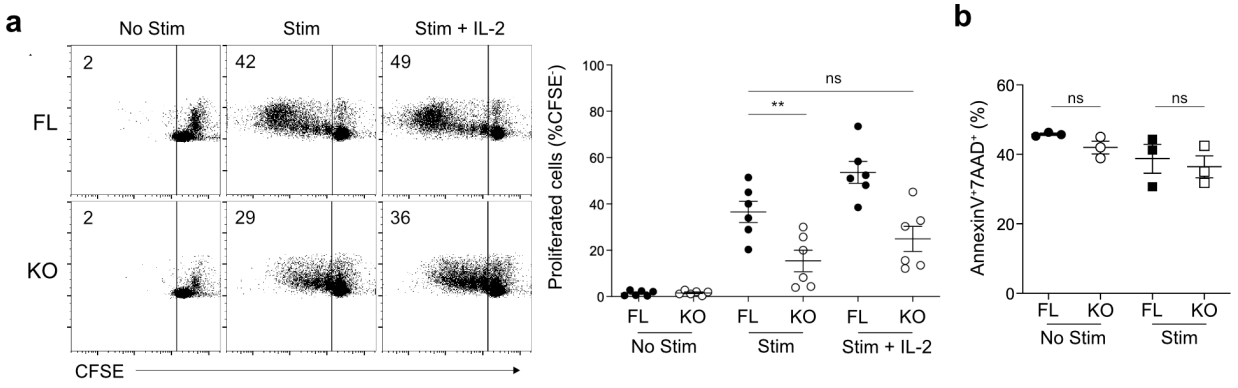

Figure 2.12 SEC23B KO T cells exhibit a proliferative defect *in vitro* that is partially rescued by the addition of exogenous IL-2

(**a**) Proliferative capacity of WT and SEC23B-deficient T cells as measured by CFSE dilutions *in vitro* (n=6/group). Partial rescue of proliferation upon addition of exogenous murine IL-2 in T cells stimulated with αCD3 and αCD28 for 3 days (n=6/group). (**b**) Cell death as measured by Annexin V and 7AAD staining (n=3/group) in SEC23B-deficient T cells compared to WT following stimulation by αCD3 and αCD28 for 3 days.

2.4.7 SEC23B-dependent COPII regulates T cell alloimmunity in experimental models of acute GVHD

To determine the relevance of SEC23B-dependent effects on T cells *in vivo*, we utilized a well-defined model of T cell stimulation, experimental allogeneic hematopoietic stem cell transplantation (allo-HCT). We hypothesized that SEC23B deficiency in donor T cells would show reduced proliferation and confer reduced pathogenicity in the clinically relevant major histocompatibility-mismatched [C57BL/6J→BALB/c] model of allo-HCT. WT or SEC23B-deficient CFSE-stained T cells were first transferred to allogeneic BALB/c mice that received total body irradiation (TBI) on day -1, and recipient spleens were analyzed 3 days post-transplant. Allogeneic SEC23B-deficient T cells proliferated significantly less than WT T cells and significantly lower numbers were recovered in the spleen (**Figure 2.13**), demonstrating an *in vivo* proliferative defect similar to *in vitro* responses.

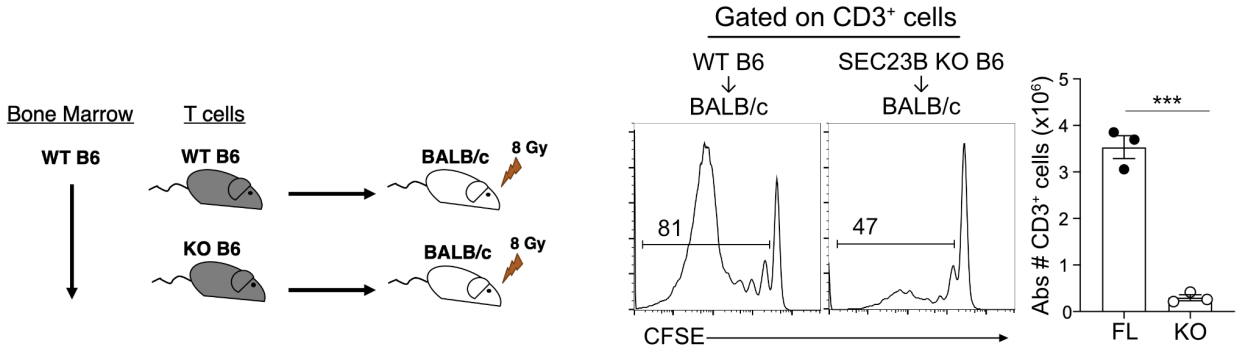

Figure 2.13 SEC23B KO T cells exhibit a proliferative defect *in vivo* in allogeneic recipients

Schematic of BMT donor and recipient pairings, and *in vivo* proliferative capacity of SEC23B-deficient T cells compared with WT as measured by CFSE dilutions following their transfer into allogeneic BALB/c recipient mice. Decreased proliferation was observed with reduced absolute numbers of SEC23B-deficient T cells in the spleen (n=3/group). Significance determined by two-tailed unpaired student's t-test ***$p < 0.001$.

Donor T cells are essential for driving Graft-versus-Host Disease (GVHD) in recipient mice[23,24], and the network of cytokines secreted by T cells are both important in the initiation and maintenance of GVHD[22]. To test whether the proliferative defect of SEC23B-deficient T cells impacted its pathogenicity *in vivo*, we assessed their ability to drive murine GVHD[17,102]. Specifically, C57BL/6J WT bone marrow combined with either C57BL/6J WT or SEC23B-deficient T cells were transferred into allogeneic BALB/c and syngeneic C57BL/6C recipient mice (**Figure 2.14a**). All recipients of syngeneic T cells survived, while all recipients of allogeneic WT T cells died by 9 weeks post-transplant (**Figure 2.14a**). However, recipients of allogeneic SEC23B KO T cells demonstrated a dramatic improvement in survival with only 6% mortality. Clinical GVHD scores in these recipients were significantly lower than those of recipients of WT T cells during the post-transplant period (**Figure 2.14a**). To rule out strain-dependent artifacts, we next corroborated these data in a second MHC matched and minor histocompatibility-mismatched model of allo-HCT using C3H.SW recipients [C57BL/6J→C3H.SW] (**Figure 2.14b**). Together, our data demonstrate a critical *in vivo* requirement for SEC23B in T cells, and suggest that targeting it may have salutary effects in T cell dependent immune pathologies.

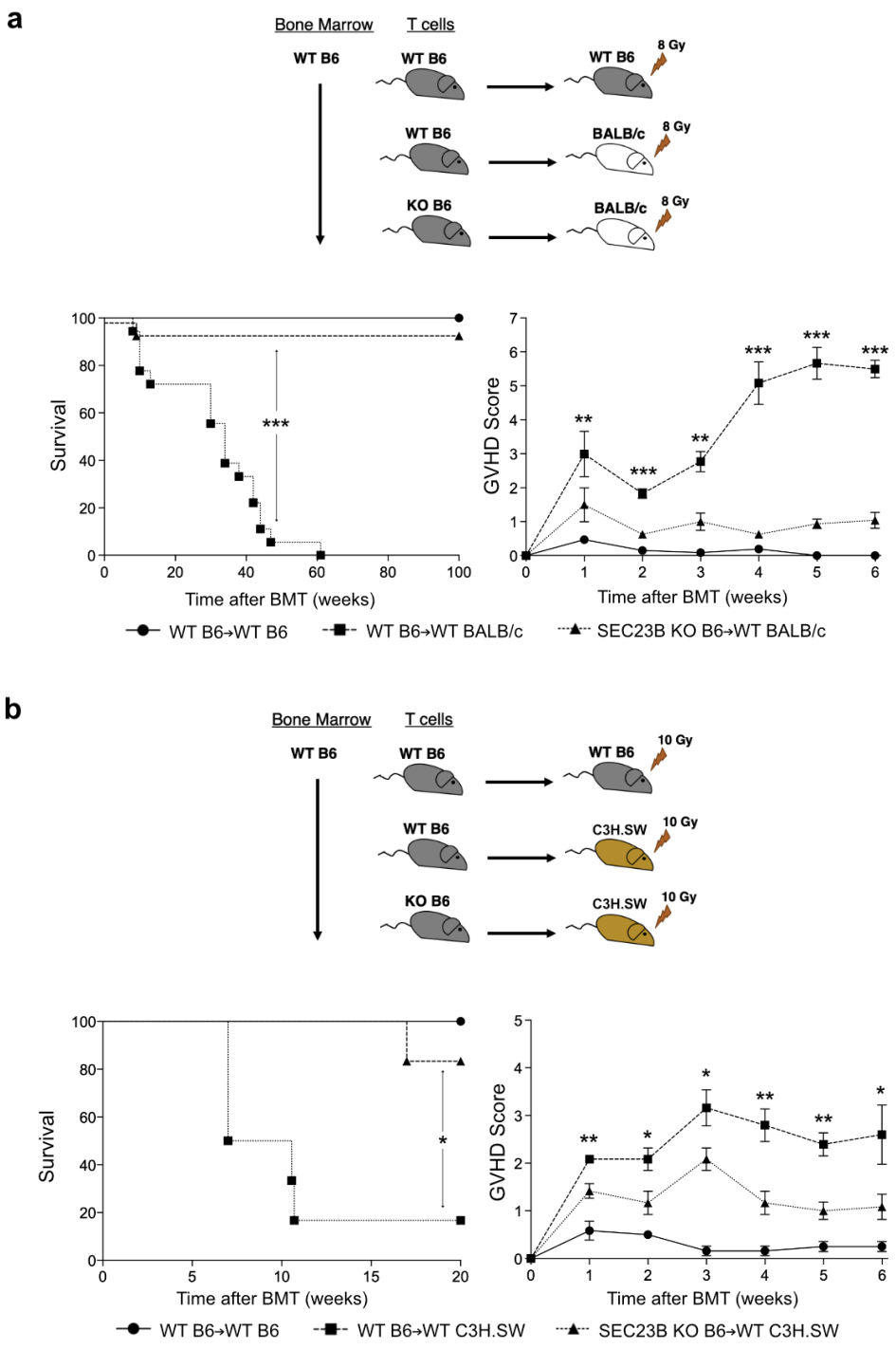

Figure 2.14 SEC23B KO T cells demonstrate reduced GVHD pathogenicity

(**a,b**) Survival and GVHD scores of mice that received syngeneic T cell-depleted bone marrow, and T cells from either syngeneic donors, allogeneic WT C57BL/6J donors, or allogeneic *Sec23b*$^{fl/-}$ *Cd4*^{Cre} C57BL/6J donors. Allogeneic recipients were BALB/c (**a**) or C3H.SW (**b**) strain. (**a,b**) Significance was determined by Mantel-Cox log rank test.

2.4.6 SEC23B-dependent COPII regulates T cell-mediated antiviral immunity

We also tested whether the absence of SEC23B affects T cell-dependent protective immune responses *in vivo*. To do this, we measured T cell-mediated antiviral immunity in LCMV Armstrong-infected mice. Following infection and interaction with viral foreign antigen, T cells undergo clonal expansion and differentiate into diverse subsets which carry out specialized effector functions[103]. A characteristic response to a primary viral infection involves three phases: expansion, contraction, and memory. Upon presentation of viral antigen with co-stimulatory and cytokine signals, T cells undergo rapid clonal expansion. Cytotoxic T cells target infected cells and secrete cytokines including IFNγ, TNFα, and IL-2 which further promote antiviral immunity[104-106]. Following a decrease in viral load and clearance of the pathogen, most antigen-specific cells undergo cell death while a subset of memory T cells persist and provide long-term immunity against a secondary challenge[107-110].

We infected *Sec23b*$^{fl/-}$ or *Sec23b*$^{fl/-}$ *Cd4*^{Cre} mice with 2x10^5 p.f.u. of LCMV Armstrong i.p., and harvested tissue samples for analysis on day 8, which represents the time point at which LCMV Armstrong is cleared in WT mice but before antigen-specific T cells undergo full contraction (**Figure 2.15a**). We performed tetramer staining to detect LCMV-specific CD8$^+$ T cells by their binding to peptide GP33, and CD4$^+$ T cells by their specificity for GP66. By day 8 post-infection, both virus-specific CD8$^+$ and CD4$^+$ T cells were reduced in *Sec23b*$^{fl/-}$ *Cd4*^{Cre} mice when compared with WT in the spleen (**Figure 2.15b**). To confirm this was not a tetramer-specific artefact, we also tested for CD8+ T cells specific for GP276, and observed the same trend (data not shown). The absence of viral peptide-specific T cells was observed in additional tissues including peripheral blood mononuclear cells (PBMCs), lung, liver (**Figure 2.15c**). This was accompanied by a reduction in CD8$^+$ T cells that produced IFNγ and TNFα (**Figure 2.15d**). Immunocompetent

mice clear the virus at by day 8 post-infection. However, at this timepoint *Sec23b*$^{fl/-}$ *Cd4*^{Cre} mice exhibited a failure to clear serum viral load, indicating loss of a normal antiviral immune response (**Figure 2.15e**).

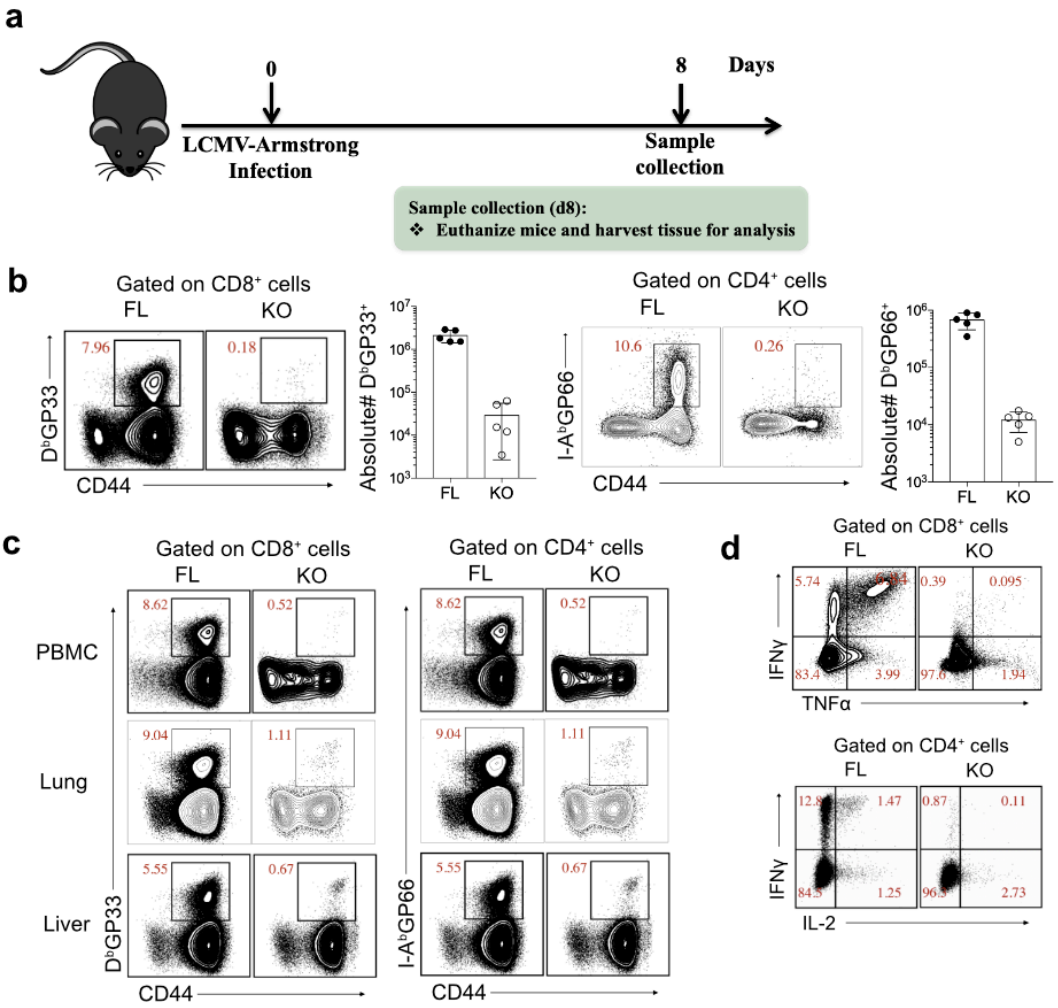

Figure 2.15 *Sec23b*$^{fl/-}$ *Cd4*^{Cre} mice exhibit reduced antiviral immunity following LCMV Armstrong infection

(**a**) LCMV Armstrong injection experimental setup (**b**) Representative flow plots gated on CD8$^+$ and CD4$^+$ T cells harvested day 8 post-infection from spleens of *Sec23b*$^{fl/-}$ (FL) and *Sec23b*$^{fl/-}$ *Cd4*^{Cre} (KO) mice that received 2x10^5 p.f.u. of LCMV Armstrong i.p. Activation was measured by CD44, and percentage of antigen-specific CD8$^+$ and CD4$^+$ T cells was detected with tetramers against GP33 and GP66 respectively. Absolute numbers of LCMV-specific CD8$^+$ and CD4$^+$ T cells are quantified on the right. (**c**) Additional flow plots indicating percentage of LCMV-specific T cells in PBMCs, Lung, and Liver. (**d**) Proportions of IFNγ and TNFα producing CD8$^+$ T cells present in the spleen (**e**) Viral titer day 8 post-infection measured in the serum. All measurements in *Sec23b*$^{fl/-}$ mice were below detection levels.

Next, we examined $CD4^+$ and $CD8^+$ T cell-dependent anti-viral processes. While $CD4^+$ T cells do not directly participate in the killing of infected cells, they provide critical helper functions. We used a peptide vaccination model that preferentially elicits $CD4^+$ T cell responses[111]. To do this, we immunized mice on day 0 with I-Ab restricted peptide GP_{61-80}. Following challenge on day 8, we harvested tissue for analysis on day 14 (**Figure 2.16a**). At this time point, absolute numbers of CD4+ T cells in the spleen were similar between *Sec23b*$^{fl/-}$ and *Sec23b*$^{fl/-}$ *Cd4*^{Cre} mice (**Figure 2.16b**). Furthermore, there was no difference in the proportions and absolute numbers of GP_{66}-specific CD4+ T cells (**Figure 2.16c**). These data did not elicit a difference in the $CD4^+$ T cell response, and altogether suggested $CD4^+$ T cells may produce normal immune responses *in vivo* in this system.

We therefore tested the requirement for SEC23B in $CD8^+$ T cells. To do this, we utilized an intracerebral (i.c.) LCMV Armstrong infection model. In this model normal immunocompetent mice die approximately 7 days following intracerebral LCMV Armstrong infection coinciding with seizures, edema, and brain herniation. $CD8^+$ T cells are essential for the pathophysiology of this process and lethal disease, as $CD8^+$ T cell-deficient mice survive i.c. LCMV challenge (**Figure 2.16d**)[112-114]. As expected, all WT mice died by day 7 post-infection. However, all *Sec23b*$^{fl/-}$ *Cd4*^{Cre} mice survived and appeared healthy by day 14. revealing the critical role of SEC23B in the $CD8^+$ T cell response during the acute phase of viral infection (**Figure 2.16e**).

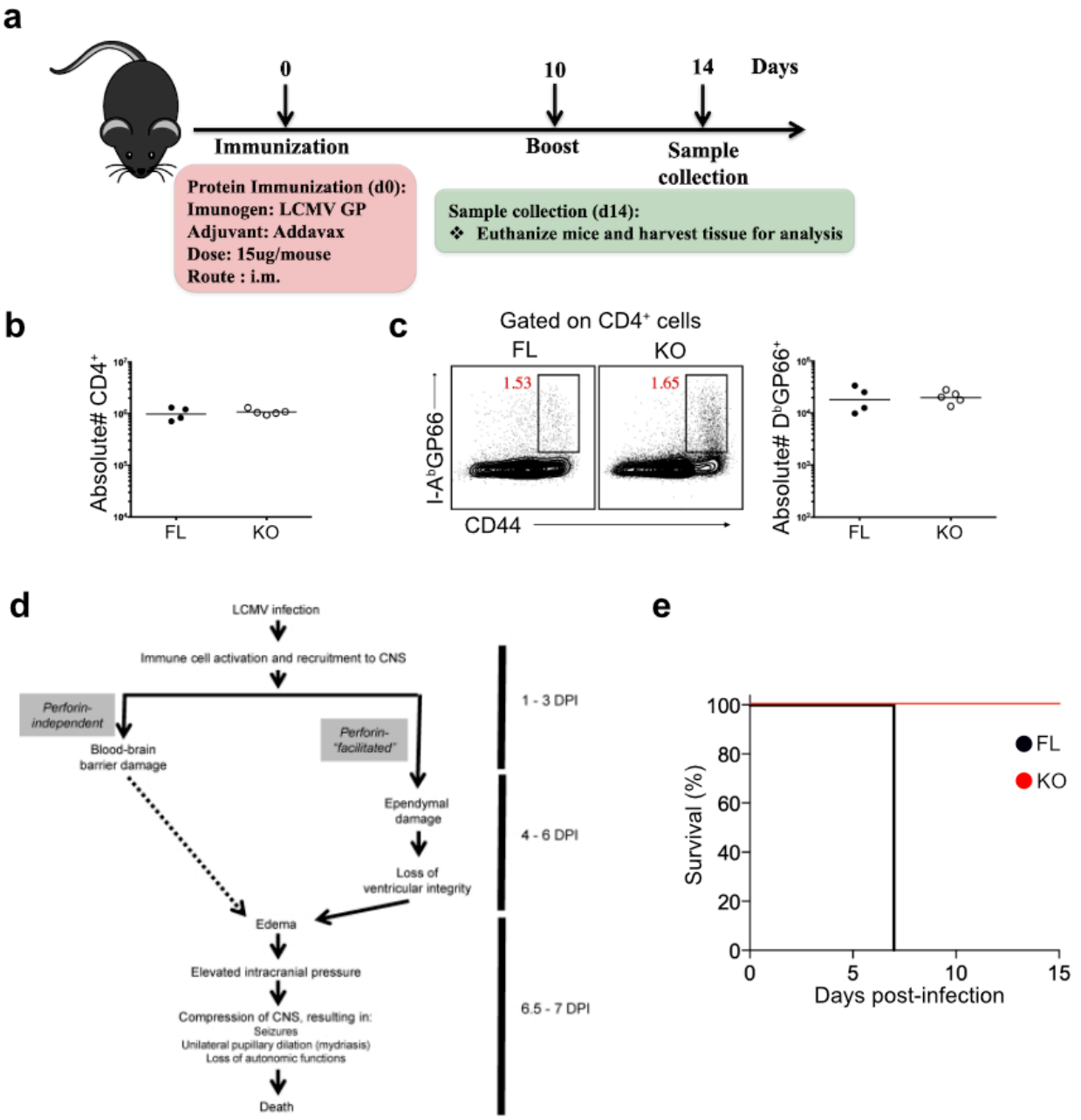

Figure 2.16 . *Sec23b*$^{fl/-}$ *Cd4*^{Cre} mice demonstrate reduced CD8^{+} T cell response following intracerebral LCMV-Armstrong infection

(**a**) Experimental setup for analyzing LCMV peptide vaccine-elicited response. (**b**) Absolute numbers of total CD4^{+} T cells present in the spleen on day 14 (n=5/group) (**c**) Representative flow plots indicated proportions and plot indicating absolute numbers of LCMV GP66-specific CD4^{+} T cells in the spleen (n=5/group). (**d**) Pathogenesis following i.c. LCMV Armstrong infection adapted from *Matullo et al*[112]. (**e**) Survival curve of *Sec23b*$^{fl/-}$ and *Sec23b*$^{fl/-}$ *Cd4*^{Cre} mice following infection i.c. (n=5/group).

2.5 Discussion

Taken together, our data demonstrate a critical role for COPII-mediated ER-to-Golgi transport in T cell immunity. Using genetically modified mice, we show that *Sec23b* mutation significantly alters the T cell secretome and impacts T cell proliferative and effector functions. Notably, we observed that the secretion of important T cell-derived factors including IL-2 is impacted by the loss of SEC23B, and that IL-2 is retained intracellularly when SEC23B is reduced. The observation that proximal TCR signaling events and transcription of secretory proteins are similar to WT in SEC23B-deficient T cells, combined with the observation that protein levels are increased intracellularly in these cells, suggests that production of these proteins is intact, but that their post-translational release is impaired.

The finding that the secretion of some cytokines but not others raises the question of specificity in the COPII pathway. Because murine T cells harbor both SEC23 paralogs, a possible explanation for the finding is that SEC23B and SEC23A mediate the secretion of a non-overlapping spectrum of secretory cargoes. SEC24 is considered the major COPII component that interacts with transmembrane cargos or cargo receptors. However, it remains open to consideration not to rule out SEC23 in this process, given its role in the COPII inner coat, the identification of multiple direct binding partners including SEC22 and TRAPPI, and the structural similarity between SEC23 and SEC24[43,115]. Chapter 3 builds on this observation using additional mouse models.

The analysis of the T cell secretome represented a novel endeavor in primary T cells, but it was met with technical challenges. This method allows for analysis of secreted proteins against the murine proteome database, and also enables the measurement of relative abundance changes among multiple samples in the same run, thus allowing for direct comparison of biological

replicates of WT and KO cultures. However, T cells in this experiment must be activated in serum-free media, as serum contamination reduces the ability to detect low abundance proteins. This is complicated by our observations as well as others' that activating T cells in the absence of serum greatly increases cell death, and the resulting cell lysis releases intracellular proteins into the supernatant[116]. To optimize this, we added bovine serum albumin (BSA) into T cell cultures which improved survival, and employed BSA depletion steps downstream of secretome collection. While we uncovered some known secreted proteins including IFNγ, others were possibly released into the sample by non-specific events such as cell lysis. In the future, it would be beneficial to revisit this experiment with further optimization of conditions that favor maximal secretion with cell viability, and employ more rigorous purification procedures, for example, by enriching for newly synthesized glycoproteins via metabolic marking and affinity purification methods[117].

Targeted analysis of the COPII pathway by specific deletion of SEC23B in T cells and hematopoietic cells provides insight into its role in specific cytokine secretion, and also raises additional questions. When we supplemented our T cell cultures with exogenous IL-2, T cell proliferation was rescued only partially, raising the likelihood that other T cell processes are also affected by *Sec23b* deletion and contribute to its overall impact. Thus, the net functional effects of disrupting *Sec23b* expression is likely a result of a reduction in the extracellular transport of effector molecules and growth factors such as IL-2, and the intracellular transport of proteins such as transcription factors, including but not limited to SREBPs. Our work exploring this is the topic of Chapter 4.

The secretion of inflammatory cytokines by T cells is central to the pathogenesis of multiple diseases, and we were able to examine two experimental models to test the ramifications of T cell-specific SEC23B deficiency *in vivo*. Our findings suggest the reduction of SEC23B-

dependent COPII formation is sufficient to significantly reduce morbidity and mortality related to GVHD in mice without affecting T cell development. These findings are dramatic, and future studies are needed to determine the full biological underpinnings of these differences. The use of both a major and minor mismatch model adds rigor to our findings.

In LCMV experiments, our data show a dramatic difference between WT and SEC23B KO mice. Our data demonstrate reduced absolute numbers of activated T cells and also reduced antigen-specific T cells that correlate with a defect in viral clearance. Our *in vitro* data would suggest that T cell activation is intact. Therefore, SEC23B-deficient T cells may exhibit a defect in clonal expansion following viral infection, or in this model system and at the specific day 8 time point analyzed, increased cell death may have occurred. Intracerebral infection with LCMV-Armstrong revealed suppression of the $CD8^+$ T cell response during the acute phase of viral infection, and we are planning follow up experiments to determine the mechanisms underlying this difference.

In future studies, examining the basis of the observed bias in select cytokine secretion may inform therapeutic applications. The notion that intracellular pathways for T cell secreted proteins including several but not all cytokines may present an opportunity to target SEC23 in COPII as a novel strategy to mitigate T cell-mediated pathologies such as GVHD in humans. Conversely, it is possible that enhancing COPII may increase T cell function as a therapeutic approach to other disorders.

CHAPTER 3

Insights into the Role of SEC23 Paralogs in T Cell Immunity

3.1 Abstract

The mammalian genome encodes for two SEC23 paralogs, SEC23A and SEC23B, which share 85% sequence identity at the amino acid level[43,56,118]. We sought to build on our observations in Chapter 2 that WT murine T cells express both paralogs, though SEC23B predominantly. We first generated *Sec23a*$^{fl/-}$ *Cd4*^{Cre} mice which lack SEC23A expression selectively in T cells. In contrast to our *Sec23b* KO model, *Sec23a* KO did not significantly affect T cell cytokine secretion or proliferation *in vitro*. We therefore tested whether SEC23B harbors unique functions in T cells, or if our observations could be attributed to the presence of greater baseline SEC23B in WT murine T cells. To do this, we examined T cells derived from *Sec23*$^{b\text{-}a/b\text{-}a}$ mice, which have been modified to express the *Sec23a* coding sequence in the *Sec23b* genomic locus. In these mice, SEC23A is expressed at the same level as total SEC23A and SEC23B. We found this modification restored T cell functions, indicating that the phenotypes we observed in our *Sec23b*$^{fl/-}$ *Cd4*^{Cre} mice were not specific to the loss of SEC23B. Rather, these observations may be a consequence of decreased overall COPII levels that does not occur to the same extent in *Sec23a*$^{fl/-}$ *Cd4*^{Cre} mice. Taken together, our data demonstrate that T cells harbor a tissue-specific bias for SEC23B in mice, as when either SEC23 paralog is expressed at adequate levels, T cell functions are normal both *in vitro* and *in vivo*.

3.2 Introduction

Mutations in *Sec23a* and *Sec23b* paralogs result in two different disorders in humans, Cranio-lenticulo-sutural dysplasia (CSLD)[64,65] and Congenital Dyserythropoietic Anemia Type II (CDAII)[67], respectively. Recent studies suggest that SEC23A and SEC23B are functionally complementary during development and have indistinguishable interactomes[57], but are expressed in a tissue- and species-specific manner, thus lending to distinct phenotypes in mice and humans when deficient or mutated[74,76-78]. In Chapter 2, we demonstrated that WT murine T cells express both SEC23A and SEC23B paralogs, and that SEC23B-deficient T cells maintained expression of SEC23A (**Figure 2.2b**). Despite the presence of SEC23A, however, the absence of SEC23B critically impacted T cell functions.

We therefore investigated mechanisms for the T cell defects in SEC23B-deficient T cells. Specifically, we focused on understanding the paralog specific roles and considered two mutually exclusive hypotheses: (a) SEC23B possesses independent functions that are not compensated for by SEC23A, or (b) as mature T cells express both SEC23B and SEC23A, the functional effect of *Sec23b* deletion is from a net loss of total SEC23. If the latter is true, we reasoned that increased expression of SEC23A, in the absence of SEC23B, to a total level of SEC23 similar to that present in WT would rescue T cell functions.

To test this, we used two genetically modified mouse models: $Sec23a^{fl/-}\ Cd4^{Cre}$ and $Sec23^{b\text{-}a/b\text{-}a}$ mice. $Sec23a^{fl/-}\ Cd4^{Cre}$ mice harbor floxed *Sec23a* alleles and express Cre-recombinase downstream of the *Cd4* promoter. They therefore achieve excision of *Sec23a* conditionally in T cells during their double positive stage of development, in which all thymocytes transiently express both CD4 and CD8. $Sec23^{b\text{-}a/b\text{-}a}$ mice express the *Sec23a* coding sequence (from C367 to A2298)

followed by a poly(A) termination signal within the *Sec23b* coding sequence as described previously[57].

In this chapter, we characterize T cells from these additional mouse models. First, we demonstrate that the absence of endogenous levels of SEC23A is not sufficient to impair T cell functions. We then show data to support the hypothesis that SEC23A can rescue T cell functions in the absence of SEC23B. Finally, we use an experimental model of allo-HCT to demonstrate that the patterns we observed *in vitro* are consistent in a T cell-dependent disease model *in vivo*. The data in this chapter advance our understanding of paralog specificity in T cell immunity and further illuminate the core COPII components required by T cells.

3.3 Materials and Methods

Mice

The generation of *Sec23b*$^{fl/-}$, *Sec23a*$^{fl/-}$, and *Sec23*$^{b\text{-}a/b\text{-}a}$ mice has been previously reported[57,76,78]. *Sec23b*$^{fl/-}$ and *Sec23a*$^{fl/-}$ mice were bred with *Cd4*^{Cre} (017336) or *Vav1*^{Cre} (008610) mice obtained from The Jackson Laboratory. Genotyping was performed using primers previously described[57,76,78]. C57BL/6C (027) and BALB/c (028) mice used as recipients in BMT experiments were obtained from Charles River Laboratories.

T cell isolation and in vitro cell culture

Primary murine T cells were purified by magnetic separation (Miltenyi Biotec) from single cell homogenates of spleens and lymph nodes, and cultured in cell media. T cells were cultured alone, or with 5 μg/mL αCD3 (145-2C11; Biolegend) and 2.5 μg/mL αCD28 (37.51; Biolegend) soluble antibodies for the specified timepoints. To measure proliferation, T cells were first labeled on day 0 with 5 μM CFSE (ThermoFisher) for 10 min at 37°C. Prior to analysis of cytokine production by intracellular flow cytometry, T cells were additionally stimulated on day 3 with PMA and ionomycin (Invitrogen) in the presence or absence of BFA (Biolegend) for 5 h at 37°C.

Flow cytometric analysis

Flow cytometric analysis was performed using fluorophore-conjugated antibodies to mouse CD3 (145-2C11), CD4 (GK1.5), CD8 (53-6.7), and IL-2 (JES6-5H4). For surface immunophenotyping, single cell suspensions were incubated with the relevant antibodies for 30 min at 4°C, washed, and fixed with 1% paraformaldehyde prior to analysis. Intracellular staining was performed following surface staining and fixation, in permeabilization buffer for 30 min at room temperature.

Western Blotting

Whole cell lysates obtained from purified T cells were fractionated by gel electrophoresis through a 10% Bis-Tris gel and transferred onto polyvinylidene difluoride membrane (Millipore) in a semi-dry transfer cell (Bio-Rad). Blots were blocked and stained in 5% nonfat milk in TBST, with primary antibodies against SEC23B and SEC23A[78], and anti-β-Actin (8226; Abcam). Incubation with secondary antibody conjugated to HRP (Santa Cruz) was performed for 2 h at room temperature. Blots were detected using the SuperSignal ECL substrate system (ThermoFisher), on a Konica SRX-101A film processor. Densitometric analysis was performed with ImageJ software.

Enzyme-linked immunosorbent assay (ELISA)

Supernatants from cell culture were harvested at the specified timepoints and analyzed for levels of IL-2 (555240; BD Biosciences) by ELISA according to the manufacturer's protocol.

Bone Marrow Transplantation (BMT)

BMTs were performed as previously described[97,98]. Briefly, syngeneic [C57BL/6J→C57BL/6C] and allogeneic [C57BL/6J→BALB/c] recipients received lethal total body irradiation on day -1. BALB/c recipients received a total of 8 Gy (^{137}Cs, split dose separated by 3 h), and C57BL/6C recipients received a single dose of 10 Gy (^{137}Cs, single dose). All mice received 1×10^6 T cells from the specified donors, and 5×10^6 WT T cell-depleted bone marrow cells. Survival was monitored daily, and recipient GVHD clinical scores were measured weekly according to the severity of disease on recipient weight loss, posture, mobility, skin, and fur integrity as described previously[97].

3.4 Results

3.4.1 Genetic SEC23A KO does not replicate the phenotype of SEC23B KO

We first generated *Sec23a*$^{fl/-}$ *Cd4*^{Cre} mice which lack SEC23A in T cells. As in *Sec23b*$^{fl/-}$ *Cd4*^{Cre} mice, Cre-recombinase is expressed in thymocytes at the double positive stage of T cell development, and therefore *Sec23a* excision occurs in both mature CD4^{+} and CD8^{+} T cells. We confirmed by western blot that these mice lack SEC23A specifically in T cells, but harbor normal levels of SEC23B (**Figure 3.1a**). We analyzed cells derived from the thymus, spleen, and peripheral lymph nodes to assess proportions and absolute numbers of CD4^{+} and CD8^{+} T cells, and measured no significant differences between SEC23A KO T cells and WT T cells, suggesting that SEC23A KO T cells developed normally and in the usual ratios (**Figure 3.3**). We next tested SEC23A KO T cells in their capacity to secrete IL-2, given our observation that IL-2 secretion is impaired in the absence of SEC23B. In contrast to this finding in SEC23B KO T cells, SEC23A KO T cells demonstrated normal IL-2 secretion, as measured by ELISA (**Figure 3.1b**). When we measured intracellular levels of IL-2, we found similar levels in both WT and SEC23A KO T cells that were stimulated both in the presence and absence of BFA (**Figure 3.1c**). Following activation with αCD3 and αCD28 for 3 days, SEC23A KO T cells also underwent similar proliferation following activation when compared to WT (**Figure 3.4**).

Given its homology with its paralog SEC23B, these data raised further questions about the relevance of SEC23A in murine T cells. We hypothesized that SEC23B may confer unique functions to T cells. Alternatively, T cells may be sensitive to levels of total available SEC23 protein, and the observed defects in *Sec23b*$^{fl/-}$ *Cd4*^{Cre} mice may result from a larger loss of total SEC23 level than in *Sec23a*$^{fl/-}$ *Cd4*^{Cre} mice, as SEC23B is predominantly expressed in murine T cells at baseline.

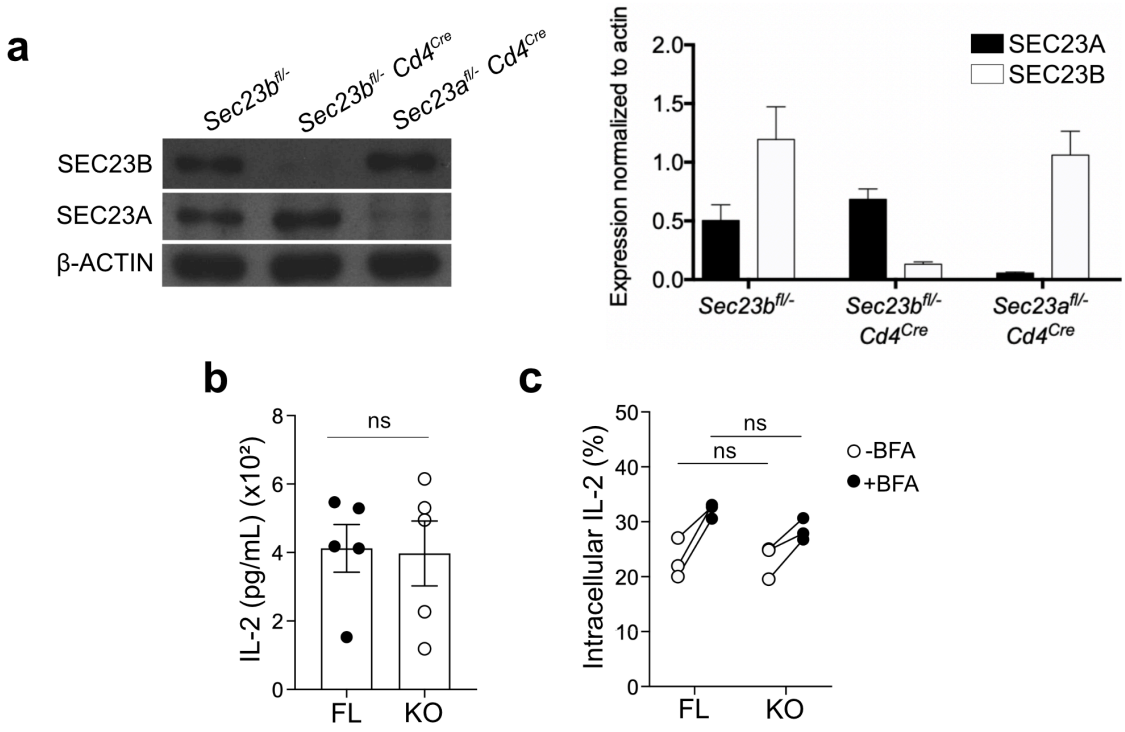

Figure 3.1 Characterization of T cells derived from *Sec23a$^{fl/-}$ Cd4^{Cre}* mice

(**a**) Representative western blot showing SEC23B and SEC23A expression in purified T cells from *Sec23b$^{fl/-}$, Sec23b$^{fl/-}$ Cd4^{Cre},* and *Sec23a$^{fl/-}$ Cd4^{Cre}* mice. Normalized levels of each protein relative to β-actin are plotted on the right. (**b**) ELISA assay measuring IL-2 secreted by WT and SEC23A-deficient T cells over 3 days in culture with αCD3 and αCD28 stimulating antibodies (n=5/group). (**c**) Flow cytometry measuring levels of intracellular IL-2 in WT and SEC23A-deficient T cells following their stimulation *in vitro* for 3 days with αCD3 and αCD28, and 5 h with PMA and ionomycin in the presence or absence of BFA (n=3/group).

3.4.2 T cells from *Sec23*$^{b\text{-}a/b\text{-}a}$ mice exhibit normal T cell functions *in vitro*

We next analyzed *Sec23*$^{b\text{-}a/b\text{-}a}$ mice which lack *Sec23b*, but express *Sec23a* from the endogenous *Sec23b* genomic locus (**Figure 3.2a**). As a result, these mice express SEC23A but only at a level comparable to the total sum of WT SEC23A and SEC23B[57]. We confirmed that *Sec23*$^{b\text{-}a/b\text{-}a}$ T cells developed normally, as indicated by normal T cell proportions in the thymus, spleen, and lymph nodes (**Figure 3.3**). We also confirmed that T cells from *Sec23*$^{b\text{-}a/b\text{-}a}$ lacked SEC23B, but contained increased levels of SEC23A (**Figure 3.2b**).

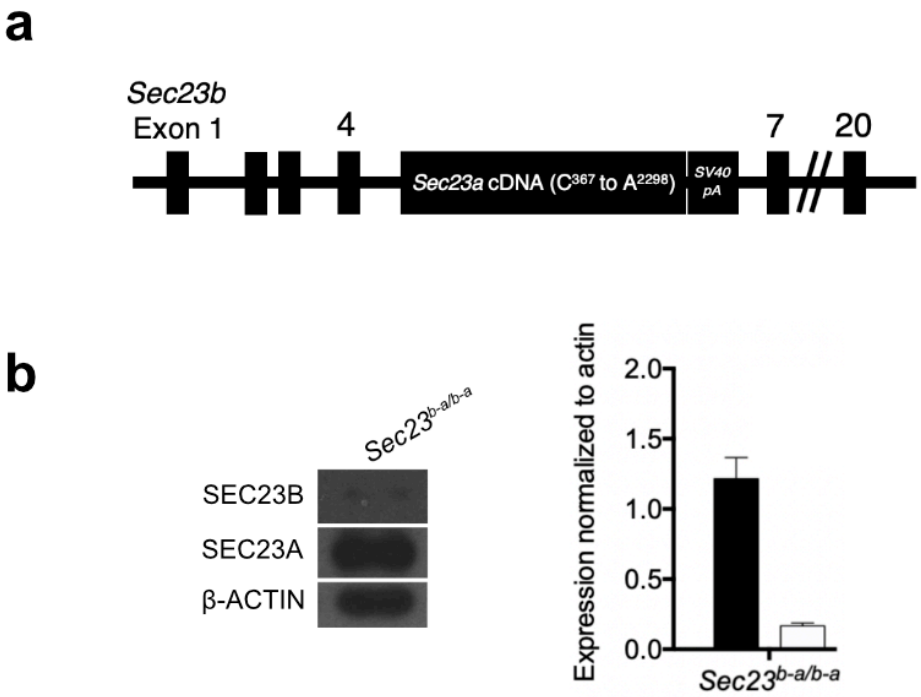

Figure 3.2 Characterization of T cells derived from *Sec23*$^{b\text{-}a/b\text{-}a}$ mice

(**a**) Schematic diagram of *Sec23b* endogenous genomic locus in *Sec23*$^{b\text{-}a/b\text{-}a}$ mice in which a portion of the *Sec23b* genomic locus is substituted by the *Sec23a* coding sequence (from C367 to A2298) followed by a poly(A) termination signal[57]. (**b**) Representative western blot showing SEC23B and SEC23A expression in purified T cells from *Sec23*$^{b\text{-}a/b\text{-}a}$ mice. Normalized levels of each protein relative to β-actin are plotted on the right.

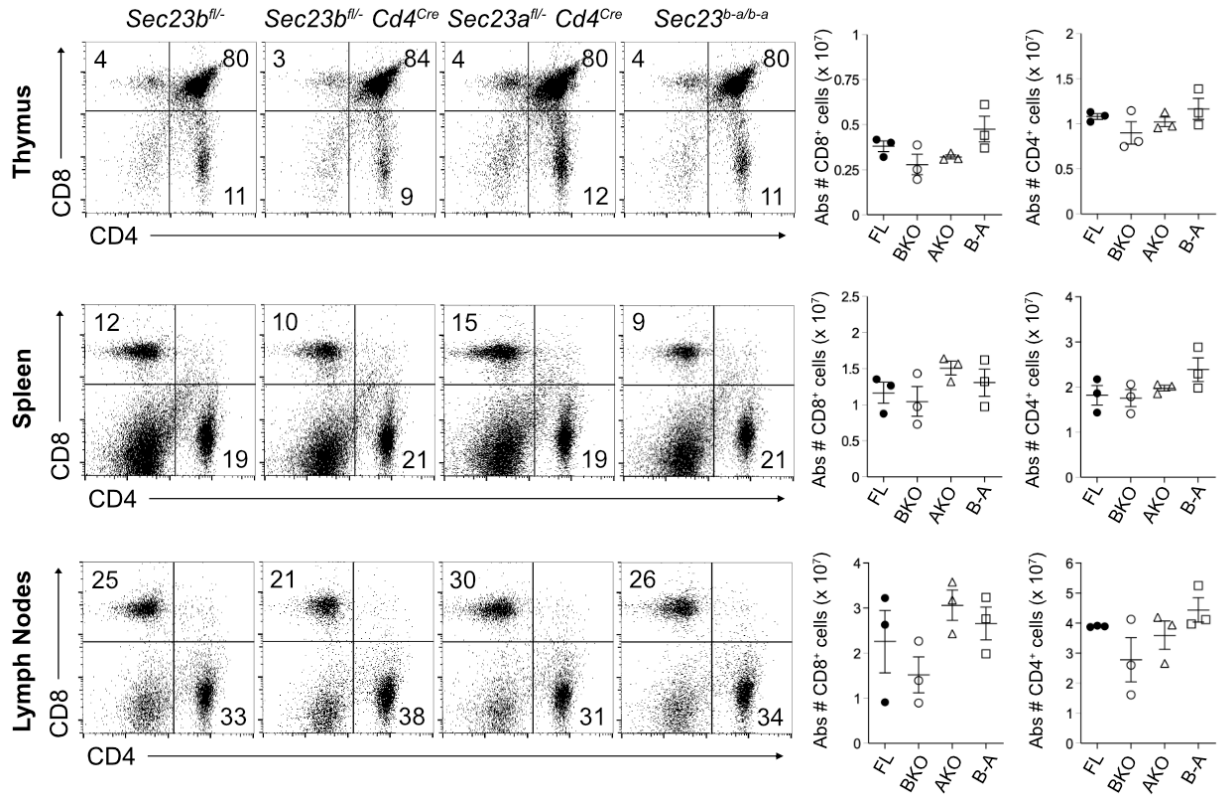

Figure 3.3 T cell development is normal in *Sec23a*$^{fl/-}$ *Cd4*^{Cre} and *Sec23*$^{b-a/b-a}$ mice

Representative flow cytometric plots indicating CD4$^+$ and CD8$^+$ ratios in thymus, spleen, and lymph nodes homogenates derived from *Sec23b*$^{fl/-}$ (FL), *Sec23b*$^{fl/-}$ *Cd4*^{Cre} (BKO), *Sec23a*$^{fl/-}$ *Cd4*^{Cre} (AKO), and *Sec23*$^{b-a/b-a}$ (B-A)mice. Absolute numbers are plotted on the right. Significance was determined by two-tailed unpaired Student's t-test. Differences between *Sec23b*$^{fl/-}$ and the remaining groups were not significantly different (n=3, $p > 0.05$ for all).

We hypothesized that this increased SEC23A expression would functionally compensate for the absence of SEC23B. Following activation with αCD3 and αCD28 for 3 days, *Sec23*$^{b-a/b-a}$ T cells exhibited normal proliferative capacity, as measured by the percentage of T cells that have undergone at least one division as measured by CFSE (**Figure 3.4**). Taken together, our data demonstrate that SEC23A and SEC23B have overlapping functions, and suggest that T cells depend on total levels of SEC23 for their secretory and effector functions *in vitro*.

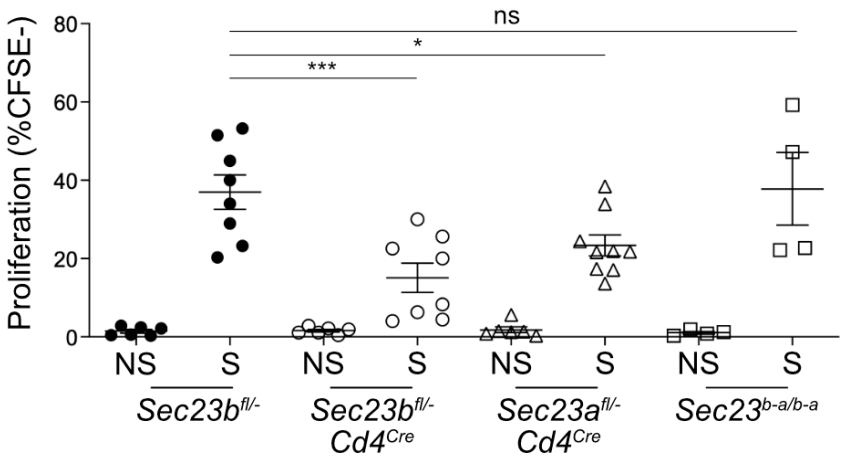

Figure 3.4 Comparison of T cell proliferative capacity in different mouse models

Proliferation of isolated T cells from the indicated mice stimulated *in vitro* with αCD3 and αCD28, as measured by CFSE dilutions. Data are mean ± SEM, *p<0.05, ***p < 0.001 (two-tailed unpaired Student's t-test).

3.4.3 T cells from *Sec23$^{b\text{-}a/b\text{-}a}$* mice demonstrate equivalent GVHD to WT T cells in allogeneic recipients

To confirm that SEC23A can compensate for SEC23B when expressed at sufficient levels *in vivo*, we performed allo-HCT to determine the pathogenic capacity of SEC23A-deficient T cells and *SEC23$^{b\text{-}a/b\text{-}a}$* T cells. We hypothesized that in contrast to SEC23B-deficient T cells, SEC23A-deficient T cells and *SEC23$^{b\text{-}a/b\text{-}a}$* T cells would cause similar severity of GVHD as WT T cells. All control recipients received a dose of WT C57BL/6J bone marrow and syngeneic T cells. Allogeneic recipients received WT C57BL/6J bone marrow, and either allogeneic WT C57BL/6J T cells, SEC23A-deficient T cells, or SEC23$^{b\text{-}a/b\text{-}a}$ T cells. Consistent with our hypothesis, all recipients of allogeneic SEC23A-deficient and SEC23$^{b\text{-}a/b\text{-}a}$ T cells died (**Figure 3.5**), and survival was similar in recipients of SEC23$^{b\text{-}a/b\text{-}a}$ and SEC23A-deficient T cells as those of WT T cells. Transfer of SEC23$^{b\text{-}a/b\text{-}a}$ and SEC23A-deficient T cells also resulted in similar GVHD clinical

scores when compared to WT T cells (**Figure 3.5**). These data demonstrate that while SEC23B is the predominantly expressed paralog in T cells, SEC23A can compensate for its loss.

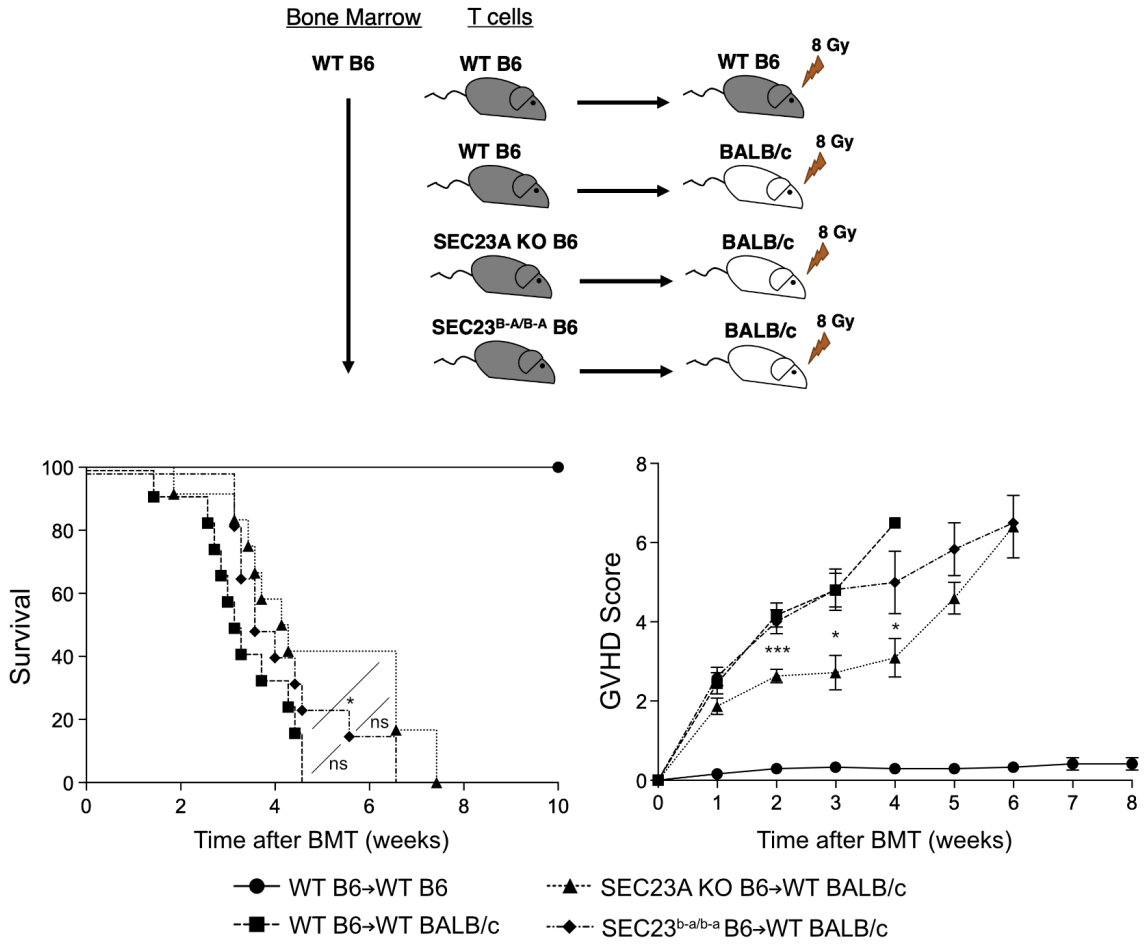

Figure 3.5 GVHD following allo-HCT with T cells from *Sec23a$^{fl/-}$ Cd4^{Cre}* or *Sec23$^{b-a/b-a}$* mice

Survival and composite GVHD scores of mice that received syngeneic T cell-depleted bone marrow and T cells from either syngeneic donors, WT C57BL/6J, *Sec23a$^{fl/-}$ Cd4^{Cre}* C57BL/6J, or *Sec23$^{b-a/b-a}$* C57BL/6J allogeneic donors. Syngeneic n=12, Allogeneic n=12 per group, significance determined by Mantel-Cox log rank test.

3.5 Discussion

Most COPII subunits in mammals exist in multiple paralogs, and mutations in different paralogs often lead to distinct disease phenotypes[34,56]. Earlier studies have proposed that SEC23A and SEC23B may contribute to increased complexity of COPII by carrying out non-overlapping functions[46,47,62]. In contrast, recent studies that have shown that mice and humans have distinct phenotypes when they lack SEC23B supported the hypothesis that tissue-specific patterns of *Sec23a* or *Sec23b* expression directed by evolutionary shifts in gene expression contribute to the differences[74,76,78]. This is corroborated by findings that SEC23A and SEC23B have indistinguishable interactomes and are interchangeable during development *in vivo*[57].

Our observations extend on these findings on the role of paralog specificity in COPII-mediated transport *in vivo*, while demonstrating for the first time a role for this intracellular pathway in T cell immunity. In light of our findings that SEC23A can compensate for SEC23B in $Sec23^{b\text{-}a/b\text{-}a}$ T cells, the absence of a secretory defect in SEC23A KO T cells suggests that when total SEC23 is reduced, T cells can carry out normal secretory functions following activation *in vitro*. Under other conditions, some differences are apparent, as in proliferation and demonstration of GVHD in Figures 3.4 and 3.5, in which SEC23A-deficient T cells strike an intermediate between SEC23B-deficient and $Sec23^{b\text{-}a/b\text{-}a}$ T cells. One interpretation is that the need for SEC23 is dose-dependent as proposed previously, as targeting SEC23A still represents a net decrease in total SEC23. Another hypothesis is that while SEC23A can fully functionally compensate for SEC23B, the same is not true vice versa. To that end, additional experiments could analyze the effects of overexpressing *Sec23b*, probe the T cell phenotype in heterozygotic $Sec23b^{+/-}$ *and* $Sec23a^{+/-}$ mice, or examine a murine model in which the *Sec23a* genomic locus is modified with the coding sequence of *Sec23b*.

Collectively, the data in this chapter support the conclusion that SEC23 paralogs have overlapping function in T cells, and that increased expression of SEC23A can rescue to the proliferative and cytokine secretion defects *in vitro* from the loss of SEC23B. This is consistent with the report that SEC23A can also rescue the perinatal lethality and pancreatic degeneration phenotype from the loss of SEC23B in murine development[57]. Importantly, rescue of T cell functions is maintained *in vivo,* as demonstrated by intact allogeneic donor T cell pathogenicity in an experimental model of GVHD.

CHAPTER 4

COPII Regulates T Cell Metabolism

4.1 Abstract

T cells undergo metabolic reprogramming upon their activation, and this is critical for the synthesis of metabolic intermediates to support T cell proliferation, differentiation, and effector functions[119-121]. However, the cell biological mechanisms that control metabolic activity remain poorly characterized in T cells. We sought to examine T cell metabolic functions in the absence of SEC23B, given the effect on proliferative functions described in Chapter 2. We demonstrate that SEC23B KO T cells exhibit a deficiency in glycolysis following activation that was associated with a decrease in transcription of Hexokinase II, as well as genes involved in cholesterol and fatty acid synthesis. SREBPs (sterol regulatory element binding proteins) are transcriptional regulators of multiple genes involved in metabolism including Hexokinase II. Furthermore, the activation of SREBPs is dependent on the COPII pathway. Thus, we examined the relationship between SEC23B and SREBP activity. We demonstrate that SREBP-1 and SREBP-2 co-localize with SEC23B in T cells. Furthermore, we show that expression of *Sec23a* in SEC23B KO T cells via analysis of *Sec23*$^{b\text{-}a/b\text{-}a}$ mice rescues SREBP-mediated gene expression, as well as glycolytic activity in T cells. Taken together, these data demonstrate a critical role for the COPII pathway in regulating T cell metabolic functions.

4.2 Introduction

In addition to enabling the extracellular transport of proteins, the COPII pathway is involved in the localization of other proteins to different intracellular compartments[31-34]. In this chapter, we explore a scenario in which COPII is involved in the nuclear transport of a transcriptional regulator.

Activated T cells undergo rapid changes in gene expression that stimulate proliferation and the adoption of diverse effector functions.[119] This process is supported by changes in metabolic pathways that increase the availability of metabolites and precursor molecules that support biosynthesis of proteins including effector molecules. Metabolic reprogramming of T lymphocytes upon their activation including changes in glycolysis, oxidative phosphorylation, and fatty acid synthesis, are critical for T cell proliferation, differentiation, and effector functions[119-121]. Thus, alterations of metabolism are tightly linked to T cell functions.

In Chapter 2, using a mouse model that is conditionally SEC23B-deficient in T cells, we found that abrogation of the COPII pathway by *Sec23b* KO led to altered T cell proliferation. However, this phenotype was only partially rescued upon addition of exogenous IL-2, which implied contributions of other cell extrinsic or intrinsic processes to this defect. As changes in metabolism can drive T cell phenotype, we explored the significance of ER-to-Golgi transport mechanisms in T cell metabolism.

We found that SEC23B-deficient T cells exhibit altered metabolic reprogramming following activation, and a defect in the upregulation of genes that play a role in glycolysis and cholesterol synthesis. On further exploration of mechanisms, we found that the COPII pathway is not only important for its classical role in transporting secreted proteins, but also for SREBP-dependent regulation of metabolism in T cells.

4.3 Materials and Methods

Mice

All animal work was performed in accordance with the recommendations of the Institutional Animal Care and Use Committee of the University of Michigan. The generation of *Sec23b*$^{fl/-}$ and *Sec23*$^{b\text{-}a/b\text{-}a}$ mice has been previously reported[57,76,78]. *Sec23b*$^{fl/-}$ mice were bred with *Cd4*^{Cre} (017336) or *Vav1*^{Cre} (008610) mice obtained from The Jackson Laboratory.

T cell isolation and in vitro cell culture

Primary murine T cells were purified by magnetic separation (Miltenyi Biotec) from single cell homogenates of spleens and lymph nodes, and cultured in cell media (1640 RPMI supplemented with 10% heat inactivated FBS, 2 mM L-glutamine, Penicillin-Streptomycin 100U/mL, 100mM HEPES, Non-essential amino acids, 1 mM sodium pyruvate, and 50 μM β-mercaptoethanol). T cells were cultured alone, or with 5 μg/mL αCD3 (145-2C11; Biolegend) and 2.5 μg/mL αCD28 (37.51; Biolegend) soluble antibodies for the specified timepoints.

Flow cytometric analysis

Flow cytometric analysis was performed using fluorophore-conjugated antibodies to mouse CD3 (145-2C11), CD4 (GK1.5), CD8 (53-6.7), CD69 (H1.2F3), and GLUT1. For surface immunophenotyping, single cell suspensions were incubated with the relevant antibodies for 30 min at 4°C, washed, and fixed with 1% paraformaldehyde prior to analysis. All samples were run on an Attune NxT flow cytometer and analysis was performed using FlowJo v10.3.

T cell immunofluorescence confocal microscopy

Purified T cells were fixed on coverslips with 3% paraformaldehyde in PBS, and quenched with 50 mM NH_4Cl in PBS. Cells were then permeabilized in 0.3% Triton X-100 in PBS and blocked with 10% normal goat serum. Cells were then sequentially stained with SREBP-1 (2A4, Santa Cruz Biotechnology) or SREBP-2 (A-12, Santa Cruz Biotechnology) and SEC23B (PA5-52533, Invitrogen) followed staining with secondary antibodies against Rat IgG2bκ and Rabbit IgG respectively. DAPI (Life Technologies) was used to detect nuclei. Acquisition of images was performed using an inverted point-scanning confocal microscope with standard PMT detectors (Nikon A1).

Metabolic Analysis

Metabolic analyses were performed on a Seahorse XFe96 Analyzer (Agilent). 3x10^5 purified T cells/well were seeded onto Cell-Tak (Corning) coated wells. Mitochondrial stress and glycolytic rate were measured by oxygen consumption rate (OCR, pmoles/min) and extracellular acidification rate (ECAR, mpH/min) respectively. In the Mito Stress test, cells were resuspended in XF assay media supplemented with L-glutamine (2mM), sodium pyruvate (1mM), and glucose (10mM). Cells were sequentially treated with oligomycin (1uM), FCCP (10uM), and rotenone (0.1uM) and antimycin (1uM). In the glyco stress test, cells were resuspended in XF assay media supplemented with L-glutamine (2mM). Cells were sequentially treated with glucose (10mM), oligomycin (1uM), and 2-Deoxy-D-glucose (50mM). Data were collected in the Seahorse Wave Desktop Software and analyzed on GraphPad Prism.

Quantitative RT-PCR

RNA was isolated from T cells with the Qiagen RNeasy kit. cDNA was synthesized using the High Capacity cDNA Reverse Transcription Kit (Applied Biosystems), and quantified on a NanoDrop Lite Spectrophotometer (ThermoFisher). Quantitative RT-PCR was performed using PowerUP SYBR Green Master Mix (Applied Biosystems) and the primers listed in **Table 4.1** on a Mastercycler RealPlex^2 (Eppendorf).

Primer	Sequence (5' to 3')
Hmgcr F	TGGTCCTAGAGCTTTCTCGTGAA
Hmgcr R	GGACCAAGCCTAAAGACATAATCATC
Hmgcs F	CAGGGTCTGATCCCCTTTG
Hmgcs R	CAGAGAACTGTGGTCTCCAGGT
Acaca F	GGCCAGTGCTATGCTGAGAT
Acaca R	CCAGGTCGTTTGACATAATGG
Sqle F	GCCTCTCAGAATGGTCGTCT
Sqle R	CGCATCTCCCAGAATAAGGA
Hk2-1 F	TGATCGCCTGCTTATTCACGG
Hk2-1 R	AACCGCCTAGAAATCTCCAGA
Hk2-2 F	TTCCGTGTGCTCCGAGTAAG
Hk2-2 R	CAGGCATTCGGCAATGTGG
Gapdh F	ATGGTGAAGGTCGGTGTGA
Gapdh R	TCGTTGATGGCAACAATCTC

Table 4.1 List of primers used for qRT-PCR in Chapter 4

Statistics

Experiments were conducted with technical and biological replicates at an appropriate sample size, as estimated by our prior experience. An unpaired Student t-test (two-tailed) was used for statistical evaluation of data between two groups, using a statistical software package (GraphPad Prism). Bars and error bars represent the mean and SEM respectively. P values <0.05 were considered significant: *$p<0.05$, **$p<0.01$, ***$p<0.001$, and ****$p<0.0001$. Sample sizes and statistical tests used are detailed in each figure legend.

4.4 Results

4.4.1 Absence of SEC23B results in altered T cell glucose metabolism

In Chapter 2, we examined *Sec23b*$^{fl/-}$ *Cd4*^{Cre} mice, which lack *Sec23b* expression in T cells. We activated T cells derived from these mice with αCD3 and αCD28 for 3 days, and observed that they have a reduced proliferative capacity when compared with WT T cells. Given the central role of COPII in secretion, we reasoned that the proliferation defect was secondary to a reduction of T cell-derived growth factors. When we supplemented the cultures with exogenous IL-2, however, *Sec23b*-deficient proliferative capacity was only partially restored (**Figure 2.12**). We also demonstrated that *Sec23b*$^{fl/-}$ *Cd4*^{Cre} T cells undergo normal development, activation, and similar levels of cell death. Therefore, we hypothesized that in addition to extrinsic factors of T cell function, T cell intrinsic processes were impacted by the loss of *Sec23b* that additionally account for the proliferative defect.

As T cell metabolism is linked to its function, we aimed to gain a better understanding of the metabolic profile of SEC23B-deficient T cells. We first probed T cell glycolytic activity and mitochondrial respiration in real-time using a Seahorse Extracellular Flux. Specifically, we examined rates of both oxygen consumption (OCR) and extracellular acidification (ECAR) by T cells before and after 24 hours of activation with αCD3 and αCD28. Following activation, there were no significant differences in OCR between WT and SEC23B KO T cells throughout the conditions of the assay. However, activated SEC23B KO T cells displayed significantly reduced glycolytic capacity when compared with WT (**Figure 4.1a**). Although ECAR was similar throughout the assay among unstimulated cells, activated SEC23B KO T cells exhibited less glycolytic activity upon addition of a saturating concentration of glucose, and decreased glycolytic capacity upon addition of oligomycin (**Figure 4.1a**).

Given the known role of SEC23B in transporting diverse cargoes including membrane proteins, we hypothesized that this phenotype may be a consequence of decreased transport of glucose transporters to the surface. GLUT1 is the primary glucose transporter expressed on T cells[119,122,123]. Therefore, we measured *Glut1* transcription by qRT-PCR, and found that *Glut1* expression was normal in SEC23B KO T cells (**Figure 4.1b**). Both at baseline and after activation, levels of GLUT1 on the surface of SEC23B KO T cells were also similar to WT as measured by flow cytometry (**Figure 4.1c**). Furthermore, when we measured glucose uptake, SEC23B KO T cells demonstrated normal 2-NBDG levels 24 hours after activation (data not shown). To further investigate this, we measured a panel of genes important in the glycolytic pathway by qRT-PCR and found that *Hexokinase II* (*Hk2*) expression was decreased in SEC23B KO T cells, which we confirmed with two separate primer pairs (**Figure 4.1d**).

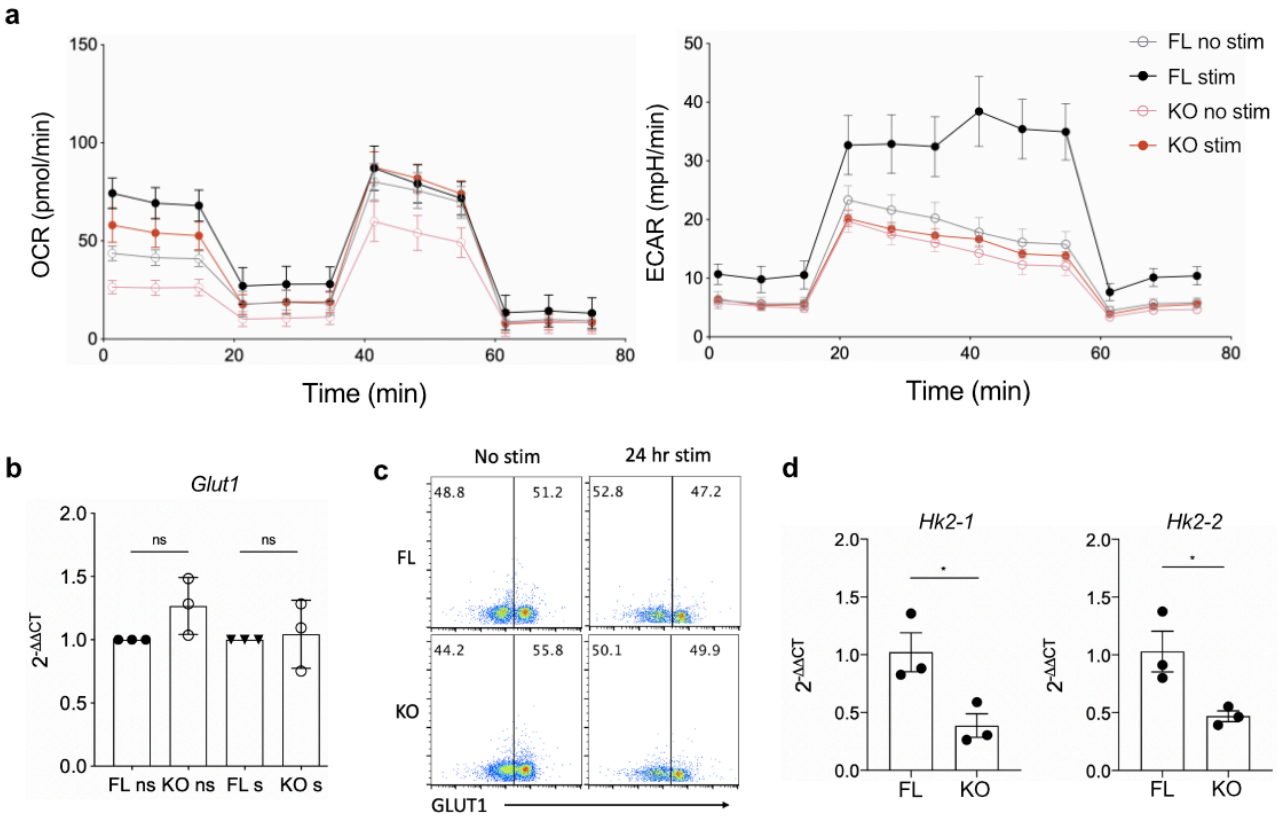

Figure 4.1 SEC23B regulates T cell glucose metabolism

(**a**) Oxidative phosphorylation of FL and KO T cells as measured by the OCR following injections with oligomycin (1uM), FCCP (10uM), and rotenone (0.1uM)/antimycin (1uM). Glycolysis of *Sec23b*$^{fl/-}$ (FL) and *Sec23b*$^{fl/-}$ *Cd4*^{Cre} (KO) T cells as measured by the ECAR following injections glucose (10mM), oligomycin (1uM), and 2-Deoxy-D-glucose (50mM) (**b**) qRT-PCR analysis of Glut1 expression in FL and KO T cells without or with stimulation with αCD3 and αCD28 for 24 hours. (c) Flow cytometric analysis of GLUT1 surface expression (d) qRT-PCR analysis of *Hk2* expression with two different primers.

Naïve T cells have low metabolic needs and undergo basal nutrient uptake and oxidative phosphorylation[119]. Following TCR stimulation, T cells undergo an increase in glycolytic flux to rapidly adapt to higher energy demand that is accompanied by a dramatic increase in expression of *Hexokinase II*[124-126]. Hexokinase II mediates the phosphorylation of glucose to glucose 6-phosphate in the glycolytic pathway, and is considered the rate limiting enzyme for glycolysis[121]. One group that generated *Hk2*$^{fl/fl}$ *Cd4*^{Cre} mice found that HK2-deficient T cells have greatly reduced ECAR, but maintain normal OCR, a pattern we observed in our own Seahorse analysis[125]. We therefore looked into the basis of decreased *Hk2* expression.

4.4.2 SEC23B KO T cells demonstrate altered SREBP-dependent transcription

Given the observation that *Hk2* transcript levels were reduced, we examined its transcriptional regulators. We found that Hexokinase II and its closely related isozyme, Glucokinase, are downstream of sterol regulatory elements which are regulated by SREBP-1[127-129]. SREBPs represent a group of transcription factors that bind sterol regulatory elements and control the expression of genes involved in metabolic processes including cholesterol and fatty acid synthesis[130-132]. While they have overlapping functions, SREBP1 is primarily involved in the synthesis of fatty acids, and SREBP2 is associated with upregulating molecules that increase in cholesterol synthesis and lipid transport. Cholesterol is an important component of cell

membranes, and it was previously demonstrated that proliferating T cells meet the increased demand for cholesterol during cell division by upregulating SREBP-dependent transcription[133].

Mechanistically, the activation of SREBP is dependent on their intracellular localization, and SREBP activity is regulated by a feedback system that controls its transport between organelles[134]. Specifically, SREPBPs utilize the classical secretory pathway, and its activation is dependent on the COPII pathway[26,27]. SREBPs are initially present as inactive precursors on the ER membrane where it is bound by the cholesterol sensor Scap (SREBP cleavage-activating protein), which itself associates with the ER membrane protein Insig (insulin-induced gene)[135]. Insig acts as a retention protein that masks the COPII sorting signal on Scap, and precludes its binding to Sec24[136]. However, in cholesterol deplete conditions, Scap undergoes a conformational change that leads to its dissociation from Insig, and incorporation into COPII vesicles[137,138]. Following its transit to the Golgi apparatus, SREBP undergoes a proteolytic cleavage that releases its amino-terminal transcription factor domain which enters the nucleus[139-144]. Thus, the intracellular transport of SREBPs is dependent on its transport from the ER to the Golgi apparatus for their activity[145,146]. SREBP activation leads to target gene transcription which includes but is not limited to the uptake and synthesis of cholesterol, and the increased availability of cholesterol negatively feeds back to inhibit the COPII-dependent ER-to-Golgi transport of SREBP[146]. It is not known whether SREBP activity is regulated by SEC23B in T cells.

Given the importance of the COPII pathway in SREBP activation, we tested whether the expression of known SREBP targets was altered in SEC23B KO T cells. We activated naïve T cells with αCD3 and αCD28 for 24 hours, and measured the transcription levels of genes commonly associated with SREBP activity. When compared with WT T cells, SEC23B-deficient T cells exhibited significantly reduced expression of *Hmgcr*, *Hmgcs*, *Acaca*, and *Sqle* (**Figure 4.2**).

As demonstrated previously, this difference in transcription is not likely attributed to differences in proximal TCR signaling events or T cell activation.

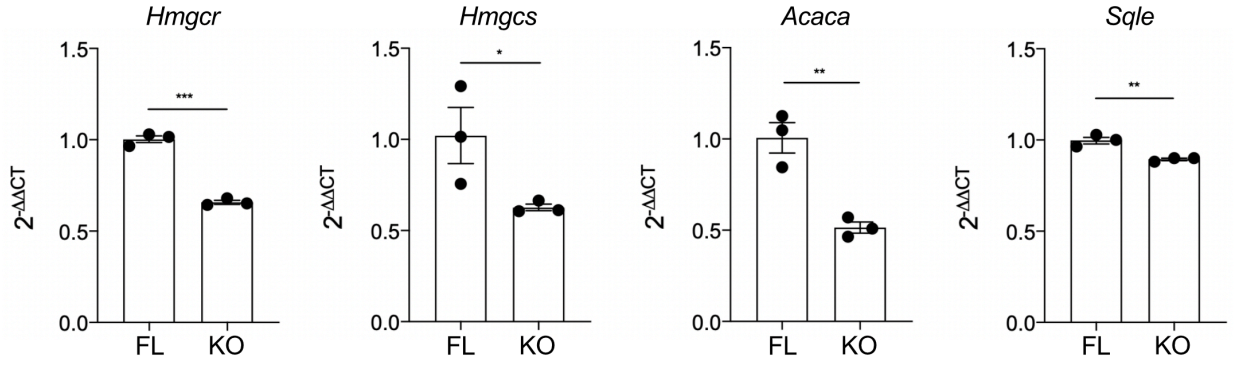

Figure 4.2 T cells lacking SEC23B exhibit transcriptional downregulation of SREBP-regulated genes following activation

qRT-PCR analysis of expression of *Hmgcr, Sqlp, Acaca,* and *Sqle* by *Sec23b*$^{fl/-}$ (FL) and *Sec23b*$^{fl/-}$ *Cd4*^{Cre} (KO) T cells following stimulation with αCD3 and αCD28 for 24 hours.

We hypothesized that while present intracellularly, SREBP activity would be reduced in SEC23B KO cells due to reduced COPII-dependent ER-to-Golgi transport. To test this, we performed confocal immunofluorescence microscopy to confirm the intracellular localization of SREBP. We found that in activated WT T cells, SREBP co-localized with SEC23B, and that SREBP is present in *Sec23b*$^{fl/-}$ *Cd4*^{Cre} T cells.

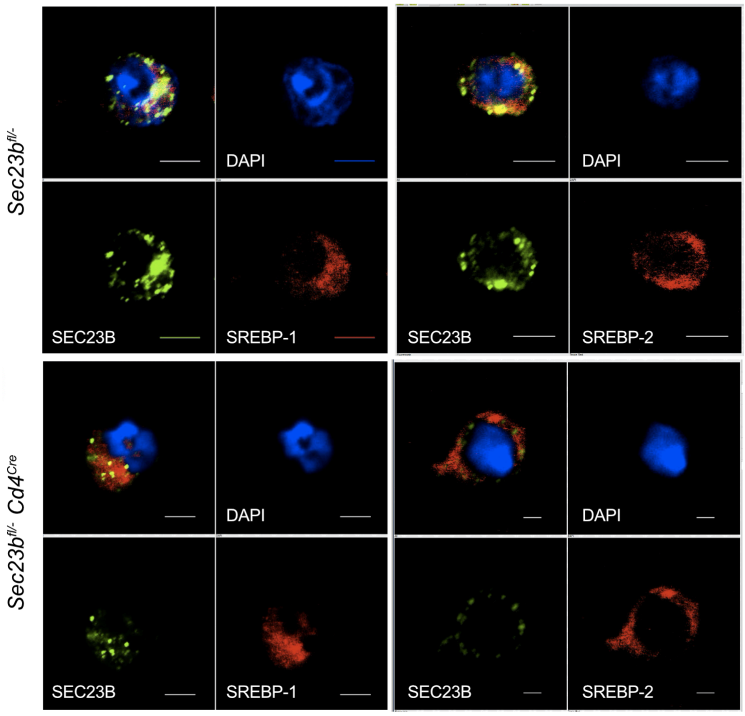

Figure 4.2 SREBP-1 and SREBP-2 co-localize with SEC23B in WT T cells

(**a**) qRT-PCR analysis of expression of *Hmgcr, Sqle, Acaca,* and *Fasn* by WT T cells following stimulation with αCD3 and αCD28 for 24 hours. (**b**) Immunofluorescence confocal micrographs of SEC23 (green) and SREBP-1 or SREBP-2 (red) with DAPI (blue) in *Sec23b*$^{fl/-}$ and *Sec23b*$^{fl/-}$ *Cd4*^{Cre} T cells after 24αCD3 and αCD28 stimulation.

4.4.3 Rescue of *Sec23b* deletion by *Sec23a* expression restores glucose metabolism

We have previously shown in Chapter 3 that in T cells, SEC23A can rescue SEC23B-deficient T cell secretory and proliferative functions. We therefore tested whether increasing *Sec23a* expression could rescue the metabolic phenotype. We first measured expression of *Hk2* in T cells derived from *Sec23*$^{b\text{-}a/b\text{-}a}$ mice. We found that following activation, *Hk2* expression was similar to WT in these cells (**Figure 4.4a**). Using the seahorse method, we also found that *Sec23*$^{b\text{-}a/b\text{-}a}$ T cells exhibited normal glycolytic capacity compared to WT T cells (**Figure 4.4b**). Additionally, the expression of *Hmgcr, Sqlp, Acaca,* and *Sqle* was rescued in activated T cells (**Figure 4.4c**).

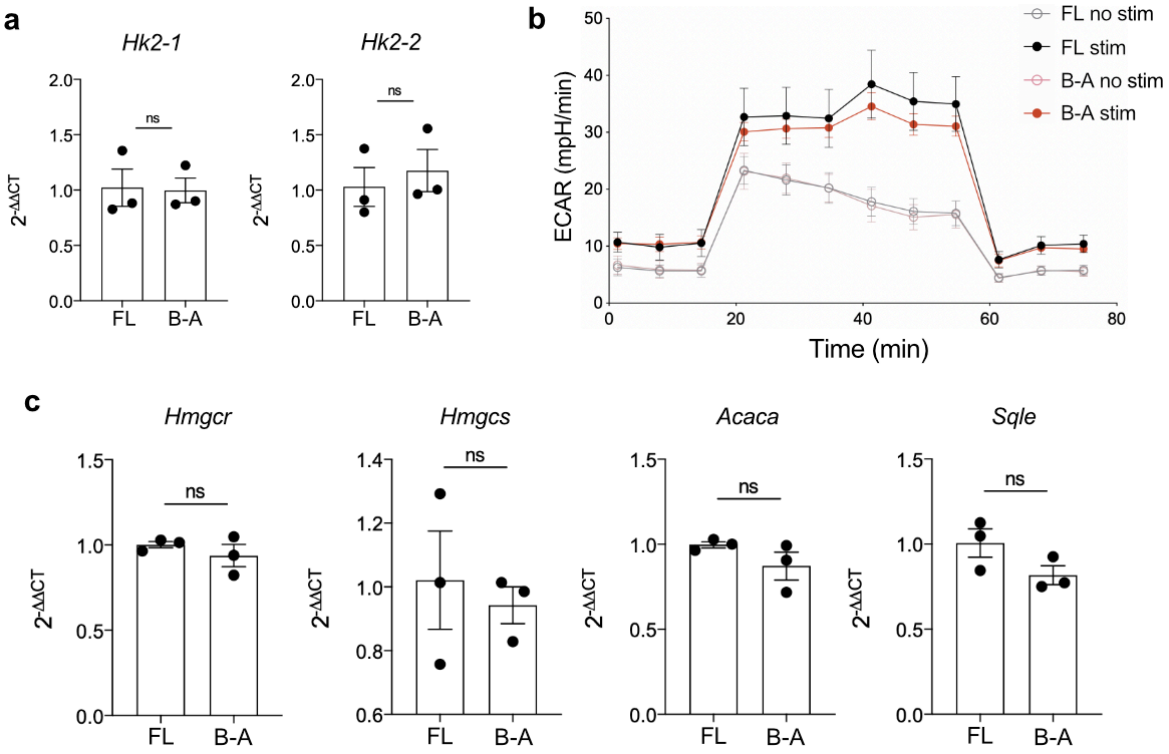

Figure 4.4 *Sec23*$^{b\text{-}a/b\text{-}a}$ T cells demonstrate normal glycolysis and SREBP-dependent gene expression

(**a**) qRT-PCR analysis of *Hk2* expression using two separate primers. (**b**) Glycolysis of *Sec23b*$^{fl/-}$ (FL) and *Sec23*$^{b\text{-}a/b\text{-}a}$ (B-A) T cells as measured by the ECAR following injections glucose (10mM), oligomycin (1uM), and 2-Deoxy-D-glucose (50mM) (**c**) qRT-PCR analysis of expression of *Hmgcr, Sqlp, Acaca,* and *Sqle* by *Sec23b*$^{fl/-}$ (FL) and *Sec23*$^{b\text{-}a/b\text{-}a}$ (B-A) T cells following stimulation with αCD3 and αCD28 for 24 hours.

Given that SREBPs act in conjunction with several different transcription factors, we performed RNA-seq to examine other pathways that are influenced by the loss of COPII-dependent SREBP activation. Principal component analysis indicates that stimulation is a major source of variation in separating *Sec23b*$^{fl/-}$ and *Sec23b*$^{fl/-}$ *Cd4*^{Cr} T cells (**Figure 4.5a**). Differential expression analysis comparing fold change in gene expression in activated *Sec23b*$^{fl/-}$ and *Sec23b*$^{fl/-}$ *Cd4*^{Cr} T cells when compared with unstimulated controls revealed differences in relative changes in gene expression (**Figure 4.5b**). In future studies, we plan to follow up on these initial results and perform gene ontology analysis.

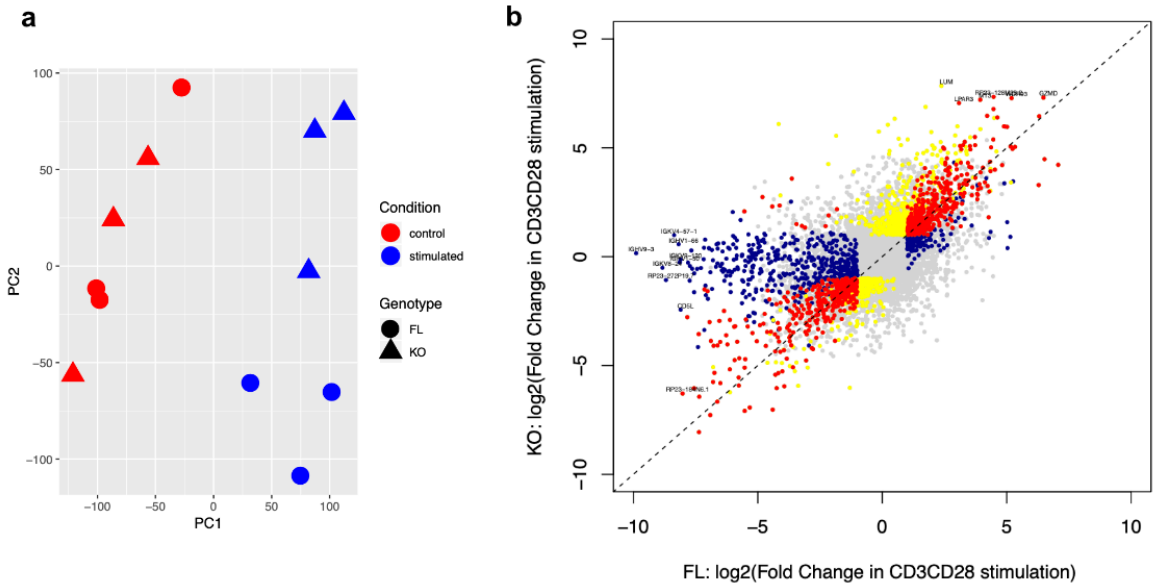

Figure 4.5 RNA-seq analysis

(**a**) Principal component analysis (**b**) Differential expression analysis comparing unstimulated vs stimulated FL T cells with KO T cells. FDR<=5% and |log2FC|>=|1| criteria were used.

4.5 Discussion

Taken together, our data demonstrate that abrogation of the COPII pathway by *Sec23b* mutation impacts SREBP-dependent gene expression. In particular, *Hk2* expression is impaired following T cell activation, and a reduction in glycolytic capacity is observed in T cells lacking SEC23B. Rescue of this phenotype is observed in T cells derived from *Sec23*$^{b\text{-}a/b\text{-}a}$ mice.

SREBPs have important functions in multiple cell types cells, and have been demonstrated to be critical in activated T cells for proliferation and effector functions[134,147,148]. T cells upregulate SREBP upon their activation, which leads to the synthesis of cholesterol and lipids critical for cell membranes, and supports the increased demand by activated T cells for growth and proliferation[133]. Alteration of SREBP availability has been demonstrated to decrease T cell proliferative capacity and reduce effector functions and anti-viral immunity in mice[147]. However, the role of the COPII pathway in regulating SREBP activity in T cells, and its downstream implications for T cell function, is not well known. In this chapter, we build on previous studies by demonstrating that the COPII pathway regulates T cell metabolism, and that SREBP-dependent gene expression is altered in the absence of SEC23B.

Altogether, our findings suggest that the COPII pathway is not only important for its classical role in transporting secreted proteins, but also for the intracellular transport of SREBP and regulation of T cell metabolism. In future studies, we plan to perform CRISPR/Cas9 studies to confirm that the targeted downregulation of SREBP activation and *Hk2* expression regulates the T cell proliferation or metabolism. Furthermore, we also plan to determine if SEC23B KO T cells can be rescued by incorporation of modified/cleaved SREBP or Hexokinase II. Finally, we will explore the contribution of the COPII pathway to SREBP activity and metabolic reprogramming in human T cells.

CHAPTER 5

Characterizing the Role of SEC23 in Human T Cells

5.1 Abstract

Homozygous or compound heterozygous mutations in SEC23B give rise to Congenital Dyserythropoietic Anemia Type II in humans[56,67]. Given our observations in SEC23B-deficient murine T cells, we examined the relevance of SEC23B in human T cells. We found that like murine T cells, healthy human T cells harbor both SEC23 paralogs. We first targeted *Sec23b* by CRISPR/Cas9 and found that this results in an IL-2 secretory defect associate with intracellular IL-2 accumulation as in murine KO T cells. T cells derived from a patient with CDAII, however, did not exhibit the same phenotype. Mechanistic studies demonstrated that unlike murine KO T cells, T cells from patients with CDAII harbored increased levels of SEC23A. This finding was reminiscent of our *Sec23*$^{b\text{-}a/b\text{-}a}$ mice in which increased expression of *Sec23a* from the *Sec23b* genomic locus restored T cell functions. Together, our data demonstrate a critical role for the COPII pathway with evidence for functional overlap *in vivo* between SEC23 paralogs in regulation of T cell immunity in both mice and humans. Furthermore, they provide a possible explanation for why immune deficiencies are not associated with CDAII.

5.2 Introduction

Patients with CDAII exhibit a mild to moderate anemia primarily due to ineffective erythropoiesis and other red blood cell abnormalities[56,70]. While CDAII manifests predominantly as a disorder of erythrocytes, a reduction in SEC23B has also been documented in lymphocytes in patients with CDAII compared with healthy controls[149]. This raised the question of whether this bears consequences for T cell functions in these patients, as we observed in our SEC23B-deficient mouse models. Previous studies have demonstrated that mice deficient in SEC23B do not exhibit the same phenotype as humans[74,76,78]. Furthermore, immunodeficiency is not a commonly associated symptom of CDAII, though this may depend on the mutation[150]. To examine the full impact of SEC23B, we sought to directly study human lymphocytes.

CRISPR/Cas9 (Clustered, Regularly Interspaced, Short Palindromic Repeats)/(CRISPR-associated protein 9) is a gene editing method that has facilitated the study of single gene KO in various cell types. One recent study optimized an approach to introducing guide RNAs complexed with Cas9 into primary human T cells by nucleofection without the need for T cell activation[151]. Using this approach, we achieved efficient *Sec23b* KO in healthy human T cells, and assayed their function. We describe the results of these experiments in this chapter.

CDAII is a rare disorder, with under 400 cases reported as of 2003[152]. However, we were able to obtain PBMCs from three patients with clinically diagnosed CDAII at the University of Michigan and University of Cincinnati. Intriguingly, T cells from the first patient we analyzed exhibited a phenotype that contrasted with those of healthy donor T cells subjected to CRISPR/Cas9-mediated *Sec23b* KO. When we measured the levels of SEC23 by western blot, we found that unlike the CRISPR/Cas9-mediated KO T cells, T cells from this patient in addition to two others harbored increased levels of SEC23A when compared with healthy human T cells.

Together, the data in this chapter data sheds light on the consequences of targeting SEC23 in human lymphocytes, and add to the conclusions derived from our experiments in mice that SEC23A can compensate for SEC23B in its absence in T cells. They also provide insight into mechanisms behind the presence of normal immunity in patients with CDAII.

5.3 Materials and Methods

Isolation and Culture of Human T Lymphocytes

PBMCs were isolated from whole blood by density centrifugation with Ficoll-Paque Premium (GE Healthcare) according to the manufacturer's instructions. PBMCs were then treated with red blood cell lysis buffer (Sigma) and cryopreserved in heat-shocked fetal calf serum (Gibco) containing 10% DMSO (Sigma). Prior to use, PBMCs were thawed in a 37°C water bath and immediately resuspended in complete cell media supplemented with 50 U/mL of Benzonase (EMDMillipore). T cells were isolated from PBMCs by magnetic separation (Miltenyi Biotec) and cultured in cell media (1640 RPMI supplemented with 10% heat inactivated FBS, 2 mM L-glutamine, Penicillin-Streptomycin 100U/mL, 100mM HEPES, Non-essential amino acids, 1 mM sodium pyruvate, and 50 μM β-mercaptoethanol). T cells were cultured alone, or with 5 μg/mL αCD3 (145-2C11; Biolegend) and 2.5 μg/mL αCD28 (37.51; Biolegend) soluble antibodies for the specified timepoints. For proliferation studies, T cells were first labeled on day 0 with 5 μM CFSE (ThermoFisher) for 10 min at 37°C. Prior to analysis of cytokine production by intracellular flow cytometry, T cells were additionally stimulated on day 3 with PMA and ionomycin (Invitrogen) in the presence or absence of BFA (Biolegend) for 5 h at 37°C.

CRISPR/Cas9-mediated KO in T cells by ribonucleoprotein (RNP) nucleofection

CRISPR/Cas9 RNP nucleofection was carried out as previously described[151]. Briefly, T cells were isolated from healthy human PBMCs by magnetic separation (Miltenyi Biotec) and incubated in media containing IL-7 (10 ng/mL) for 2-24 h (37ºC, 5% CO_2). Control non-targeting crRNA (IDT) or Sec23b-targeting crRNA (AGGTCTGGACGTTCTTTCAA, GACGTTCTTTCAAAGGAGTA, AAGAGACCTTTGCGATCCAC) were complexed with

tracrRNA (IDT) at equimolar concentrations and annealed at 95℃ for 5 min. crRNA-tracrRNA duplexes were complexed with Cas9 protein (IDT) at room temperature for 10 min. T cells were resuspended in primary cell nucleofector solution (Lonza) and mixed with Cas9/RNPs for 2 min at room temperature. Combined samples were transferred to a nucleofection cuvette, and electroporated on a Lonza 4D Nucleofector. Nucleofected T cells were incubated in media at 37°C for 3 days in the presence of IL-7 (10 ng/mL). KO efficiency was confirmed by qRT-PCR and western blot. T cells were used on day 3 for downstream applications.

Flow cytometric analysis

Flow cytometric analysis was performed using fluorophore-conjugated antibodies to human CD3 (UCHT1), CD69 (FN50), CD25 (BC96), IL-2 (MQ1-17H12), IFNγ (4S.B3), and TNFα (Mab11). For surface immunophenotyping, single cell suspensions were incubated with the relevant antibodies for 30 min at 4°C, washed, and fixed with 1% paraformaldehyde prior to analysis. Intracellular staining was performed following surface staining and fixation, in permeabilization buffer (eBioscience) for 30 min at room temperature. All samples were run on an Attune NxT flow cytometer and analysis was performed using FlowJo v10.3.

Quantitative RT-PCR

RNA was isolated from T cells with the Qiagen RNeasy kit. cDNA was synthesized using the High Capacity cDNA Reverse Transcription Kit (Applied Biosystems), and quantified on a NanoDrop Lite Spectrophotometer (ThermoFisher). Quantitative RT-PCR was performed using PowerUP SYBR Green Master Mix (Applied Biosystems) on a Mastercycler RealPlex^2 (Eppendorf), using

the primers Sec23b F: TGGCACGAGTCAGTGGAAAA, and Sec23b R: AAACTGGATGGCTCCTCTGC.

Western Blotting

Whole cell lysates obtained from purified T cells were fractionated by gel electrophoresis through a 10% Bis-Tris gel and transferred onto polyvinylidene difluoride membrane (Millipore) in a semi-dry transfer cell (Bio-Rad). Blots were blocked and stained in 5% nonfat milk in TBST, with primary antibodies against SEC23B and SEC23A[78], and anti-β-Actin (8226; Abcam). Incubation with secondary antibody conjugated to HRP (Santa Cruz) was performed for 2 h at room temperature. Blots were detected using the SuperSignal ECL substrate system (ThermoFisher), on a Konica SRX-101A film processor. Densitometric analysis was performed with ImageJ software.

Enzyme-linked immunosorbent assay (ELISA)

Supernatants from cell culture were harvested at the specified timepoints and analyzed for levels of IL-2 (555190; BD Biosciences), IFNγ (555142; BD Biosciences), and TNFα (555212; BD Biosciences) by ELISA according to manufacturer instructions.

Statistics

Experiments were conducted with technical and biological replicates. An unpaired Student t-test (two-tailed) was used for statistical evaluation of data between two groups, using a statistical software package (GraphPad Prism). Bars and error bars represent the mean and SEM respectively. P values <0.05 were considered significant: $*p<0.05$, $**p<0.01$, $***p<0.001$, and $****p<0.0001$. Sample sizes and statistical tests used are detailed in each figure legend.

5.4 Results

5.4.1 Healthy human T cells express both SEC23 paralogs

We first measured the levels of SEC23A and SEC23B in healthy human T cells. Like mice, humans express both SEC23A and SEC23B in T cells (**Figure 5.1**). However, the relative expression of both paralogs in human T cells is similar, with neither paralog being predominant as indicated by densitometric analysis of western blot band intensity.

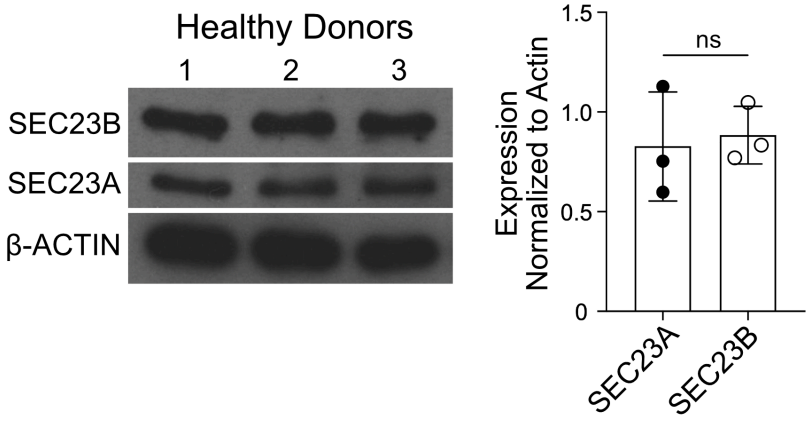

Figure 5.1 Protein expression levels of SEC23 paralogs in healthy human T cells

(**a**) Western blot measuring SEC23B and SEC23A expression in naive T cells isolated from healthy humans. Densitometric analysis indicating normalized expression levels relative to β-actin is quantified on the right (n=3).

5.4.2 *Sec23b* KO by CRISPR/Cas9 in primary human T cells

Given the presence of SEC23B in healthy human T cells, we examined the consequences of SEC23B KO via CRISPR/Cas9 (**Figure 5.2**). We chose to perform *Sec23b* KO in primary human T cells by CRISPR/Cas9, as it presented important advantages to other methods of genetic KO. First, this method enables transfection of Cas9/RNPs without TCR stimulation. Previous methods such as lentiviral delivery or electroporation of guide RNAs with Cas9 have been less

efficient and toxic to primary T cells[153-156]. Furthermore, the activation required by these methods to achieve increased efficiency is suboptimal for functional studies downstream that seek to analyze T cells following initial activation. Upon confirming a reduction in SEC23B expression by qRT-PCR and western blot (**Figure 5.3a**), we assessed T cell functions and observed an increase in IL-2 retention as measured by intracellular flow cytometry (**Figure 5.3b**). When stimulated with PMA and ionomycin in the presence of BFA, control and KO T cells contained similar levels of IL-2. However, when stimulated in the absence of BFA, only KO T cells maintained those same levels, consistent with observations in murine T cells as noted in Chapter 2. These data suggested that patients with CDAII who are deficient in SEC23B might have similar T cell defects.

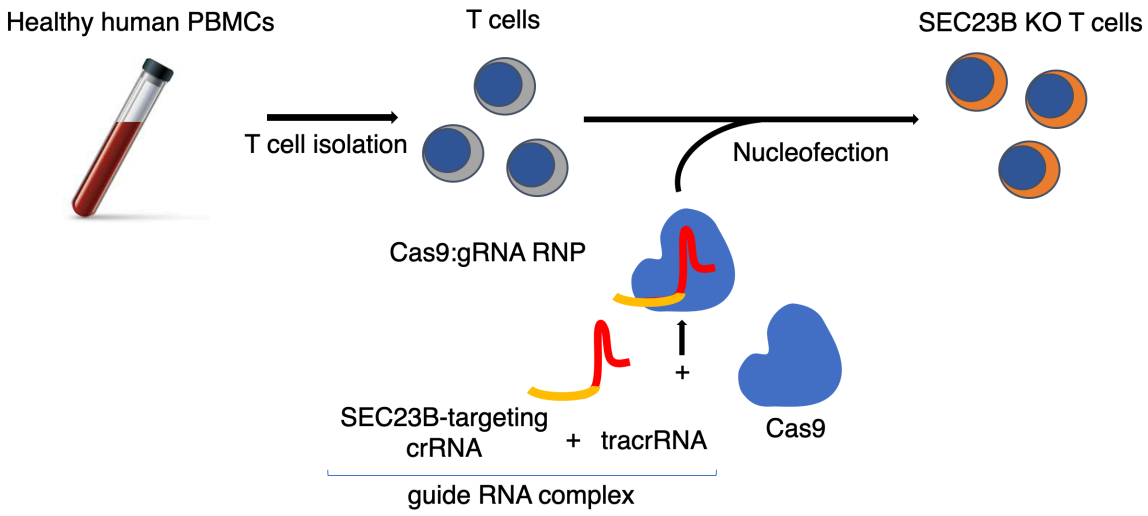

Figure 5.2 Schematic of RNP transfection for CRISPR/Cas9-mediated *Sec23b* KO

T cells isolated from healthy human PBMCs by magnetic separation underwent nucleofection of *Sec23b*-specific guide RNAs pre-complexed with Cas9 Protein by nucleofection. Non-specific guide RNAs were used as a control. T cells were used for downstream functional assays 3 days post-nucleofection, at which detected protein levels were reduced.

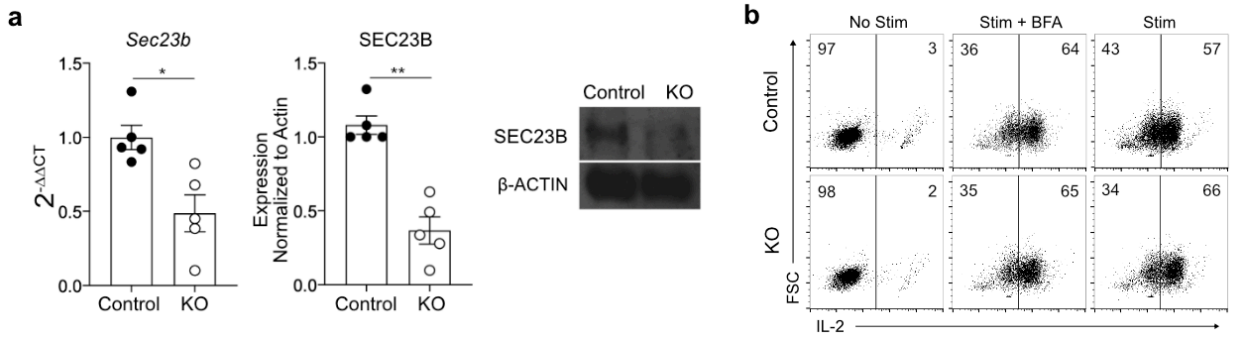

Figure 5.3 Functional impact of CRISPR/Cas9 *Sec23b* KO in primary human T cells

(**a**) qRT-PCR analysis and Western blots indicating the KO efficiency of T cells that underwent CRISPR/Cas9-mediated *Sec23b* KO. T cells were analyzed 3 days following nucleofection with control or *Sec23b*-targeting crRNA-tracrRNA duplexes complexed with Cas9 protein. (**b**) Flow cytometry measuring intracellular IL-2 in healthy T cells that underwent CRISPR/Cas9-based *Sec23b* KO compared with those that received control guide RNA. T cells were stimulated *in vitro* for 3 days with αCD3 and αCD28, and additionally stimulated for 5 h with PMA and ionomycin in the presence or absence of BFA.

5.4.3 Analysis of T cells from a patients with CDAII

We next analyzed T cells obtained from a patient with CDAII. We first activated these T cells for 3 days with αCD3 and αCD28, and measured their proliferation and cytokine secretion. In contrast to murine SEC23B KO T cells and healthy human T cells that underwent acute KO of *Sec23b*, T cells from this patient exhibited normal proliferative capacity (**Figure 5.4a**). They also appeared to produce and release IL-2 normally, as well as TNFα and IFNγ, as indicated by the presence of normal intracellular cytokine following stimulation in the presence or absence of BFA (**Figure 5.4b**). The patient's T cells also expressed similar levels of surface CD69 and CD25, indicating they were similarly activated (**Figure 5.4c**). Because mechanistic murine studies demonstrated that SEC23A, when expressed in sufficient quantities, can rescue cytokine secretion in the absence of SEC23B, we hypothesized that preservation of the T cell response from this patient with CDAII may be from a compensatory increase in SEC23A. Consistent with this hypothesis, we measured SEC23A levels in this patient's T cells, and found that it was expressed

at about twice the levels observed in healthy controls (**Figure 5.4d**). We further corroborated this finding in T cells from two additional patients. Together, these data confirm the interchangeability of SEC23 paralogs in T cells from mice and humans, and also provide a potential explanation for the lack of significant immunodeficiencies in patients with CDAII[150,152].

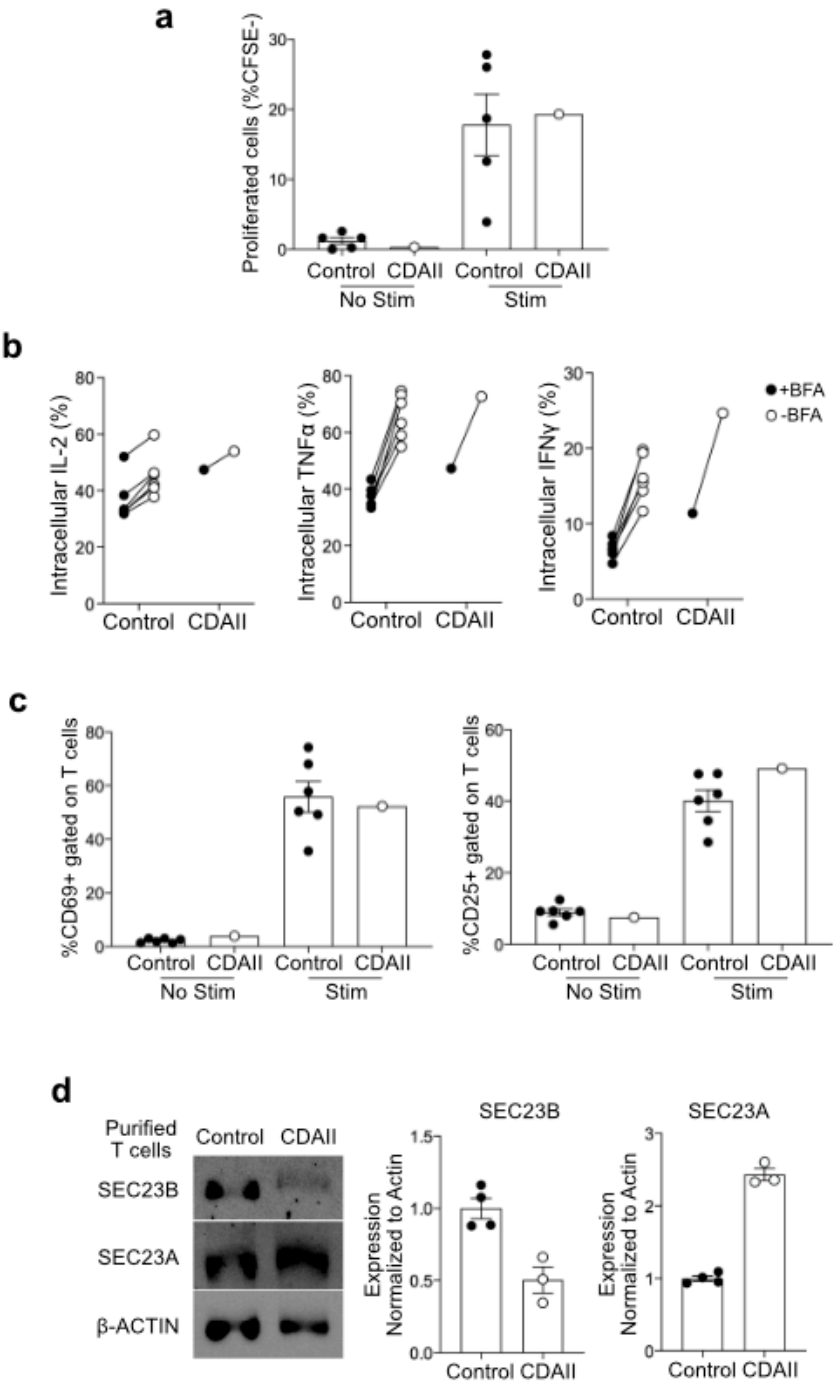

Figure 5.4 Phenotype of T cells derived from a patient with CDAII

(**a**) Proliferative capacity of T cells derived from a patient with CDAII compared with healthy controls, as measured by CFSE dilutions following stimulation *in vitro* with αCD3 and αCD28 for 3 days (n=5/controls, n=1/CDAII). (**b**) Flow cytometry measuring the levels of intracellular IL-2, TNFα, and IFNγ in T cells from a patient with CDAII and healthy controls, following their stimulation *in vitro* with αCD3 and αCD28 for 3 days, and an additional 5 h with PMA and ionomycin in the presence or absence of BFA (n=5/controls, n=1/CDAII). (**c**) Quantification of surface CD69 and CD25 expression as measured by flow cytometry in T cells from healthy T cells or T cells from a patient with CDAII on day 3 after no stimulation, or stimulation with αCD3 and αCD28 (n=6/controls, n=1/CDAII). (**b**) Western blots showing expression of SEC23B and SEC23A relative to β-actin in naive unmanipulated T cells from healthy human donors or patients with CDAII. (n=4/controls, n=3/CDAII).

5.5 Discussion

In this chapter, we first demonstrate that human T cells express both SEC23B and SEC23A. Given this observation, we tested the impact of targeting SEC23B by CRISPR/Cas9 and found that this impacts IL-2 release. In contrast to this, T cells from a patient with CDAII did not exhibit the same functional defect. Importantly, T cells from three different patients with CDAII exhibited increased expression of SEC23A, while CRISPR/Cas9-mediated KO of *Sec23b* in mature T cells from healthy humans did not accompany an upregulation of SEC23A, potentially due to the acute nature of the knockdown method. Assayed functions of T cells from the patient with CDAII are comparable to those derived from healthy controls in their ability to become activated, proliferate, and secrete cytokines.

These observations may be due to differences in genetic compensation mechanisms in human T cells that manifest in gene KO when compared with knock-down methods[157]. Although poorly understood, functional compensation by paralogs is a common phenomenon in mouse KO studies[158], and the regulated expression of a protein by its paralog has been observed in T cells in other contexts[159]. BBF2 human homolog on chromosome 7 (BBF2H7) is a transcription factor that directly binds to the *Sec23a* promoter region and is implicated in the secretion of collagen, a process that is deficient in patients with CLSD[160,161]. One study transduced the transcriptionally active N-terminal p60 fragment of BBF2H7 into PBMC-derived erythroblasts from healthy humans and patients with CDAII[162]. They observed a concomitant increase in SEC23A expression in both conditions. Importantly, overexpression of this transcription factor rescued the hypo-glycosylation of proteins that is observed in patients with CDAII[162]. In a separate study, *Sec23b* expression has been associated with EGF-dependent upregulation of the transcriptional regulator RNF11, which normally localizes in endosomes, but is translocated to the nucleus following EGF

receptor engagement[163]. The data in this chapter suggest that strategies to target SEC23A or SEC23B may also have implications for functions in T cells.

In future studies, understanding the molecular regulators of SEC23A and SEC23B expression may be informative in efforts to therapeutically target SEC23A or SEC23B. If a patient harbors a germline mutation in one paralog, growing evidence would support that upregulation of the other paralog can rescue the resulting phenotype. In addition to increasing the availability of COPII subunits, strategies to increase the efficiency of coat formation and disassembly may also play an important role. A recent example that highlights this is a study that demonstrated that alternative splicing of ER resident protein SEC16 can determine the efficiency of its binding to SEC23 and formation of ER exit sites, and increase COPII-dependent ER-to-Golgi transport[164]. Thus, different regulatory strategies have been identified as critical to the COPII pathway.

CDAII is a rare disorder, and therefore we were only able to perform functional assays in blood from a single patient, and perform expression analysis in three patients. We understand the limitations given the rarity of this disorder and are actively seeking additional patient samples to analyze in future studies. Further studies will also include the analysis of SREBP-dependent processes in human T cells, which will contribute to our efforts in arriving at a more integrated interpretation of the role for COPII in T cells and possible implications for therapy.

CHAPTER 6

Conclusion

In summary, our data demonstrate a critical role for COPII-mediated ER-to-Golgi transport in T cell functions. Through the generation of a novel mouse model with a T cell-specific deletion in *Sec23b*, we demonstrate that SEC23B KO T cells develop normally and in the usual proportions. Furthermore, following activation, TCR signaling and transcription of cytokines is intact in these cells. However, they produce an altered secretome following activation as determined by mass spectrometry and a cytokine multiplex assay. Using IL-2 as an example, we confirm that in the absence of adequate levels of SEC23B, T cells exhibit defective secretion that is coupled with accumulation intracellularly. Taken together, these data show that the COPII pathway is involved in the transport of important T cell-derived factors. In addition to *in vitro* functional studies, we show that deletion of SEC23B has profound implications for T cell-mediated protective and pathogenic functions *in vivo*. In the absence of SEC23B, T cells are deficient in conferring anti-viral immunity in mice infected with LCMV Armstrong, and also demonstrate reduced GVHD-related pathogenicity in allogeneic recipients.

Our data also yield insights into the significance of SEC23 paralogs in immunity. Intriguingly, T cells derived from $Sec23b^{fl/-}\ Cd4^{Cre}$ and $Sec23a^{fl/-}\ Cd4^{Cre}$ mice exhibited different phenotypes. Specifically, while SEC23B KO T cells demonstrated a secretory and proliferative defect, SEC23A KO T cells were comparable to WT. We made the initial observation that murine

T cells express both SEC23B and SEC23A, but harbor greater baseline levels of SEC23B. Therefore, it was possible that SEC23B harbored unique functions critical for T cell secretion. T cells from *Sec23*$^{b\text{-}a/b\text{-}a}$ mice, however, exhibited normal functions *in vitro* and were fully pathogenic *in vivo* in an experimental model of allo-HCT. These findings together suggest that both SEC23 paralogs, when present at adequate levels, are sufficient to support T cell effector functions.

We also demonstrate that SEC23B KO T cells exhibit a deficiency in glycolytic metabolic reprogramming following activation. Given the diverse roles of COPII not only in secretion but in other cellular functions, we examined the SREBP-dependent pathway and found that the metabolic phenotype is linked to decreased expression of SREBP-dependent genes critical for glycolysis and cholesterol synthesis. We demonstrate that expression of *Sec23a* in SEC23B KO T cells via analysis of *Sec23*$^{b\text{-}a/b\text{-}a}$ mice rescues SREBP-mediated gene expression as well as glycolytic activity in T cells. T cell metabolism is linked to its activity and differentiation, and therefore modulating metabolic functions dependent on the COPII pathway may be a strategy for driving specific T cell phenotypes.

Finally, we demonstrate the relevance of our data to human lymphocytes. CRISPR/Cas9-mediated *Sec23b* KO in healthy human T cells conferred a secretory and proliferative defect similar to that observed in murine T cells. T cells derived from a patient with CDAII did not exhibit the same defects, and upon further examination, these T cells were discovered to harbor increased levels of SEC23A. The mechanisms of this increase are not known, but it may arise from either tissue-specific bias for SEC23A or a compensatory increase in expression following the lack of functional SEC23B.

Future Directions

The data presented in this dissertation touch on the complexity of contributions of COPII-dependent processes to T cell biology. There are several future directions we would like to pursue.

Elucidating the role of SEC23B in other immune cell subsets

While our work focuses on bulk T cells, our LCMV peptide immunization data and intracerebral infection studies indicate that much remains to be learned about the differential impact on $CD8^+$ and $CD4^+$ cell functions. To extend this to our GVHD studies, different experimental models will be used to determine the context-specific requirements for these differences. Specifically, we will use the $CD8^+$ dependent [C57BL/6→bm1] and $CD4^+$ dependent [C57BL/6→bm12] transplant schemes.

$CD4^+$ cells can be further separated into distinct T helper subtypes (e.g. T_H1, T_H2, T_H17, T_{reg}) prior to analysis, as they have distinct secretory profiles, and it is becoming increasingly appreciated that they have different metabolic requirements. We have preliminary data that suggest the impact of COPII is significant in T_{reg} cells. T_{reg} suppression assay data indicate that suppressive capacity is not significantly impacted in SEC23B KO $FoxP3^+$ cells. Intriguingly, however, 3 days following transfer of SEC23B KO T cells into allogeneic hosts, SEC23B KO FoxP3+ cells undergo a profound expansion when compared with WT (**Figure 6.1**). While the mechanisms remain unclear, this phenomenon may play a role in the survival difference we see in our Allo-HCT recipients of SEC23B KO T cells when compared with WT.

In addition to T cell subsets, innate immune cells will be analyzed in future studies. We gathered preliminary data in BMDCs derived from our $Sec23b^{fl/-}$ $Vav1^{Cre}$ model that suggest that abrogating COPII in DCs affects select cytokine secretion. Specifically, while the secretion of IL-

12 and TNFα is impaired, IL-6 is released normally by SEC23B KO DCs (**Figure 6.2**). As DC-derived secreted factors contribute significantly to controlling immune responses, we plan to follow up on these studies.

Potential directions for further elucidating basic T cell mechanisms

The impact of *Sec23b* knock-out is striking, and we gained valuable insights from analyzing the impacted secretome. Additional agnostic approaches may be warranted to appreciate the full phenotypic spectrum of our model. For instance, as COPII is critical for the transport of surface membrane proteins, many of which act as functional receptors or markers on T cells, mass cytometry could uncover which among these proteins are critically dependent on COPII. Furthermore, as Chapter 4 alluded to, the absence of SEC23B can lead to some transcriptional differences, and thus we plan to follow up on our RNA-seq experiments with gene ontology analysis to identify additional processes and cargoes with regulatory roles that may be affected.

In this study, we focus on SEC23 due to its central role in COPII formation, but examining the contribution of other COPII proteins may yield additional insights. One question that remains from our data is one of specificity. Some hypotheses for the observed differences in cytokine secretion may be that the cytokines differ in their signal sequences, post-translational modifications, or post-Golgi sequestration into differentially regulated intracellular compartments. Alternatively, there may be contributions from the COPII cargo component SEC24.

Future human studies

Future work could extend into informing the development of novel treatments. Targeting COPII activity might be approached from several different angles, such as modulating COPII stability, efficiency, selectivity, or kinetics. A framework for contextualizing our findings in the frontiers of GVHD treatment is described in the Appendix. Given our observation that select

cytokine secretion is impaired following targeting of SEC23B, the COPII pathway may present an opportunity to target an intracellular pathway that is shared by some cytokines but not others. Our observation that T cells from a patient with CDAII upregulate SEC23A when *Sec23b* is mutated raises questions about the mechanisms of this upregulation. Future studies could also focus on understanding distinct regulators of *Sec23a* and *Sec23b* expression, and on developing strategies to selectively modulate the expression of one paralog.

Much remains to be learned about the intracellular pathways and molecular determinants that regulate T cell secretion. Taken together, pursuing these future directions may further illuminate details of the COPII pathway in immune cell biology, and also inform their practical application.

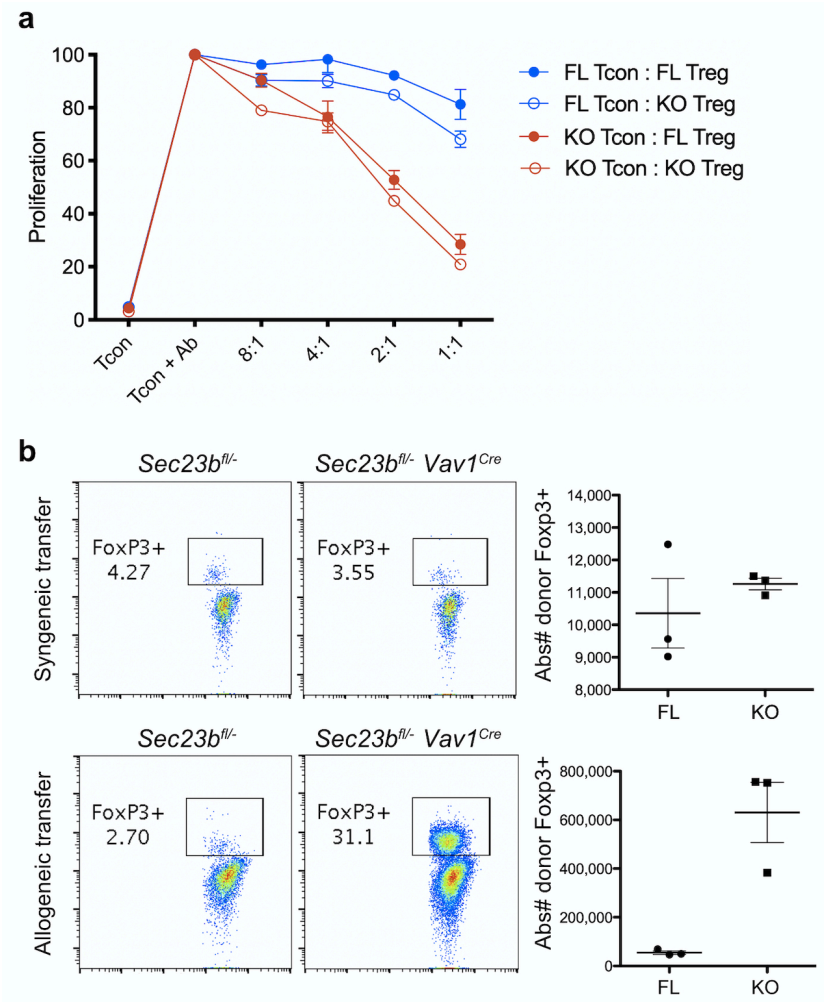

Figure 6.1 Expansion of SEC23B Tregs following transfer into allogeneic hosts

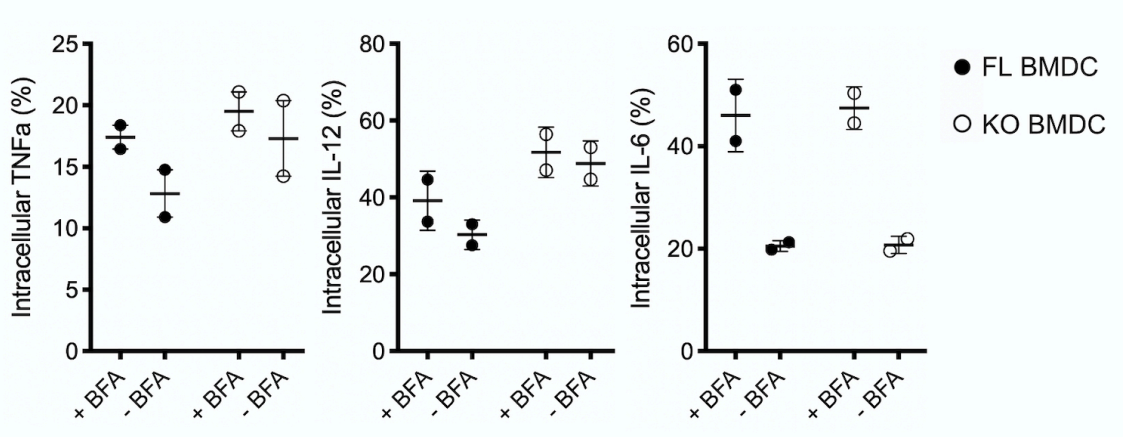

Figure 6.2 Select cytokine retention by SEC23B KO BMDCs following LPS stimulation

Appendix

Allogeneic donor T lymphocytes are essential for causing GVHD, and their activation relies on the coordination of TCR engagement and co-stimulation, also known as Signal 1 and Signal 2. In addition to these signals, a network of secreted cytokines by immune cells provides a third signal, Signal 3, that is critical for the initiation and maintenance of GVHD. Strategies to target Signal 3 in human diseases have shown therapeutic benefit for inflammatory disorders such as Rheumatoid Arthritis and Inflammatory Bowel Disease. However, despite our growing understanding of their role in GVHD, the success of targeting individual cytokines has been modest with some notable exceptions (**Figure A1**). Our findings add to the cell biological understanding of T cells that may be harnessed for better clinical translation.

Direct T cell intrinsic cytokines and proliferative responses: Strategies to control donor T cell activity begin with broadly acting anti-inflammatory prophylactic agents. The most widely used approaches today include methotrexate in combination with cyclosporine or tacrolimus. Methotrexate, a folate antagonist, can target rapidly proliferating allogeneic T cells and be cytotoxic to their growth. Cyclosporine and Tacrolimus inhibit the calcineurin-dependent activation of NFAT transcription factors and their translocation from the cytoplasm to the nucleus, reducing the transcription of inflammatory cytokines such as IL-2 and IFNγ by T cells. Targeting the immune response at this level inhibits key T effector functions as well as their proliferation.

While instrumental in reducing GVHD risk, however, standard prophylaxis measures are not completely effective in preventing the onset of GVHD. Furthermore, they confer non-specific

anti-inflammatory functions that can increase the risk of tumor relapse and infection. Systemic glucocorticoids which remain the mainstay of first-line treatment of acute GVHD is also broadly immunosuppressive. However, T cells are responsive to the influence of select cytokine signals which promote their growth, proliferation, cytotoxicity, and secretion of effector molecules. Important signals include cytokines that promote inflammation and which also tend to be increased following conditioning and allo-HCT such as IL-12, IL-4, IL-1, TNFα, and IL-6[165,166]. Therefore, agents that attenuate the cytokine signals that promote the overactivity of T cells could be beneficial in GVHD treatment. While all of these cytokines have been shown to be critical sources of Signal 3, agents that block TNF, IL-6, and IL-1, as well as the T cell-derived growth factor IL-2 have been studied as potential modes of treatment in acute GVHD. There remains active interest in the use of specific anti-inflammatory cytokine blockade including agents that directly target activating cytokine signals to T cells extracellularly.

Targeting the intracellular afferent arm of Signal 3 cytokine release: Following their activation, T cells engage distinct signaling pathways that lead to the increased synthesis of important effector molecules including cytokines and cytotoxic factors. These culminate in a pro-inflammatory milieu that shapes the allogeneic T cell response and also causes direct tissue damage. While targeting cytokines following their release by immune cells is gaining increasing interest for their promising outcomes in both experimental models and clinical trials, there has been renewed interest in targeting earlier steps following T cell activation such as the intracellular signaling pathways that increase cytokine production. Therapeutic strategies have included targeting the intracellular signaling pathways that lead to proinflammatory cytokine transcription and translation with agents such as calcineurin inhibitors as described above, mTOR inhibitors, JAK inhibitors, Alpha-1 Antitrypsin, histone deacetylase inhibitors, and proteasome inhibitors.

Targeting the intracellular efferent arm of Signal 3 cytokine release: The majority of pre-clinical studies have provided the foundation for the development of therapies that target cytokines or cytokine receptors directly, or the signaling pathways that govern their transcription and translation. A gap in knowledge remains, however, in the post-translational intracellular pathways that coordinate the transport mechanisms that regulate cytokine release by immune cells. Multiple transport steps coordinate the membrane biogenesis, transport, and fusion events that carry cytokines between intracellular compartments and towards the cell surface for secretion. Better understanding of these intracellular secretory pathways utilized by cytokines in immune cells may provide important insights into novel therapeutic targets.

The relevance of cytokines that serve as Signal 3 for robust T cell responses is increasingly well established in their role in promoting GVHD, and as promising therapeutic targets. However, current approaches have yielded modest success and additional strategies are warranted. Moving forward, identifying shared intracellular trafficking pathways that control cytokine release may be of value in developing newer approaches to target Signal 3. Basic science research on the fundamental and critical determinants of intracellular trafficking pathways that coordinate their release remain to be understood. With a better mechanistic understanding of these pathways, the identification of key molecular mediators in the allogeneic setting will be essential. Exploring these questions will both enhance our fundamental understanding of immune regulation, and may pave the way for controlling T cell immunity in inflammatory disorders.

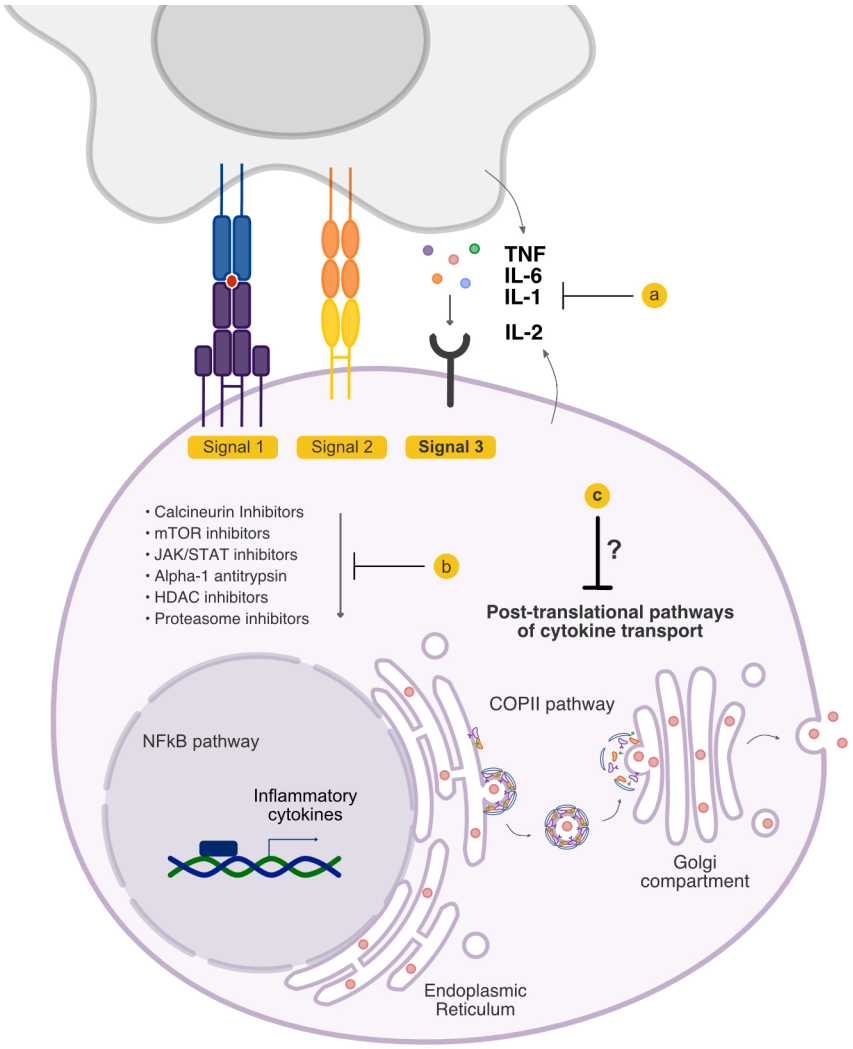

Figure A1: Signal 3 pathways that are targeted in GVHD

Signal 3 critically shapes the allo-response, and existing treatment options have the potential to modulate the cytokine milieu that accompanies allogeneic T cell activation. Current treatment strategies include **a)** blockade of cytokines extracellularly and blockade of cytokine receptors, and **b)** inhibition of the downstream signaling cascades that culminate in the production of inflammatory cytokines. **c)** The pathways that regulate cytokine secretion following their synthesis but preceding their release have not been therapeutically targeted.

Approaches to targeting Signal 3 extracellularly in acute GVHD

Anti-TNF

Tumor Necrosis Factor (TNF) is a cytokine that acts on multiple immune cell types, and promotes the production of Signal 3 cytokines including IL-1 and IL-6[167]. Overexpression of TNF is implicated in the development of multiple autoimmune and inflammatory disorders, and its blockade has improved disease management and quality of life for patients with rheumatoid arthritis, inflammatory bowel disease, and others[168]. In addition to innate immune cell-derived TNFα, T cell-derived TNFα is implicated in the development of GVHD in experimental murine models, and in humans, it was observed that early increased serum levels of TNFα are associated with major transplant-related complications[169,170]. TNFα levels are initially increased following conditioning treatments as measured by levels of TNF receptor-1 which correlate with those of plasma TNFα[171,172]. TNFα is appreciated to play direct roles in acute GVHD pathogenesis by both effecting direct tissue damage and by promoting allogeneic T cell cytotoxicity[173]. Therefore, the use of neutralizing anti-TNFα agents has been studied for efficacy in GVHD prevention and treatment. One such agent is Infliximab, an anti-TNFα monoclonal antibody that has been studied in prophylaxis, and treatment of steroid-refractory acute GVHD (SR-aGVHD)[174,175]. However, in patients with SR-aGVHD, the addition of infliximab did not improve survival and instead increased post-transplant risk of infection when compared with treatment with corticosteroids alone[175,176]. Clinical trials have also been performed to test the efficacy of Etanercept for the blockade of soluble TNF. However, early results were not borne out by a multi-center randomized study that demonstrated no impact of Etanercept on GVHD or on overall survival, infection, and relapse of the primary malignancy[177-181]. While TNFα is best known for its inflammatory properties that promote T cell effector responses, its dual role as a suppressive cytokine is

increasingly being appreciated with the characterization of functionally disparate TNF receptors and their actions on different cell types such as Tregs[182]. While the vast majority of current therapies target TNF directly, future studies of specific inhibitors of TNF production, signaling, and oligomerization, may clarify their potential in the treatment of GVHD[168].

Anti-IL-6

IL-6 is a member of a family of cytokines that shares the receptor complex gp130, a widely expressed signaling complex that leads to the activation of associated Janus kinase (JAK) and signal transducer and activation of transcription (STAT) pathways. Levels of circulating IL-6 can increase dramatically in settings of inflammation, and consequently, IL-6 is associated with the acute phase inflammatory response[183]. The biological consequences of IL-6 are wide-ranging and include the pathologic stimulation of proinflammatory responses, such as by promoting Th17 cell development and inhibition of regulatory T cell differentiation[184]. In murine models of GVHD, donor T cell-derived IL-6 critically contributes to disease severity, and donor T cell-specific deficiency of IL-6 decreases GVHD-related mortality[185]. Blockade of the IL-6 signaling in experimental models also improved GVHD survival and led to an increase in regulatory T cells, and decreased Th1 and Th17 cells in target organs while preserving GVT effects[185,186]. A clinical study examining the effect of tocilizumab, a humanized monoclonal antibody against the IL-6 receptor, showed favorable outcomes in a small number of patients with either acute or chronic GVHD[187]. A phase I/II clinical trial further studied the effect tocilizumab administered one day prior to allogeneic peripheral blood stem cell transplantation in patients that received cyclosporine and methotrexate as GVHD prophylaxis[188]. A phase II trial in which patients received busulfan-based conditioning prior to receiving tocilizumab with tacrolimus and methotrexate showed a low

incidence of gastrointestinal GVHD[189]. Recently, a phase III randomized and double-blinded trial observed a trend towards a reduced overall incidence of grade II-IV GVHD in patients receiving tocilizumab, but no difference in long term survival compared to controls[190].

Anti-IL-1

In addition to TNF and IL-6, IL-1 is an inflammatory cytokine that is increased following conditioning and is critical for immune homeostasis, but when dysregulated, potentiate the pathogenesis of GVHD[22]. Although small early studies showed that targeting soluble IL-1 with a recombinant human IL-1 receptor or administration of a recombinant IL-1 receptor antagonist could ameliorated SR-aGVHD, these results were not confirmed in a randomized controlled trial[191-193]. Given its known potency in inflammatory disorders and association with GVHD in both experimental models and humans, strategies that target IL-1 may be effective depending on the phase of acute and/or chronic GVHD[194,195]. Key upstream regulators of IL-1 include intracellular immune sensors NLRP3 and NLRP6, which assemble into inflammasomes in settings of cellular damage and stress such as those induced by pre-transplant conditioning therapies. Following allogeneic transplant in experimental models, NLRP3 inflammasomes induced the secretion of pathogenic levels of IL-1β by multiple intestinal cellular sources, and also controlled the IL-1β-dependent skewing of Th17 differentiation critical to the development of GVHD[195]. By contrast, donor myeloid derived suppressor cells, which have immunoregulatory functions in GVHD, can lose suppressive capacity following activation of the inflammasome[196]. Thus, the cellular source is an important determinant of the impact of inflammasome dependent effects on GVHD. In host non-hematopoietic target tissues, NLRP3 inflammasomes serve a protective role in promoting intestinal epithelial cell integrity and repair by increasing IL-18 secretion[197]. NLRP6, which has

protective roles in intestinal colitis, plays a role in aggravating gastrointestinal GVHD when expressed in host-nonhematopoietic tissue, and its absence in host intestinal epithelial cells helps maintain gut homeostasis following allogeneic BMT in experimental models[198]. It is likely that the effects mediated by NLRP6 may be IL-1 independent or dependent depending on the type of immunopathology.

Anti-IL-2

IL-2 expression is increased upon activation, is released by T cells, and serves as a growth factor for T effector cells and Tregs. IL-2 is one of the earliest cytokines to be studied as a target for immunosuppression therapeutically[199-201]. Intracellular targeting of the production and secretion of IL-2 with Calcineurin inhibitors remains the first line prophylaxis strategy in the prevention of GVHD. Studies have also explored the use of monoclonal antibodies against IL-2 receptor including daclizumab, basiliximab, and inolimomab, to target the activity of secreted IL-2. One randomized trial found that the addition of daclizumab to corticosteroids as an initial therapy for acute GVHD resulted in increased GVHD-related mortality[202]. A phase II study found that while treatment of SR-aGVHD with daclizumab led to an increased complete response rate, it was associated with higher rates of long-term complications of chronic GVHD[203]. Although basiliximab appears to be better tolerated by patients and not associated to the same degree of adverse events in initial studies, future studies are needed to determine its safety and efficacy[204-206]. Targeting IL-2 is nuanced by its dual roles in that addition to promoting the T cell-mediated toxicity in GVHD, it is essential for the development and maintenance of Tregs which are important regulators of immune tolerance, and may in turn be employed in the prevention of GVHD[207-211]. Therefore, efforts to target IL-2 must balance its inflammatory and

immunoregulatory effects that minimize GVHD but still prevent relapse of the primary disease. The administration of low-dose IL-2 is of interest in the treatment of chronic GVHD, and has been associated with expansion of Tregs, suppression of conventional T cell proliferation, and long-term reduction of chronic GVHD symptoms[212-214].

Approaches to targeting Signal 3 intracellularly in acute GVHD

mTOR inhibition

The mammalian target of rapamycin (mTOR) pathway is a major regulator of cellular growth and metabolism that is also critical for T cell activation, differentiation, and function[215]. Sirolimus, an inhibitor of mTOR, has been demonstrated to exhibit anti-inflammatory effects through multiple mechanisms including inhibition of both conventional T cell and dendritic cell activity, and promotion of Treg development[216-218]. Early studies showed that sirolimus can be well tolerated in patients and may be associated with a lower risk of GVHD[219,220]. A prospective randomized trial found that in combination with tacrolimus, sirolimus is a safe alternative to cyclosporine and methotrexate for GVHD prophylaxis[221]. A recent phase III trial reported that the addition of sirolimus to cyclosporine and mycophenolate mofetil for prophylaxis showed efficacy in lowering the incidence of GVHD[222]. However, its efficacy as a therapy for SR-aGVHD in combination with other agents may be limited depending on the stage of GVHD, and warrants further studies[223].

JAK1/2 inhibition

T cells are responsive to inflammatory cytokines including IL-6 and interferons via their propagation of JAK/STAT pathways. Activation of the JAK family of proteins leads to the phosphorylation of STATs, which translocate to the nucleus and are critical regulators of T cell

alloreactivity[224]. Pre-clinical models demonstrated that targeting JAK1/2 targets GVHD but preserves GVL, with the contribution of decreased serum levels of proinflammatory cytokines including IL-6[225-227]. This led to testing the effects of JAK inhibitors such as ruxolitinib, baricitinib, and itacitinib. Ruxolitinib, a selective inhibitor of JAK1/2, in patients with SR-aGVHD. In an early study, 6 patients experienced reduced GVHD in correlation with a decrease in proinflammatory cytokines in the serum[226]. Additional clinical trials are underway to examine the effects of ruxolitinib in patients with SR-aGVHD[228]. Itacitinib, a selective JAK1 inhibitor, has also demonstrated safety in a Phase I trial and studies of its efficacy in the treatment of SR-aGVHD are ongoing[229].

Alpha-1 antitrypsin

Alpha-1 Antitrypsin (AAT) is an endogenously circulating serine protease inhibitor that, when deficient or mutated, has been described in the pathogenesis of disorders including COPD, cirrhosis, and multiple neurodegenerative diseases[230]. In addition, AAT has a suppressive role in inflammatory settings with an appreciable inhibitory effect on TNF levels[231,232]. When AAT is administered in models of murine allo-HCT, it has been shown to reduce GVHD-induced mortality while preserving the allogeneic T cell GVL effect[233-235]. The therapeutic benefit in these models has been linked to a decrease in alloreactive effector T cells and inflammatory cytokines, and an increase in Tregs and immunoregulatory cytokines such as IL-10[235]. AAT is an effective modulator of the profile of circulating cytokines following allo-HCT leading to significantly reduced disease murine models, underscoring the therapeutic potential of AAT and strengthening the rationale for studying the effect of AAT therapy in humans. Recent studies showed complete recovery in 4 of 12 patients and improvement in the other 8 patients with SR-aGVHD[236]. A prospective multi-

center study that followed tested AAT as a first line therapy for SR-aGVHD led to an overall response rate of 65% and complete response rate of 35% by day 28[237]. Findings on the ratio of T effector cells and Tregs were consistent with those observed in experimental models[237]. Both studies found that AAT is well tolerated by patients, is not associated with an excessive risk of infection, and are now being studied in a randomized manner in a Phase III study.

Histone deacetylase inhibition

Histone deacetylase (HDAC) inhibitors represent a diverse class of drugs that cause reversible inhibition of HDAC enzymes, remodel chromatin structure, and modify gene expression in different ways depending on the specific HDAC, cell type, and context. HDAC inhibitors have been widely studied as anti-cancer agents. A clinically significant consideration of HDAC inhibitors is that in addition to acting on histones, they can have non-specific effects on other protein deacetylases that broadly regulate cell growth and signaling[238]. However, at non-cytotoxic doses, HDAC inhibitors have recently been appreciated to be well tolerated and exhibit immunoregulatory properties, lending to growing interest in their potential to treat inflammatory diseases[239]. Among their diverse effects, HDAC inhibitors have shown immunomodulatory effects on dendritic cell and macrophage antigen presentation, TLR pathways, and IFN signaling[239]. As a consequence, they can reduce the expression of cytokines involved in Th1 and Th17 differentiation such as IL-6 and IL-12[240,241]. In experimental models of GVHD, HDAC inhibition has been observed to lead to reduced secretion of proinflammatory cytokines including IL-12, IL-6, and TNFα by dendritic cells through enhancing the expression of indoleamine 2,3 dioxygenase[98,242,243]. Two phase II clinical trials have examined oral HDAC inhibitor vorinostat in the prevention of GVHD. One study investigated the addition of vorinostat to tacrolimus and mycophenolate in

patients that received reduced intensity conditioning prior to related donor hematopoietic stem cell transplantation[244]. Another study tested the effect of vorinostat when combined with tacrolimus and methotrexate following myeloablative conditioning prior to unrelated donor allo-HCT[245]. Both studies showed that vorinostat is well tolerated and associated with a lower incidence of acute GVHD[244,245]. A third study is ongoing to evaluate vorinostat as preventive therapy in adolescents and young adults receiving allogeneic BMT when combined with standard preventive therapy (NCT03842696). Future studies will elucidate the clinical benefit of HDAC inhibitors including vorinostat, as well as other agents such as panobinostat that are more recently being evaluated as primary therapy for acute GVHD[246].

Proteasome inhibition

The ubiquitin proteasome pathway is central to the selective of maintenance of proteins, and regulates a diverse set of intracellular processes including quality control for misfolded proteins, regulation of the cell cycle, and peptide processing for antigen presentation[247]. In immune cells, the proteasome is also involved in cell signaling, notably by regulating the expression of NF-κB, a transcription factor that promotes cell survival as well as the expression of numerous inflammatory cytokines[248]. Proteasome inhibitors have thus emerged as a drug class that is associated with a number of immunomodulatory effects, and are currently approved for the treatment of a number of hematologic disorders[249]. Proteasome inhibitors have been shown suppress NF-κB activation, in part due to the reduction of proteasome-dependent degradation of IκB[250,251]. The inhibition of NF-κB is associated with reduced proliferation, survival, and toxicity of allogeneic T cells, and has also been shown to abrogate T cell cytokine production[252,253]. In addition to its effect on T cells, proteasome inhibitors such as bortezomib have suppressive effect

on dendritic cell maturation and inflammatory cytokine production, while increasing dendritic cell apoptosis, highlighting their influence on multiple processes and cell types[254]. In murine models of acute GVHD, treatment of recipients with proteasome inhibitor bortezomib led to increased survival and protection from GVHD while maintaining GVT activity[255,256]. However, the timing of bortezomib administration may be critical in determining its efficacy as well as its overall safety, as delayed administration (i.e. 5 or more days after BMT compared to 0 to 3 days following BMT results in increased gastrointestinal toxicity that mechanistically correlates in other studies with amplified IL-1β production by dendritic cells[257,258]. While an early Phase I/II study to test a prophylaxis regimen of bortezomib combined with tacrolimus and methotrexate showed that the combination was well tolerated and associated with a lower incidence of GVHD, a randomized controlled trial failed to show an improvement in grade II-IV acute GVHD incidence with the addition of bortezomib, compared to methotrexate and tacrolimus alone[259,260]. Another proteasome inhibitor ixazomib improves acute GVHD upon early administration, impairs dendritic cell development, cytokine production, and expression of co-stimulatory molecules consistent with reduced proliferation of T cells, and clinical trials are underway to determine its efficacy in post-transplant patients[261].

REFERENCES

1. Bonifacino, J.S. Vesicular transport earns a Nobel. *Trends Cell Biol* **24**, 3-5 (2014).
2. Barlowe, C. Twenty-five years after coat protein complex II. *Mol Biol Cell* **31**, 3-6 (2020).
3. Miller, J.F. The discovery of thymus function and of thymus-derived lymphocytes. *Immunol Rev* **185**, 7-14 (2002).
4. Deftos, M.L. & Bevan, M.J. Notch signaling in T cell development. *Curr Opin Immunol* **12**, 166-172 (2000).
5. Shah, D.K. & Zuniga-Pflucker, J.C. An overview of the intrathymic intricacies of T cell development. *J Immunol* **192**, 4017-4023 (2014).
6. Kersh, G.J. & Hedrick, S.M. Role of TCR specificity in CD4 versus CD8 lineage commitment. *J Immunol* **154**, 1057-1068 (1995).
7. Germain, R.N. T-cell development and the CD4-CD8 lineage decision. *Nat Rev Immunol* **2**, 309-322 (2002).
8. Koch, U. & Radtke, F. Mechanisms of T cell development and transformation. *Annu Rev Cell Dev Biol* **27**, 539-562 (2011).
9. Smith-Garvin, J.E., Koretzky, G.A. & Jordan, M.S. T cell activation. *Annu Rev Immunol* **27**, 591-619 (2009).
10. Curtsinger, J.M. & Mescher, M.F. Inflammatory cytokines as a third signal for T cell activation. *Curr Opin Immunol* **22**, 333-340 (2010).
11. Curtsinger, J.M., Lins, D.C. & Mescher, M.F. Signal 3 determines tolerance versus full activation of naive CD8 T cells: dissociating proliferation and development of effector function. *J Exp Med* **197**, 1141-1151 (2003).
12. Curtsinger, J.M.*, et al.* Inflammatory cytokines provide a third signal for activation of naive CD4+ and CD8+ T cells. *J Immunol* **162**, 3256-3262 (1999).
13. Taniuchi, I. CD4 Helper and CD8 Cytotoxic T Cell Differentiation. *Annu Rev Immunol* **36**, 579-601 (2018).
14. Zhu, J., Yamane, H. & Paul, W.E. Differentiation of effector CD4 T cell populations (*). *Annu Rev Immunol* **28**, 445-489 (2010).
15. Kalia, V. & Sarkar, S. Regulation of Effector and Memory CD8 T Cell Differentiation by IL-2-A Balancing Act. *Front Immunol* **9**, 2987 (2018).
16. Ferrara, J.L., Levine, J.E., Reddy, P. & Holler, E. Graft-versus-host disease. *Lancet* **373**, 1550-1561 (2009).
17. Shlomchik, W.D. Graft-versus-host disease. *Nat Rev Immunol* **7**, 340-352 (2007).
18. Antin, J.H. & Ferrara, J.L. Cytokine dysregulation and acute graft-versus-host disease. *Blood* **80**, 2964-2968 (1992).
19. Hill, G.R.*, et al.* Total body irradiation and acute graft-versus-host disease: the role of gastrointestinal damage and inflammatory cytokines. *Blood* **90**, 3204-3213 (1997).
20. Xun, C.Q., Thompson, J.S., Jennings, C.D., Brown, S.A. & Widmer, M.B. Effect of total body irradiation, busulfan-cyclophosphamide, or cyclophosphamide conditioning on

inflammatory cytokine release and development of acute and chronic graft-versus-host disease in H-2-incompatible transplanted SCID mice. *Blood* **83**, 2360-2367 (1994).
21. Toubai, T., Mathewson, N.D., Magenau, J. & Reddy, P. Danger Signals and Graft-versus-host Disease: Current Understanding and Future Perspectives. *Front Immunol* **7**, 539 (2016).
22. Henden, A.S. & Hill, G.R. Cytokines in Graft-versus-Host Disease. *J Immunol* **194**, 4604-4612 (2015).
23. Wallace, P.M.*, et al.* CTLA4Ig treatment ameliorates the lethality of murine graft-versus-host disease across major histocompatibility complex barriers. *Transplantation* **58**, 602-610 (1994).
24. Briones, J., Novelli, S. & Sierra, J. T-cell costimulatory molecules in acute-graft-versus host disease: therapeutic implications. *Bone Marrow Res* **2011**, 976793 (2011).
25. Poirier, N.*, et al.* Preclinical efficacy and immunological safety of FR104, an antagonist anti-CD28 monovalent Fab' antibody. *Am J Transplant* **12**, 2630-2640 (2012).
26. Ghaemmaghami, S.*, et al.* Global analysis of protein expression in yeast. *Nature* **425**, 737-741 (2003).
27. Huh, W.K.*, et al.* Global analysis of protein localization in budding yeast. *Nature* **425**, 686-691 (2003).
28. Hegde, R.S. & Bernstein, H.D. The surprising complexity of signal sequences. *Trends Biochem Sci* **31**, 563-571 (2006).
29. Oakes, S.A. & Papa, F.R. The role of endoplasmic reticulum stress in human pathology. *Annu Rev Pathol* **10**, 173-194 (2015).
30. Hetz, C. The unfolded protein response: controlling cell fate decisions under ER stress and beyond. *Nat Rev Mol Cell Biol* **13**, 89-102 (2012).
31. Matsuoka, K.*, et al.* COPII-coated vesicle formation reconstituted with purified coat proteins and chemically defined liposomes. *Cell* **93**, 263-275 (1998).
32. Barlowe, C.*, et al.* COPII: a membrane coat formed by Sec proteins that drive vesicle budding from the endoplasmic reticulum. *Cell* **77**, 895-907 (1994).
33. Matsuoka, K., Morimitsu, Y., Uchida, K. & Schekman, R. Coat assembly directs v-SNARE concentration into synthetic COPII vesicles. *Mol Cell* **2**, 703-708 (1998).
34. Zanetti, G., Pahuja, K.B., Studer, S., Shim, S. & Schekman, R. COPII and the regulation of protein sorting in mammals. *Nat Cell Biol* **14**, 20-28 (2011).
35. Novick, P., Field, C. & Schekman, R. Identification of 23 complementation groups required for post-translational events in the yeast secretory pathway. *Cell* **21**, 205-215 (1980).
36. Novick, P. & Schekman, R. Secretion and cell-surface growth are blocked in a temperature-sensitive mutant of Saccharomyces cerevisiae. *Proc Natl Acad Sci U S A* **76**, 1858-1862 (1979).
37. Lederkremer, G.Z.*, et al.* Structure of the Sec23p/24p and Sec13p/31p complexes of COPII. *Proc Natl Acad Sci U S A* **98**, 10704-10709 (2001).
38. Schlacht, A. & Dacks, J.B. Unexpected ancient paralogs and an evolutionary model for the COPII coat complex. *Genome Biol Evol* **7**, 1098-1109 (2015).
39. Nakano, A., Brada, D. & Schekman, R. A membrane glycoprotein, Sec12p, required for protein transport from the endoplasmic reticulum to the Golgi apparatus in yeast. *J Cell Biol* **107**, 851-863 (1988).

40. Barlowe, C. & Schekman, R. SEC12 encodes a guanine-nucleotide-exchange factor essential for transport vesicle budding from the ER. *Nature* **365**, 347-349 (1993).
41. Bielli, A.*, et al.* Regulation of Sar1 NH2 terminus by GTP binding and hydrolysis promotes membrane deformation to control COPII vesicle fission. *J Cell Biol* **171**, 919-924 (2005).
42. Lee, M.C.*, et al.* Sar1p N-terminal helix initiates membrane curvature and completes the fission of a COPII vesicle. *Cell* **122**, 605-617 (2005).
43. Fromme, J.C., Orci, L. & Schekman, R. Coordination of COPII vesicle trafficking by Sec23. *Trends Cell Biol* **18**, 330-336 (2008).
44. Yoshihisa, T., Barlowe, C. & Schekman, R. Requirement for a GTPase-activating protein in vesicle budding from the endoplasmic reticulum. *Science* **259**, 1466-1468 (1993).
45. Bi, X., Corpina, R.A. & Goldberg, J. Structure of the Sec23/24-Sar1 pre-budding complex of the COPII vesicle coat. *Nature* **419**, 271-277 (2002).
46. Miller, E., Antonny, B., Hamamoto, S. & Schekman, R. Cargo selection into COPII vesicles is driven by the Sec24p subunit. *Embo j* **21**, 6105-6113 (2002).
47. Miller, E.A.*, et al.* Multiple cargo binding sites on the COPII subunit Sec24p ensure capture of diverse membrane proteins into transport vesicles. *Cell* **114**, 497-509 (2003).
48. Aridor, M., Weissman, J., Bannykh, S., Nuoffer, C. & Balch, W.E. Cargo selection by the COPII budding machinery during export from the ER. *J Cell Biol* **141**, 61-70 (1998).
49. Kuehn, M.J., Herrmann, J.M. & Schekman, R. COPII-cargo interactions direct protein sorting into ER-derived transport vesicles. *Nature* **391**, 187-190 (1998).
50. Stagg, S.M.*, et al.* Structural basis for cargo regulation of COPII coat assembly. *Cell* **134**, 474-484 (2008).
51. Aridor, M. & Traub, L.M. Cargo selection in vesicular transport: the making and breaking of a coat. *Traffic* **3**, 537-546 (2002).
52. Stagg, S.M.*, et al.* Structure of the Sec13/31 COPII coat cage. *Nature* **439**, 234-238 (2006).
53. Kirk, S.J. & Ward, T.H. COPII under the microscope. *Semin Cell Dev Biol* **18**, 435-447 (2007).
54. Zeuschner, D.*, et al.* Immuno-electron tomography of ER exit sites reveals the existence of free COPII-coated transport carriers. *Nat Cell Biol* **8**, 377-383 (2006).
55. Bi, X., Mancias, J.D. & Goldberg, J. Insights into COPII coat nucleation from the structure of Sec23.Sar1 complexed with the active fragment of Sec31. *Dev Cell* **13**, 635-645 (2007).
56. Khoriaty, R., Vasievich, M.P. & Ginsburg, D. The COPII pathway and hematologic disease. *Blood* **120**, 31-38 (2012).
57. Khoriaty, R.*, et al.* Functions of the COPII gene paralogs SEC23A and SEC23B are interchangeable in vivo. *Proc Natl Acad Sci U S A* **115**, E7748-e7757 (2018).
58. Lee, M.C. & Miller, E.A. Molecular mechanisms of COPII vesicle formation. *Semin Cell Dev Biol* **18**, 424-434 (2007).
59. Watson, P., Forster, R., Palmer, K.J., Pepperkok, R. & Stephens, D.J. Coupling of ER exit to microtubules through direct interaction of COPII with dynactin. *Nat Cell Biol* **7**, 48-55 (2005).
60. Lord, C.*, et al.* Sequential interactions with Sec23 control the direction of vesicle traffic. *Nature* **473**, 181-186 (2011).
61. Cai, H.*, et al.* TRAPPI tethers COPII vesicles by binding the coat subunit Sec23. *Nature* **445**, 941-944 (2007).
62. Mancias, J.D. & Goldberg, J. The transport signal on Sec22 for packaging into COPII-coated vesicles is a conformational epitope. *Mol Cell* **26**, 403-414 (2007).

63. Mossessova, E., Bickford, L.C. & Goldberg, J. SNARE selectivity of the COPII coat. *Cell* **114**, 483-495 (2003).
64. Boyadjiev, S.A.*, et al.* Cranio-lenticulo-sutural dysplasia is caused by a SEC23A mutation leading to abnormal endoplasmic-reticulum-to-Golgi trafficking. *Nat Genet* **38**, 1192-1197 (2006).
65. Lang, M.R., Lapierre, L.A., Frotscher, M., Goldenring, J.R. & Knapik, E.W. Secretory COPII coat component Sec23a is essential for craniofacial chondrocyte maturation. *Nat Genet* **38**, 1198-1203 (2006).
66. Boyadjiev, S.A.*, et al.* Cranio-lenticulo-sutural dysplasia associated with defects in collagen secretion. *Clin Genet* **80**, 169-176 (2011).
67. Schwarz, K.*, et al.* Mutations affecting the secretory COPII coat component SEC23B cause congenital dyserythropoietic anemia type II. *Nat Genet* **41**, 936-940 (2009).
68. Bianchi, P.*, et al.* Congenital dyserythropoietic anemia type II (CDAII) is caused by mutations in the SEC23B gene. *Hum Mutat* **30**, 1292-1298 (2009).
69. Russo, R.*, et al.* Mutational spectrum in congenital dyserythropoietic anemia type II: identification of 19 novel variants in SEC23B gene. *Am J Hematol* **85**, 915-920 (2010).
70. Iolascon, A., Heimpel, H., Wahlin, A. & Tamary, H. Congenital dyserythropoietic anemias: molecular insights and diagnostic approach. *Blood* **122**, 2162-2166 (2013).
71. Yang, C.*, et al.* Mutations in the coat complex II component SEC23B promote colorectal cancer metastasis. *Cell Death & Disease* **11**, 157 (2020).
72. Wang, Y.*, et al.* Identification of Rare Variants Predisposing to Thyroid Cancer. *Thyroid* **29**, 946-955 (2019).
73. Yehia, L.*, et al.* Germline Heterozygous Variants in SEC23B Are Associated with Cowden Syndrome and Enriched in Apparently Sporadic Thyroid Cancer. *The American Journal of Human Genetics* **97**, 661-676 (2015).
74. Tao, J.*, et al.* SEC23B is required for the maintenance of murine professional secretory tissues. *Proc Natl Acad Sci U S A* **109**, E2001-2009 (2012).
75. Zhu, M.*, et al.* Neural tube opening and abnormal extraembryonic membrane development in SEC23A deficient mice. *Sci Rep* **5**, 15471 (2015).
76. Khoriaty, R.*, et al.* Pancreatic SEC23B deficiency is sufficient to explain the perinatal lethality of germline SEC23B deficiency in mice. *Sci Rep* **6**, 27802 (2016).
77. Khoriaty, R.*, et al.* SEC23B is required for pancreatic acinar cell function in adult mice. *Mol Biol Cell* **28**, 2146-2154 (2017).
78. Khoriaty, R.*, et al.* Absence of a red blood cell phenotype in mice with hematopoietic deficiency of SEC23B. *Mol Cell Biol* **34**, 3721-3734 (2014).
79. Boncompain, G. & Weigel, A.V. Transport and sorting in the Golgi complex: multiple mechanisms sort diverse cargo. *Curr Opin Cell Biol* **50**, 94-101 (2018).
80. Gomez-Navarro, N. & Miller, E. Protein sorting at the ER-Golgi interface. *J Cell Biol* **215**, 769-778 (2016).
81. Kienzle, C. & von Blume, J. Secretory cargo sorting at the trans-Golgi network. *Trends Cell Biol* **24**, 584-593 (2014).
82. Ritter, A.T., Angus, K.L. & Griffiths, G.M. The role of the cytoskeleton at the immunological synapse. *Immunol Rev* **256**, 107-117 (2013).
83. Masson, D. & Tschopp, J. Isolation of a lytic, pore-forming protein (perforin) from cytolytic T-lymphocytes. *J Biol Chem* **260**, 9069-9072 (1985).

84. Podack, E.R., Konigsberg, P.J., Acha-Orbea, H., Pircher, H. & Hengartner, H. Cytolytic T-cell granules: biochemical properties and functional specificity. *Adv Exp Med Biol* **184**, 99-119 (1985).
85. Young, J.D.*, et al.* Isolation and characterization of a serine esterase from cytolytic T cell granules. *Cell* **47**, 183-194 (1986).
86. Stinchcombe, J.C., Majorovits, E., Bossi, G., Fuller, S. & Griffiths, G.M. Centrosome polarization delivers secretory granules to the immunological synapse. *Nature* **443**, 462-465 (2006).
87. Feldmann, J.*, et al.* Munc13-4 is essential for cytolytic granules fusion and is mutated in a form of familial hemophagocytic lymphohistiocytosis (FHL3). *Cell* **115**, 461-473 (2003).
88. Iida, T.*, et al.* Regulation of cell surface expression of CTLA-4 by secretion of CTLA-4-containing lysosomes upon activation of CD4+ T cells. *J Immunol* **165**, 5062-5068 (2000).
89. Lettau, M.*, et al.* The adaptor protein Nck interacts with Fas ligand: Guiding the death factor to the cytotoxic immunological synapse. *Proc Natl Acad Sci U S A* **103**, 5911-5916 (2006).
90. Kupfer, A., Mosmann, T.R. & Kupfer, H. Polarized expression of cytokines in cell conjugates of helper T cells and splenic B cells. *Proc Natl Acad Sci U S A* **88**, 775-779 (1991).
91. Poo, W.J., Conrad, L. & Janeway, C.A., Jr. Receptor-directed focusing of lymphokine release by helper T cells. *Nature* **332**, 378-380 (1988).
92. Huse, M., Lillemeier, B.F., Kuhns, M.S., Chen, D.S. & Davis, M.M. T cells use two directionally distinct pathways for cytokine secretion. *Nat Immunol* **7**, 247-255 (2006).
93. Huse, M., Quann, E.J. & Davis, M.M. Shouts, whispers and the kiss of death: directional secretion in T cells. *Nat Immunol* **9**, 1105-1111 (2008).
94. Jolly, C. & Sattentau, Q.J. Regulated secretion from CD4+ T cells. *Trends Immunol* **28**, 474-481 (2007).
95. Russell, J.H. & Ley, T.J. Lymphocyte-mediated cytotoxicity. *Annu Rev Immunol* **20**, 323-370 (2002).
96. Miller, E.A. & Schekman, R. COPII - a flexible vesicle formation system. *Curr Opin Cell Biol* **25**, 420-427 (2013).
97. Reddy, P.*, et al.* A crucial role for antigen-presenting cells and alloantigen expression in graft-versus-leukemia responses. *Nat Med* **11**, 1244-1249 (2005).
98. Reddy, P.*, et al.* Histone deacetylase inhibition modulates indoleamine 2,3-dioxygenase-dependent DC functions and regulates experimental graft-versus-host disease in mice. *J Clin Invest* **118**, 2562-2573 (2008).
99. Fujiwara, T., Oda, K., Yokota, S., Takatsuki, A. & Ikehara, Y. Brefeldin A causes disassembly of the Golgi complex and accumulation of secretory proteins in the endoplasmic reticulum. *J Biol Chem* **263**, 18545-18552 (1988).
100. Murphy, K.M. & Reiner, S.L. The lineage decisions of helper T cells. *Nature Reviews Immunology* **2**, 933-944 (2002).
101. Muul, L.M., Silvin, C., James, S.P. & Candotti, F. Measurement of proliferative responses of cultured lymphocytes. *Curr Protoc Immunol* **Chapter 7**, Unit 7.10.11-17.10.24 (2008).
102. Welniak, L.A., Blazar, B.R. & Murphy, W.J. Immunobiology of allogeneic hematopoietic stem cell transplantation. *Annu Rev Immunol* **25**, 139-170 (2007).
103. Wong, P. & Pamer, E.G. CD8 T Cell Responses to Infectious Pathogens. *Annual Review of Immunology* **21**, 29-70 (2003).

104. Virgin, H.W., Wherry, E.J. & Ahmed, R. Redefining chronic viral infection. *Cell* **138**, 30-50 (2009).
105. Butz, E.A. & Bevan, M.J. Massive expansion of antigen-specific CD8+ T cells during an acute virus infection. *Immunity* **8**, 167-175 (1998).
106. Wherry, E.J., Blattman, J.N., Murali-Krishna, K., van der Most, R. & Ahmed, R. Viral persistence alters CD8 T-cell immunodominance and tissue distribution and results in distinct stages of functional impairment. *J Virol* **77**, 4911-4927 (2003).
107. Laidlaw, B.J., Craft, J.E. & Kaech, S.M. The multifaceted role of CD4(+) T cells in CD8(+) T cell memory. *Nat Rev Immunol* **16**, 102-111 (2016).
108. Kaech, S.M. & Cui, W. Transcriptional control of effector and memory CD8+ T cell differentiation. *Nat Rev Immunol* **12**, 749-761 (2012).
109. Kaech, S.M. & Wherry, E.J. Heterogeneity and cell-fate decisions in effector and memory CD8+ T cell differentiation during viral infection. *Immunity* **27**, 393-405 (2007).
110. Kurtulus, S., Tripathi, P. & Hildeman, D.A. Protecting and rescuing the effectors: roles of differentiation and survival in the control of memory T cell development. *Front Immunol* **3**, 404 (2012).
111. Penaloza-MacMaster, P.*, et al.* Vaccine-elicited CD4 T cells induce immunopathology after chronic LCMV infection. *Science* **347**, 278-282 (2015).
112. Matullo, C.M., O'Regan, K.J., Hensley, H., Curtis, M. & Rall, G.F. Lymphocytic choriomeningitis virus-induced mortality in mice is triggered by edema and brain herniation. *J Virol* **84**, 312-320 (2010).
113. Matullo, C.M., O'Regan, K.J., Curtis, M. & Rall, G.F. CNS recruitment of CD8+ T lymphocytes specific for a peripheral virus infection triggers neuropathogenesis during polymicrobial challenge. *PLoS Pathog* **7**, e1002462 (2011).
114. Kang, S.S. & McGavern, D.B. Lymphocytic choriomeningitis infection of the central nervous system. *Front Biosci* **13**, 4529-4543 (2008).
115. Lee, M.C., Miller, E.A., Goldberg, J., Orci, L. & Schekman, R. Bi-directional protein transport between the ER and Golgi. *Annu Rev Cell Dev Biol* **20**, 87-123 (2004).
116. Bonzon-Kulichenko, E.*, et al.* Quantitative in-depth analysis of the dynamic secretome of activated Jurkat T-cells. *J Proteomics* **75**, 561-571 (2011).
117. Witzke, K.E.*, et al.* Quantitative Secretome Analysis of Activated Jurkat Cells Using Click Chemistry-Based Enrichment of Secreted Glycoproteins. *J Proteome Res* **16**, 137-146 (2017).
118. Paccaud, J.P.*, et al.* Cloning and functional characterization of mammalian homologues of the COPII component Sec23. *Mol Biol Cell* **7**, 1535-1546 (1996).
119. MacIver, N.J., Michalek, R.D. & Rathmell, J.C. Metabolic regulation of T lymphocytes. *Annu Rev Immunol* **31**, 259-283 (2013).
120. van der Windt, G.J. & Pearce, E.L. Metabolic switching and fuel choice during T-cell differentiation and memory development. *Immunol Rev* **249**, 27-42 (2012).
121. Chapman, N.M., Boothby, M.R. & Chi, H. Metabolic coordination of T cell quiescence and activation. *Nat Rev Immunol* **20**, 55-70 (2020).
122. Macintyre, A.N.*, et al.* The glucose transporter Glut1 is selectively essential for CD4 T cell activation and effector function. *Cell Metab* **20**, 61-72 (2014).
123. Cammann, C.*, et al.* Early changes in the metabolic profile of activated CD8(+) T cells. *BMC Cell Biol* **17**, 28 (2016).

124. Jones, N.*, et al.* Metabolic Adaptation of Human CD4+ and CD8+ T-Cells to T-Cell Receptor-Mediated Stimulation. *Frontiers in Immunology* **8**(2017).
125. Tan, H.*, et al.* Integrative Proteomics and Phosphoproteomics Profiling Reveals Dynamic Signaling Networks and Bioenergetics Pathways Underlying T Cell Activation. *Immunity* **46**, 488-503 (2017).
126. Gerriets, V.A.*, et al.* Metabolic programming and PDHK1 control CD4+ T cell subsets and inflammation. *J Clin Invest* **125**, 194-207 (2015).
127. Gosmain, Y., Lefai, E., Ryser, S., Roques, M. & Vidal, H. Sterol regulatory element-binding protein-1 mediates the effect of insulin on hexokinase II gene expression in human muscle cells. *Diabetes* **53**, 321-329 (2004).
128. Foretz, M., Guichard, C., Ferre, P. & Foufelle, F. Sterol regulatory element binding protein-1c is a major mediator of insulin action on the hepatic expression of glucokinase and lipogenesis-related genes. *Proc Natl Acad Sci U S A* **96**, 12737-12742 (1999).
129. Kim, S.Y.*, et al.* SREBP-1c mediates the insulin-dependent hepatic glucokinase expression. *J Biol Chem* **279**, 30823-30829 (2004).
130. Shao, W. & Espenshade, P.J. Expanding roles for SREBP in metabolism. *Cell Metab* **16**, 414-419 (2012).
131. Ye, J. & DeBose-Boyd, R.A. Regulation of cholesterol and fatty acid synthesis. *Cold Spring Harb Perspect Biol* **3**(2011).
132. Shimano, H. & Sato, R. SREBP-regulated lipid metabolism: convergent physiology - divergent pathophysiology. *Nat Rev Endocrinol* **13**, 710-730 (2017).
133. Bensinger, S.J.*, et al.* LXR signaling couples sterol metabolism to proliferation in the acquired immune response. *Cell* **134**, 97-111 (2008).
134. Espenshade, P.J. SREBPs: sterol-regulated transcription factors. *J Cell Sci* **119**, 973-976 (2006).
135. Radhakrishnan, A., Sun, L.P., Kwon, H.J., Brown, M.S. & Goldstein, J.L. Direct binding of cholesterol to the purified membrane region of SCAP: mechanism for a sterol-sensing domain. *Mol Cell* **15**, 259-268 (2004).
136. Sun, L.P., Li, L., Goldstein, J.L. & Brown, M.S. Insig required for sterol-mediated inhibition of Scap/SREBP binding to COPII proteins in vitro. *J Biol Chem* **280**, 26483-26490 (2005).
137. Adams, C.M.*, et al.* Cholesterol and 25-hydroxycholesterol inhibit activation of SREBPs by different mechanisms, both involving SCAP and Insigs. *J Biol Chem* **279**, 52772-52780 (2004).
138. Feramisco, J.D.*, et al.* Intramembrane aspartic acid in SCAP protein governs cholesterol-induced conformational change. *Proc Natl Acad Sci U S A* **102**, 3242-3247 (2005).
139. Duncan, E.A., Brown, M.S., Goldstein, J.L. & Sakai, J. Cleavage site for sterol-regulated protease localized to a leu-Ser bond in the lumenal loop of sterol regulatory element-binding protein-2. *J Biol Chem* **272**, 12778-12785 (1997).
140. Espenshade, P.J., Cheng, D., Goldstein, J.L. & Brown, M.S. Autocatalytic processing of site-1 protease removes propeptide and permits cleavage of sterol regulatory element-binding proteins. *J Biol Chem* **274**, 22795-22804 (1999).
141. Rawson, R.B. Control of lipid metabolism by regulated intramembrane proteolysis of sterol regulatory element binding proteins (SREBPs). *Biochem Soc Symp*, 221-231 (2003).
142. Lee, S.J.*, et al.* The structure of importin-beta bound to SREBP-2: nuclear import of a transcription factor. *Science* **302**, 1571-1575 (2003).

143. Brown, M.S. & Goldstein, J.L. The SREBP pathway: regulation of cholesterol metabolism by proteolysis of a membrane-bound transcription factor. *Cell* **89**, 331-340 (1997).
144. Wang, X., Sato, R., Brown, M.S., Hua, X. & Goldstein, J.L. SREBP-1, a membrane-bound transcription factor released by sterol-regulated proteolysis. *Cell* **77**, 53-62 (1994).
145. Antonny, B. & Schekman, R. ER export: public transportation by the COPII coach. *Curr Opin Cell Biol* **13**, 438-443 (2001).
146. Espenshade, P.J., Li, W.P. & Yabe, D. Sterols block binding of COPII proteins to SCAP, thereby controlling SCAP sorting in ER. *Proc Natl Acad Sci U S A* **99**, 11694-11699 (2002).
147. Kidani, Y.*, et al.* Sterol regulatory element-binding proteins are essential for the metabolic programming of effector T cells and adaptive immunity. *Nat Immunol* **14**, 489-499 (2013).
148. Horton, J.D., Goldstein, J.L. & Brown, M.S. SREBPs: activators of the complete program of cholesterol and fatty acid synthesis in the liver. *J Clin Invest* **109**, 1125-1131 (2002).
149. Punzo, F.*, et al.* Congenital dyserythropoietic anemia type II: molecular analysis and expression of the SEC23B gene. *Orphanet J Rare Dis* **6**, 89 (2011).
150. Zhang, H.*, et al.* A case report of congenital erythropoietic anemia II in China with a novel mutation. *Ann Hematol* **98**, 1041-1043 (2019).
151. Seki, A. & Rutz, S. Optimized RNP transfection for highly efficient CRISPR/Cas9-mediated gene knockout in primary T cells. *J Exp Med* **215**, 985-997 (2018).
152. Heimpel, H.*, et al.* Congenital dyserythropoietic anemia type II: epidemiology, clinical appearance, and prognosis based on long-term observation. *Blood* **102**, 4576-4581 (2003).
153. Mandal, P.K.*, et al.* Efficient ablation of genes in human hematopoietic stem and effector cells using CRISPR/Cas9. *Cell Stem Cell* **15**, 643-652 (2014).
154. Su, S.*, et al.* CRISPR-Cas9 mediated efficient PD-1 disruption on human primary T cells from cancer patients. *Sci Rep* **6**, 20070 (2016).
155. Liu, X.*, et al.* CRISPR-Cas9-mediated multiplex gene editing in CAR-T cells. *Cell Res* **27**, 154-157 (2017).
156. Wang, W.*, et al.* CCR5 gene disruption via lentiviral vectors expressing Cas9 and single guided RNA renders cells resistant to HIV-1 infection. *PLoS One* **9**, e115987 (2014).
157. El-Brolosy, M.A. & Stainier, D.Y.R. Genetic compensation: A phenomenon in search of mechanisms. *PLoS Genet* **13**, e1006780 (2017).
158. Liang, H. & Li, W.H. Functional compensation by duplicated genes in mouse. *Trends Genet* **25**, 441-442 (2009).
159. O'Leary, M.N.*, et al.* The ribosomal protein Rpl22 controls ribosome composition by directly repressing expression of its own paralog, Rpl22l1. *PLoS Genet* **9**, e1003708 (2013).
160. Saito, A.*, et al.* Regulation of endoplasmic reticulum stress response by a BBF2H7-mediated Sec23a pathway is essential for chondrogenesis. *Nat Cell Biol* **11**, 1197-1204 (2009).
161. Kondo, S.*, et al.* BBF2H7, a novel transmembrane bZIP transcription factor, is a new type of endoplasmic reticulum stress transducer. *Mol Cell Biol* **27**, 1716-1729 (2007).
162. Pellegrin, S.*, et al.* Transduction with BBF2H7/CREB3L2 upregulates SEC23A protein in erythroblasts and partially corrects the hypo-glycosylation phenotype associated with CDAII. *Br J Haematol* **184**, 876-881 (2019).
163. Scharaw, S.*, et al.* The endosomal transcriptional regulator RNF11 integrates degradation and transport of EGFR. *J Cell Biol* **215**, 543-558 (2016).

164. Wilhelmi, I.*, et al.* Sec16 alternative splicing dynamically controls COPII transport efficiency. *Nat Commun* **7**, 12347 (2016).
165. Tanaka, J.*, et al.* Cytokine gene expression in peripheral blood mononuclear cells during graft-versus-host disease after allogeneic bone marrow transplantation. *Br J Haematol* **85**, 558-565 (1993).
166. Tvedt, T.H.A., Ersvaer, E., Tveita, A.A. & Bruserud, O. Interleukin-6 in Allogeneic Stem Cell Transplantation: Its Possible Importance for Immunoregulation and As a Therapeutic Target. *Front Immunol* **8**, 667 (2017).
167. O'Shea, J.J., Ma, A. & Lipsky, P. Cytokines and autoimmunity. *Nat Rev Immunol* **2**, 37-45 (2002).
168. Brenner, D., Blaser, H. & Mak, T.W. Regulation of tumour necrosis factor signalling: live or let die. *Nat Rev Immunol* **15**, 362-374 (2015).
169. Holler, E.*, et al.* Increased serum levels of tumor necrosis factor alpha precede major complications of bone marrow transplantation. *Blood* **75**, 1011-1016 (1990).
170. Schmaltz, C.*, et al.* Donor T cell-derived TNF is required for graft-versus-host disease and graft-versus-tumor activity after bone marrow transplantation. *Blood* **101**, 2440-2445 (2003).
171. Holler, E.*, et al.* Modulation of acute graft-versus-host-disease after allogeneic bone marrow transplantation by tumor necrosis factor alpha (TNF alpha) release in the course of pretransplant conditioning: role of conditioning regimens and prophylactic application of a monoclonal antibody neutralizing human TNF alpha (MAK 195F). *Blood* **86**, 890-899 (1995).
172. Kitko, C.L.*, et al.* Plasma elevations of tumor necrosis factor-receptor-1 at day 7 postallogeneic transplant correlate with graft-versus-host disease severity and overall survival in pediatric patients. *Biol Blood Marrow Transplant* **14**, 759-765 (2008).
173. Korngold, R., Marini, J.C., de Baca, M.E., Murphy, G.F. & Giles-Komar, J. Role of tumor necrosis factor-alpha in graft-versus-host disease and graft-versus-leukemia responses. *Biol Blood Marrow Transplant* **9**, 292-303 (2003).
174. Hamadani, M.*, et al.* Addition of infliximab to standard acute graft-versus-host disease prophylaxis following allogeneic peripheral blood cell transplantation. *Biol Blood Marrow Transplant* **14**, 783-789 (2008).
175. Couriel, D.*, et al.* Tumor necrosis factor-alpha blockade for the treatment of acute GVHD. *Blood* **104**, 649-654 (2004).
176. Couriel, D.R.*, et al.* A phase III study of infliximab and corticosteroids for the initial treatment of acute graft-versus-host disease. *Biol Blood Marrow Transplant* **15**, 1555-1562 (2009).
177. Gatza, E.*, et al.* Etanercept plus topical corticosteroids as initial therapy for grade one acute graft-versus-host disease after allogeneic hematopoietic cell transplantation. *Biol Blood Marrow Transplant* **20**, 1426-1434 (2014).
178. De Jong, C.N.*, et al.* Etanercept for steroid-refractory acute graft-versus-host disease: A single center experience. *PLoS One* **12**, e0187184 (2017).
179. van Groningen, L.F.*, et al.* Combination Therapy with Inolimomab and Etanercept for Severe Steroid-Refractory Acute Graft-versus-Host Disease. *Biol Blood Marrow Transplant* **22**, 179-182 (2016).

180. Ma, C.K.K., *et al.* Poor prognosis in patients with steroid refractory acute graft versus host disease treated with etanercept: a multi-centre analysis. *Bone Marrow Transplant* **53**, 1478-1482 (2018).
181. Busca, A., Locatelli, F., Marmont, F., Ceretto, C. & Falda, M. Recombinant human soluble tumor necrosis factor receptor fusion protein as treatment for steroid refractory graft-versus-host disease following allogeneic hematopoietic stem cell transplantation. *Am J Hematol* **82**, 45-52 (2007).
182. Wajant, H. & Beilhack, A. Targeting Regulatory T Cells by Addressing Tumor Necrosis Factor and Its Receptors in Allogeneic Hematopoietic Cell Transplantation and Cancer. *Front Immunol* **10**, 2040 (2019).
183. Jones, S.A., Scheller, J. & Rose-John, S. Therapeutic strategies for the clinical blockade of IL-6/gp130 signaling. *J Clin Invest* **121**, 3375-3383 (2011).
184. Tanaka, T., Narazaki, M. & Kishimoto, T. IL-6 in inflammation, immunity, and disease. *Cold Spring Harb Perspect Biol* **6**, a016295 (2014).
185. Tawara, I., *et al.* Interleukin-6 modulates graft-versus-host responses after experimental allogeneic bone marrow transplantation. *Clin Cancer Res* **17**, 77-88 (2011).
186. Chen, X., *et al.* Blockade of interleukin-6 signaling augments regulatory T-cell reconstitution and attenuates the severity of graft-versus-host disease. *Blood* **114**, 891-900 (2009).
187. Drobyski, W.R., *et al.* Tocilizumab for the treatment of steroid refractory graft-versus-host disease. *Biol Blood Marrow Transplant* **17**, 1862-1868 (2011).
188. Kennedy, G.A., *et al.* Addition of interleukin-6 inhibition with tocilizumab to standard graft-versus-host disease prophylaxis after allogeneic stem-cell transplantation: a phase 1/2 trial. *Lancet Oncol* **15**, 1451-1459 (2014).
189. Drobyski, W.R., *et al.* Tocilizumab, tacrolimus and methotrexate for the prevention of acute graft-versus-host disease: low incidence of lower gastrointestinal tract disease. *Haematologica* **103**, 717-727 (2018).
190. Kennedy, G.A., *et al.* Results of a Phase III Double-Blind Study of the Addition of Tocilizumab Vs. Placebo to Cyclosporin/Methotrexate Gvhd Prophylaxis after HLA-Matched Allogeneic Stem Cell Transplantation. *Blood* **134**, 368-368 (2019).
191. McCarthy, P.L., Jr., *et al.* A clinical phase I/II study of recombinant human interleukin-1 receptor in glucocorticoid-resistant graft-versus-host disease. *Transplantation* **62**, 626-631 (1996).
192. Antin, J.H., *et al.* Recombinant human interleukin-1 receptor antagonist in the treatment of steroid-resistant graft-versus-host disease. *Blood* **84**, 1342-1348 (1994).
193. Antin, J.H., *et al.* Interleukin-1 blockade does not prevent acute graft-versus-host disease: results of a randomized, double-blind, placebo-controlled trial of interleukin-1 receptor antagonist in allogeneic bone marrow transplantation. *Blood* **100**, 3479-3482 (2002).
194. McCarthy, P.L., Jr., *et al.* Inhibition of interleukin-1 by an interleukin-1 receptor antagonist prevents graft-versus-host disease. *Blood* **78**, 1915-1918 (1991).
195. Jankovic, D., *et al.* The Nlrp3 inflammasome regulates acute graft-versus-host disease. *J Exp Med* **210**, 1899-1910 (2013).
196. Koehn, B.H., *et al.* GVHD-associated, inflammasome-mediated loss of function in adoptively transferred myeloid-derived suppressor cells. *Blood* **126**, 1621-1628 (2015).
197. Fujiwara, H., *et al.* Microbial metabolite sensor GPR43 controls severity of experimental GVHD. *Nat Commun* **9**, 3674 (2018).

198. Toubai, T.*, et al.* Host NLRP6 exacerbates graft-versus-host disease independent of gut microbial composition. *Nat Microbiol* **4**, 800-812 (2019).
199. Reed, M.H., Shapiro, M.E., Milford, E.L., Carpenter, C.B. & Kirkman, R.L. Interleukin 2 receptor expression on peripheral blood lymphocytes in association with renal allograft rejection. *Transplantation* **48**, 361-366 (1989).
200. Kirkman, R.L.*, et al.* Administration of an anti-interleukin 2 receptor monoclonal antibody prolongs cardiac allograft survival in mice. *J Exp Med* **162**, 358-362 (1985).
201. Abbas, A.K., Trotta, E., D, R.S., Marson, A. & Bluestone, J.A. Revisiting IL-2: Biology and therapeutic prospects. *Sci Immunol* **3**(2018).
202. Lee, S.J.*, et al.* Effect of up-front daclizumab when combined with steroids for the treatment of acute graft-versus-host disease: results of a randomized trial. *Blood* **104**, 1559-1564 (2004).
203. Bordigoni, P.*, et al.* Daclizumab, an efficient treatment for steroid-refractory acute graft-versus-host disease. *Br J Haematol* **135**, 382-385 (2006).
204. Massenkeil, G.*, et al.* Basiliximab is well tolerated and effective in the treatment of steroid-refractory acute graft-versus-host disease after allogeneic stem cell transplantation. *Bone Marrow Transplant* **30**, 899-903 (2002).
205. Wang, J.Z.*, et al.* Basiliximab for the treatment of steroid-refractory acute graft-versus-host disease after unmanipulated HLA-mismatched/haploidentical hematopoietic stem cell transplantation. *Transplant Proc* **43**, 1928-1933 (2011).
206. Schmidt-Hieber, M.*, et al.* Efficacy of the interleukin-2 receptor antagonist basiliximab in steroid-refractory acute graft-versus-host disease. *Br J Haematol* **130**, 568-574 (2005).
207. Betts, B.C.*, et al.* IL-2 promotes early Treg reconstitution after allogeneic hematopoietic cell transplantation. *Haematologica* **102**, 948-957 (2017).
208. Malek, T.R. & Bayer, A.L. Tolerance, not immunity, crucially depends on IL-2. *Nat Rev Immunol* **4**, 665-674 (2004).
209. Taylor, P.A., Lees, C.J. & Blazar, B.R. The infusion of ex vivo activated and expanded CD4(+)CD25(+) immune regulatory cells inhibits graft-versus-host disease lethality. *Blood* **99**, 3493-3499 (2002).
210. Hoffmann, P., Ermann, J., Edinger, M., Fathman, C.G. & Strober, S. Donor-type CD4(+)CD25(+) regulatory T cells suppress lethal acute graft-versus-host disease after allogeneic bone marrow transplantation. *J Exp Med* **196**, 389-399 (2002).
211. Edinger, M.*, et al.* CD4+CD25+ regulatory T cells preserve graft-versus-tumor activity while inhibiting graft-versus-host disease after bone marrow transplantation. *Nat Med* **9**, 1144-1150 (2003).
212. Matsuoka, K.*, et al.* Low-dose interleukin-2 therapy restores regulatory T cell homeostasis in patients with chronic graft-versus-host disease. *Sci Transl Med* **5**, 179ra143 (2013).
213. Koreth, J.*, et al.* Interleukin-2 and regulatory T cells in graft-versus-host disease. *N Engl J Med* **365**, 2055-2066 (2011).
214. Koreth, J.*, et al.* Efficacy, durability, and response predictors of low-dose interleukin-2 therapy for chronic graft-versus-host disease. *Blood* **128**, 130-137 (2016).
215. Chi, H. Regulation and function of mTOR signalling in T cell fate decisions. *Nat Rev Immunol* **12**, 325-338 (2012).
216. Chiang, P.H.*, et al.* Mechanistic insights into impaired dendritic cell function by rapamycin: inhibition of Jak2/Stat4 signaling pathway. *J Immunol* **172**, 1355-1363 (2004).

217. Abouelnasr, A., Roy, J., Cohen, S., Kiss, T. & Lachance, S. Defining the role of sirolimus in the management of graft-versus-host disease: from prophylaxis to treatment. *Biol Blood Marrow Transplant* **19**, 12-21 (2013).
218. Zeiser, R.*, et al.* Differential impact of mammalian target of rapamycin inhibition on CD4+CD25+Foxp3+ regulatory T cells compared with conventional CD4+ T cells. *Blood* **111**, 453-462 (2008).
219. Antin, J.H.*, et al.* Sirolimus, tacrolimus, and low-dose methotrexate for graft-versus-host disease prophylaxis in mismatched related donor or unrelated donor transplantation. *Blood* **102**, 1601-1605 (2003).
220. Cutler, C. & Antin, J.H. Sirolimus for GVHD prophylaxis in allogeneic stem cell transplantation. *Bone Marrow Transplant* **34**, 471-476 (2004).
221. Torlen, J.*, et al.* A prospective randomized trial comparing cyclosporine/methotrexate and tacrolimus/sirolimus as graft-versus-host disease prophylaxis after allogeneic hematopoietic stem cell transplantation. *Haematologica* **101**, 1417-1425 (2016).
222. Sandmaier, B.M.*, et al.* Addition of sirolimus to standard cyclosporine plus mycophenolate mofetil-based graft-versus-host disease prophylaxis for patients after unrelated non-myeloablative haemopoietic stem cell transplantation: a multicentre, randomised, phase 3 trial. *Lancet Haematol* **6**, e409-e418 (2019).
223. Xhaard, A.*, et al.* A monocentric study of steroid-refractory acute graft-versus-host disease treatment with tacrolimus and mTOR inhibitor. *Bone Marrow Transplant* **55**, 86-92 (2020).
224. Schroeder, M.A., Choi, J., Staser, K. & DiPersio, J.F. The Role of Janus Kinase Signaling in Graft-Versus-Host Disease and Graft Versus Leukemia. *Biol Blood Marrow Transplant* **24**, 1125-1134 (2018).
225. Choi, J.*, et al.* Pharmacologic blockade of JAK1/JAK2 reduces GvHD and preserves the graft-versus-leukemia effect. *PLoS One* **9**, e109799 (2014).
226. Spoerl, S.*, et al.* Activity of therapeutic JAK 1/2 blockade in graft-versus-host disease. *Blood* **123**, 3832-3842 (2014).
227. Carniti, C.*, et al.* Pharmacologic Inhibition of JAK1/JAK2 Signaling Reduces Experimental Murine Acute GVHD While Preserving GVT Effects. *Clin Cancer Res* **21**, 3740-3749 (2015).
228. Jagasia, M.*, et al.* Ruxolitinib for the treatment of patients with steroid-refractory GVHD: an introduction to the REACH trials. *Immunotherapy* **10**, 391-402 (2018).
229. Chen, Y.-B., Arbushites, M., Delaite, P., Yan, Y. & Zeiser, R. Trial in Progress: Gravitas-301, a Randomized, Double-Blind Phase 3 Study of Itacitinib or Placebo with Corticosteroids (CS) for the First-Line Treatment of Patients with Acute Gvhd (aGVHD). *Biology of Blood and Marrow Transplantation* **24**, S208-S209 (2018).
230. Carrell, R.W. & Lomas, D.A. Alpha1-antitrypsin deficiency--a model for conformational diseases. *N Engl J Med* **346**, 45-53 (2002).
231. Jonigk, D.*, et al.* Anti-inflammatory and immunomodulatory properties of alpha1-antitrypsin without inhibition of elastase. *Proc Natl Acad Sci U S A* **110**, 15007-15012 (2013).
232. Bergin, D.A.*, et al.* The circulating proteinase inhibitor alpha-1 antitrypsin regulates neutrophil degranulation and autoimmunity. *Sci Transl Med* **6**, 217ra211 (2014).
233. Marcondes, A.M.*, et al.* α-1-Antitrypsin (AAT)–modified donor cells suppress GVHD but enhance the GVL effect: a role for mitochondrial bioenergetics. *Blood* **124**, 2881-2891 (2014).

234. Marcondes, A.M., *et al.* Inhibition of IL-32 activation by alpha-1 antitrypsin suppresses alloreactivity and increases survival in an allogeneic murine marrow transplantation model. *Blood* **118**, 5031-5039 (2011).
235. Tawara, I., *et al.* Alpha-1-antitrypsin monotherapy reduces graft-versus-host disease after experimental allogeneic bone marrow transplantation. *Proc Natl Acad Sci U S A* **109**, 564-569 (2012).
236. Marcondes, A.M., *et al.* Response of Steroid-Refractory Acute GVHD to alpha1-Antitrypsin. *Biol Blood Marrow Transplant* **22**, 1596-1601 (2016).
237. Magenau, J.M., *et al.* alpha1-Antitrypsin infusion for treatment of steroid-resistant acute graft-versus-host disease. *Blood* **131**, 1372-1379 (2018).
238. Narita, T., Weinert, B.T. & Choudhary, C. Functions and mechanisms of non-histone protein acetylation. *Nat Rev Mol Cell Biol* **20**, 156-174 (2019).
239. Shakespear, M.R., Halili, M.A., Irvine, K.M., Fairlie, D.P. & Sweet, M.J. Histone deacetylases as regulators of inflammation and immunity. *Trends Immunol* **32**, 335-343 (2011).
240. Brogdon, J.L., *et al.* Histone deacetylase activities are required for innate immune cell control of Th1 but not Th2 effector cell function. *Blood* **109**, 1123-1130 (2007).
241. Bosisio, D., *et al.* Blocking TH17-polarizing cytokines by histone deacetylase inhibitors in vitro and in vivo. *J Leukoc Biol* **84**, 1540-1548 (2008).
242. Reddy, P., *et al.* Histone deacetylase inhibitor suberoylanilide hydroxamic acid reduces acute graft-versus-host disease and preserves graft-versus-leukemia effect. *Proc Natl Acad Sci U S A* **101**, 3921-3926 (2004).
243. Choi, S. & Reddy, P. HDAC inhibition and graft versus host disease. *Mol Med* **17**, 404-416 (2011).
244. Choi, S.W., *et al.* Vorinostat plus tacrolimus and mycophenolate to prevent graft-versus-host disease after related-donor reduced-intensity conditioning allogeneic haemopoietic stem-cell transplantation: a phase 1/2 trial. *Lancet Oncol* **15**, 87-95 (2014).
245. Choi, S.W., *et al.* Vorinostat plus tacrolimus/methotrexate to prevent GVHD after myeloablative conditioning, unrelated donor HCT. *Blood* **130**, 1760-1767 (2017).
246. Perez, L., *et al.* Phase I trial of histone deacetylase inhibitor panobinostat in addition to glucocorticoids for primary therapy of acute graft-versus-host disease. *Bone Marrow Transplantation* **53**, 1434-1444 (2018).
247. Ciechanover, A. The ubiquitin-proteasome proteolytic pathway. *Cell* **79**, 13-21 (1994).
248. Chen, Z.J. Ubiquitin signalling in the NF-kappaB pathway. *Nat Cell Biol* **7**, 758-765 (2005).
249. Manasanch, E.E. & Orlowski, R.Z. Proteasome inhibitors in cancer therapy. *Nat Rev Clin Oncol* **14**, 417-433 (2017).
250. Sunwoo, J.B., *et al.* Novel proteasome inhibitor PS-341 inhibits activation of nuclear factor-kappa B, cell survival, tumor growth, and angiogenesis in squamous cell carcinoma. *Clin Cancer Res* **7**, 1419-1428 (2001).
251. Palombella, V.J., *et al.* Role of the proteasome and NF-kappaB in streptococcal cell wall-induced polyarthritis. *Proc Natl Acad Sci U S A* **95**, 15671-15676 (1998).
252. Vodanovic-Jankovic, S., Hari, P., Jacobs, P., Komorowski, R. & Drobyski, W.R. NF-kappaB as a target for the prevention of graft-versus-host disease: comparative efficacy of bortezomib and PS-1145. *Blood* **107**, 827-834 (2006).

253. Blanco, B.*, et al.* Bortezomib induces selective depletion of alloreactive T lymphocytes and decreases the production of Th1 cytokines. *Blood* **107**, 3575-3583 (2006).
254. Al-Homsi, A.S.*, et al.* Bortezomib for the prevention and treatment of graft-versus-host disease after allogeneic hematopoietic stem cell transplantation. *Exp Hematol* **44**, 771-777 (2016).
255. Sun, K.*, et al.* Inhibition of acute graft-versus-host disease with retention of graft-versus-tumor effects by the proteasome inhibitor bortezomib. *Proc Natl Acad Sci U S A* **101**, 8120-8125 (2004).
256. Pai, C.C.*, et al.* Therapeutic benefit of bortezomib on acute graft-versus-host disease is tissue specific and is associated with interleukin-6 levels. *Biol Blood Marrow Transplant* **20**, 1899-1904 (2014).
257. Sun, K.*, et al.* Differential effects of proteasome inhibition by bortezomib on murine acute graft-versus-host disease (GVHD): delayed administration of bortezomib results in increased GVHD-dependent gastrointestinal toxicity. *Blood* **106**, 3293-3299 (2005).
258. Liang, Y.*, et al.* IL-1beta and TLR4 signaling are involved in the aggravated murine acute graft-versus-host disease caused by delayed bortezomib administration. *J Immunol* **192**, 1277-1285 (2014).
259. Koreth, J.*, et al.* Bortezomib-based graft-versus-host disease prophylaxis in HLA-mismatched unrelated donor transplantation. *J Clin Oncol* **30**, 3202-3208 (2012).
260. Koreth, J.*, et al.* Bortezomib-based immunosuppression after reduced-intensity conditioning hematopoietic stem cell transplantation: randomized phase II results. *Haematologica* **103**, 522-530 (2018).
261. Al-Homsi, A.S.*, et al.* Ixazomib suppresses human dendritic cell and modulates murine graft-versus-host disease in a schedule-dependent fashion. *Exp Hematol* **48**, 50-57 (2017).